INFORMATION CONTENT OF GRAIN-SIZE FREQUENCY DISTRIBUTIONS IN COASTAL DEPOSITS ON THE EASTERN SHORE OF LAKE MICHIGAN

By

Richard Lee Chambers

A DISSERTATION

Submitted to
Michigan State University
in partial fulfillment of the requirements
for the degree of

DOCTOR OF PHILOSOPHY

Department of Geology

1975

ABSTRACT

INFORMATION CONTENT OF GRAIN-SIZE
FREQUENCY DISTRIBUTIONS IN COASTAL DEPOSITS
ON THE EASTERN SHORE OF LAKE MICHIGAN

by

Richard Lee Chambers

The problem of discriminating sediments deposited by different sedimentary processes in adjacent environments from two recent depositional systems on the eastern coast of Lake Michigan has been investigated by multivariate statistical methods. These two systems are located at 1) Little Sable Point and 2) the Sleeping Bear Point/Manitou Passage area. Each system has four adjacent depositional environments. The Little Sable Point environments are: beach, aeolian, fluvial, and offshore bar and trough; while the environments in the Sleeping Bear Point/Manitou Passage area are: beach, shoal and nearshore (<20m in water depth), transitional (>20m<75m in water depth), and profundal (>75m>100m in water depth). The sediment from the Little Sable Point area has a limited grain-size range (0Ø to 3Ø) and is derived from a single source area. The Sleeping Bear Point/Manitou Passage sediments are derived from several source areas and are characterized by grain-sizes ranging from lag gravels to fine silt and clay.

Principal-components analysis was performed on frequencies of occurrence of sediment within grain-size intervals in order to group

the size classes into independent clusters which may reflect deposition from different transport mechanisms. It was found that in both systems, the size classes were clustered mainly around two factors which account for 70-90% of the total grain-size variance. Generally, specific size classes clustered around specific factors and each cluster corresponds to one of the log-normal sub-populations observed on traditional cumulative probability graphs of grain-size frequency distributions. The main clusters generally correspond to 1) sizes coarser than 1Ø; 2) sizes from 1Ø to 3.5Ø to 4Ø; and 3) sizes 4Ø and finer. These groups are thought to represent respectively surface creep bed load, mixed suspension bed-load (saltation and non-uniform suspension), and uniform suspension.

Discriminant-function analysis of sediment samples from the Sleeping Bear Point/Manitou Passage area demonstrates that grain-size distributions can be used for discrimination providing that available grain-sizes do not limit the resulting distributions and that the environments are characterized by different energy conditions. Discriminant-function analysis and Q-mode factor analysis of the Little Sable Point sediment samples show that when available grain-sizes are limited in size range, similar grain-size distribution can occur in environments that are characterized by supposedly different energy conditions. It is apparent from this study that source areas which provide a variety of grain-sizes, the presence of sediment in the size range 4Ø and finer and differing energy conditions are prerequisite for effective environmental discrimination.

It has been shown that sediment texture (Little Sable Point sediments) is not always effective for discriminating recent environments. The problem of identifying ancient environments is further complicated because of lithification and diagenesis of the sediment. Even if sedimentary environments, be they recent or ancient, cannot be uniquely identified by grain-size studies, the knowledge of energy transport levels obtained by principal-components analysis of presently operative systems will aid in the interpretation of paleo-flow regimes.

For my parents,
Aileen and Bob

ACKNOWLEDGMENTS

I would like to take this opportunity to thank Dr. Sam B. Upchurch, dissertation advisor and good friend, for his continued encouragement throughout this project. Sam originally suggested this study and contributed much to its completion. We had some good discussions on the golf course, sorry about all the times you lost Sam.

I would also like to thank the other members of my committee for their comments on the manuscript, they are: Drs. J. Alan Holman, James Fisher, Maynard M. Miller and Arthur P. Pinsak. Many thanks to Dr. "Chip" Prouty for joining the committee only one week before the oral defense. Thanks are extended to Dr. Edward Rothman, University of Michigan, Department of Statistics, for his time discussing various aspects of the multivariate techniques used in this study.

Special thanks to the Great Lakes Environmental Research Laboratory, NOAA,ERL. Dr. Pinsak made it possible for me to be permanently employed with the Limnology Division of the Lake Survey Center (now part of the NOAA,ERL,GLERL research group in Ann Arbor, Michigan) and work full time on my dissertation. The Lake Survey's research vessel SHENEHON was made available to me for sample collection in the Sleeping Bear Point/Manitou Passage area in northern Lake Michigan. The time, funds, and materials made available to me by these organizations are gratefully acknowledged.

Last, but not least, thanks to my wife Linda who put up with all the chaos that goes with a dissertation.

TABLE OF CONTENTS

Table of Contents (cont'd)

LIST OF TABLES

LIST OF FIGURES

Figures (cont'd) Page

Figures (cont'd) Page

NOMENCLATURE

Canonical variable - these are weights refer to the standard scores of the responses. $Z_{ij} = \frac{X_{ij} - X_j}{S_j}$ where X_{ij} refers to the S_j ith individual on the jth measurements, X_j equals the mean and S_j equals the standard deviations, computed from the correlation matrix.

Communality - this value indicates the degree to which the extracted factors, with eigenvalues >1 represent variations in a correlation matrix.

Eigenvalue and eigenvector - a value λ such that $Ax - \lambda x = 0$, where A is some symmetrical matrix, has a non-zero solution is called an eigenvalue (characteristic root) of the matrix A, and the non-zero solutions of this equation are called eigenvectors (characteristic vectors) corresponding to λ.

Factor analysis - multivariate technique used to discern simplifying relationships in complex data. It may be used to study relationships between variables (R-mode) or between cases (Q-mode).

Factor axes - these represent best fitted lines through data clusters in a hyper-ellipsoidal space.

Hyper-ellipsoidal space - an ellipse described mathematically as one with more than 3 orthogonal axes.

Loading profile - a graphical representation of loading values versus the variables.

Loading value - this value represents the degree to which a variable correlates with a factor axis; the closer the value is to unity the better the correlation.

Mahalanobis D^2 - this is a measure of the distance between two sample cluster multivariate means.

Principal-components - the jth principal-component of the sample of P - variate observations is the linear compound

$$Y_j = A_{1j}X_1 + \ldots + A_{Pj}X_P$$

whose coefficients are the elements of the characteristic vector of the sample matrix corresponding to the jth largest root $\lambda \neq \lambda_j$, the coefficients of the ith and jth components are orthogonal. The sample variance of the jth component is λ_j.

Profundal - in limnology, this term means deep water, with quiet circulation.

Rankits - a non-parametric statistic used to test normality of values falling into some ranked order.

Saltation - the mode of movement of particles in a series of jumps upwards from the bed; it is intermediate in character between surface creep and suspension.

Surface creep - in sedimentological terms, this refers to larger particles transported by rolling or sliding, intermittently along the bed.

Suspension - the mode of movement of particles which are supported by the fluid; two types of suspension are recognized: in non-uniform suspension there is an increased gradient of particles nearer the bed, while uniform suspension denotes wholly fluid supported particles.

Varimax rotation - one of several types of axis rotations used in factor analysis; for this type of rotation the axes remain orthogonal to each other.

INTRODUCTION

Sedimentological models often use concepts based on fundamental relationships between grain-size frequency distributions and depositional environments. Considerable controversey has developed over the usefulness of sediment texture and summary statistics (e.g., mean, standard deviation, skewness, and kurtosis) as environmental indicators. This dispute arises in part from the multitudinous grain-size measurements and computational methods developed since the turn of the century. Many authors (e.g., Friedman, 1967; Visher, 1969; Upchurch, 1970a) have demonstrated the usefulness of different combinations of summary statistics for environmental discrimination, while others (e.g., Shepard and Young, 1961; Schlee, et al., 1964; Solohub and Klovan, 1970) using the same or different statistics claim the environments cannot be discriminated on texture alone. Further complications in the use of grain-size statistics to make environmental interpretations are derived from the insensitivity of the statistics to subtle differences in sample textures and to polymodal mixtures of sediment from different sources. In order to effectively discriminate between depositional environments it is important to understand the sources of environmentally sensitive textural information within sediment samples. This requires identification of the most useful statistics for characterization of sediments. These statistics are those which are least variable within

sediment types and most variable across sediment types (Davis, 1973).

The use of multivariate statistics in sedimentology (e.g., Imbrie, 1963; Imbrie and Van Andel, 1964; Klovan, 1966; Davis, 1970; Upchurch, 1970a, 1972; Allen, et al., 1971; Mather, 1972; Davies and Ethridge, 1975) has shown a considerable increase in the literature during the past twelve years stemming from the availability of high speed computers. With the computational capacity of the computer it has become possible to use a large number variables in order to characterize size distributions, rather than limiting comparisons to summary statistics. For example, the percent of sediment in 1/2 phi intervals can be used as variables. Use of size frequency data as variables allows principal-components and Q-mode factor analyses to identify those size frequency variables which cluster into independent groups and are environmentally sensitive variables. These variables may then be related to specific sediment distributions which reflect depositional environments and to the energy levels in these environments that control sediment textures. This study tests the effectiveness of sediment size distributions as environmental discriminators by means of multivariate techniques. This study also shows why for certain sediment types discrimination is not always possible.

Two contrasting Recent depositional systems were chosen for this study to provide an opportunity to evaluate the effects of provenance and hydrodynamics on sediment texture in adjacent environments. The first system studied is located at Little Sable Point,

Michigan (Fig. 1). This area was chosen because of the limited grain-size range available to the system (Upchurch, 1970b). Most of the sediments in the beach, offshore bar and trough, aeolian, and fluvial environments of the main study area are limited such that differences in texture between the respective environments should be a function of hydrodynamics, rather than of provenance and hydrodynamics.

The second study area is located in the Manitou Passage area of Sleeping Bear Point, Michigan (Fig. 1). This site was selected because of the presence of a variety of sediment provenances and hydrodynamic environments (French, 1964). The sediment in this area ranges from lag gravels and coarse sands on shoals to fine fractions including deep water silt and clay.

Figure 1: Index map of study areas located on the eastern shore of Lake Michigan. Littoral currents and wind vectors (W) are indicated by arrows

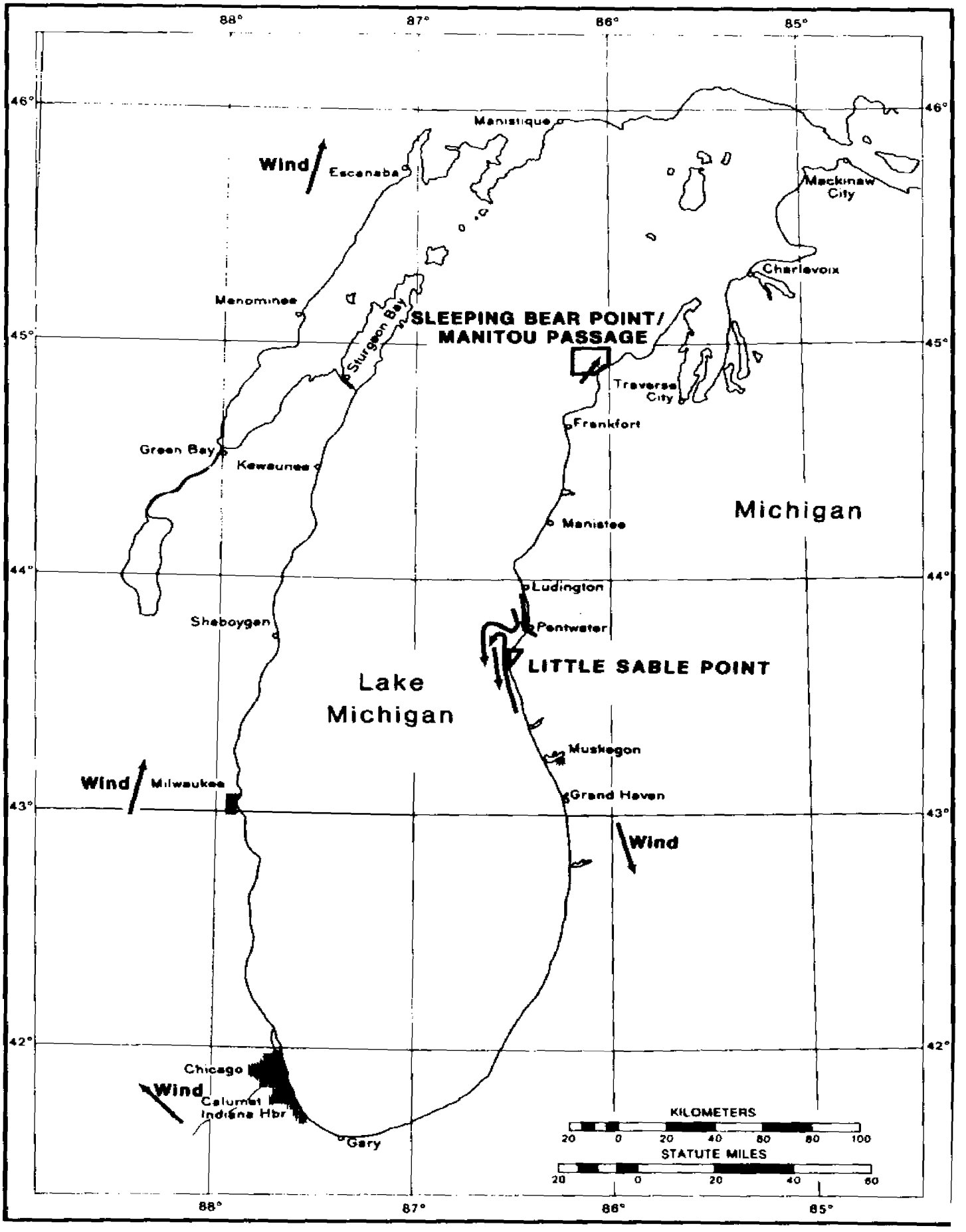
88°
87°
86°
85°
46°
45°
44°
43°
42°
Manistique
Wind
Escanaba
Mackinaw City
Charlevoix
Menominee
Sturgeon Bay
SLEEPING BEAR POINT/
MANITOU PASSAGE
Traverse City
Frankfort
Green Bay
Kewaunee
Michigan
Manistee
Ludington
Sheboygan
Pentwater
LITTLE SABLE POINT
Lake
Michigan
Muskegon
Wind
Milwaukee
Grand Haven
Wind
Chicago
Wind
Calumet
Indiana Hbr
Gary
KILOMETERS
20 0 20 40 60 80 100
STATUTE MILES
20 0 20 40 60

PREVIOUS WORK

Every depositional environment is assumed to have characteristic energy conditions and fluctuations through time and space (Sahu, 1964). Recent workers (Folk and Ward, 1975; Sahu, 1964; Visher, 1965, 1969; Klovan, 1966; Friedman, 1967; Upchurch, 1970a, b; Allen et al., 1971; and Buller and McManus, 1972) have suggested that sediment textures seem to reflect different energy conditions. However, Visher (1969) states that similar transport mechanisms operate within a number of environments and the consequent sediment textural responses may be similar. Klovan (1966), Bagnold (1967), and Davis (1970) concluded that the entire grain-size spectrum reflects transport energy and should be analyzed in order to characterize environments of deposition.

Many authors have shown that most size distributions are composed of two or more log-normal sub-populations rather than a single, log-linear curve (Krumbein, 1937, 1938; Otto, 1939; Doeglas, 1946; Inman, 1949; Bagnold, 1956; Fuller, 1961; Spencer, 1963; Visher, 1969; and Upchurch, 1970b). Moss (1962, 1963) suggests that three sub-populations could exist within the same sample and that they are produced by different transport mechanisms: 1) surface creep; 2) saltation; and 3) suspension. Moss related these transport mechanisms in terms of fluid mechanics concepts developed earlier by Bagnold (1956).

In 1969, Visher discussed a number of processes which he felt were uniquely depicted in log-probability plots of grain-size distributions. These processes include: 1) currents; 2) swash and backwash; 3) waves; 4) tidal channel currents; 5) fall out from suspension; 6) turbidity currents; and 7) wind. Visher suggested that log-normal sub-populations are related to the mechanisms described by Moss (1962, 1963); and that the number of sub-populations present in the total distribution, the percent of sediment in each sub-population, the size range of each sub-population, the sorting of each sub-population, and mixing between the sub-populations vary systematically in relation tc provenance, transport mechanisms present, and relative energy intensity.

Bagnold (1966), Allen, et al. (1971), and Blatt, et al. (1972) have attempted to relate specific grain-size intervals to transport processes in terms of fluid mechanics, mainly on an experimental and theoretical basis. Bagnold (1966) noted that grains coarser than 2Ø tend to be moved as bedload at the onset of grain motion, while those grains from 2Ø to approximately 3.5Ø to 4Ø are transported by nonuniform suspension (Allen, et al., 1971), which denotes an increase in particle density nearer the bed. Bagnold (1966) states that uniform suspension would be fully developed in grains finer than 3.3Ø. Blatt, et al. (1972) noted that sand in the size range of -1Ø to 3Ø tends to move mainly by traction and intermittent suspension while finer sizes are probably transported by suspension. Therefore, these different size modes represent different sediment transport mechanisms, and the relative portions and size ranges of the modes should reflect different energy levels.

Davis (1970), Allen, et al. (1971) and Mather (1972) were the first to use a form of R-mode factor analysis in an attempt to show statistical relationships between grain-size intervals. Davis (1970) showed that for samples from Barataria Bay, Louisiana, sixty percent of the sample variability could be explained by simply comparing the ratio of sediment finer than 4 Ø to the material coarser than 4 Ø. In a study of the sediment of the Gironde Estuary, France, Allen et al. (1971) showed that seventy-three percent of the total grain-size variability was accounted for by three factor axes. The sediments in the estuary range in size from -3 Ø to 6 Ø. Factor I is associated with sizes coarser than 0.6 Ø, representing the surface creep process. Factor II is associated with sizes finer than 3 Ø and is interpreted to represent a pure suspension load. The sediment sizes between 0.6 Ø and 3 Ø are associated with factor III. Allen et al. (1971) suggested that factor III reflects the interaction of two transport mechanisms. The grains between 0.6 Ø and 1.6 Ø are interpreted to represent the saltation mode, while those between 1.6 Ø and 3.0 Ø represent a non-uniform suspension mode. Mather (1972) noted that six factors were needed to explain the total variance in glacio-fluvial sediments and each factor was related to a small part of the total distribution. He did not relate these factors to any process, but noted that the sand fractions accounted for sixty-eight percent of the variance.

The terminology and fluid mechanics concepts used in this study are taken from these previous workers. Visher (1969) has developed a very useful approach for analyzing grain-size

distribution curves, and comparisons between the multivariate approach used in this study and Visher's approach will be made whenever possible.

LOCATION AND PROCEDURE

Location and Collection of Samples

Two independent Recent depositional systems were chosen for this study; the Little Sable Point area (Fig. 1), and the Sleeping Bear Point/Manitou Passage area (Fig. 1). Both are located in Michigan on the eastern shore of Lake Michigan.

Little Sable Point - The surficial deposits of this area are predominately of glacial origin (Saylor and Hands, 1970). At the lakeshore, Recent, beach, aeolian, and fluvial sediments are accumulating (Fig. 2). The source material for sediments in the Silver Lake sand dunes and adjacent Lake Michigan beach system comes from Pleistocene morainic sediment approximately 2.5 km south of Silver Lake (Upchurch, 1970b). Upchurch (1970b) found the following sorting conditions at the source area: 1) the pebble-cobble fraction forms a lag beach deposit; 2) the silt-clay population is winnowed and carried lakeward; and 3) the sand population is transported by littoral currents. The dominant littoral current for this area is northward (Ayers, et al. 1958) (Fig. 1 and 2). Thus, beach sediment transported northward from the source area has a restricted grain-size distribution, limited by the sand size population at the source and competence of the transporting mechanism, namely littoral drift. There is much feedback between the beach and adjacent dunes (Upchurch, 1970b) and presumably between the beach, offshore bars,

Figure 2: Sample locations at Little Sable Point, Lake Michigan. Site 1 locates aeolian samples west of Silver Lake. Site 2 locates beach, Silver Creek and offshore bar and trough samples. Site 3 locates the beach samples collected at the morainal source area

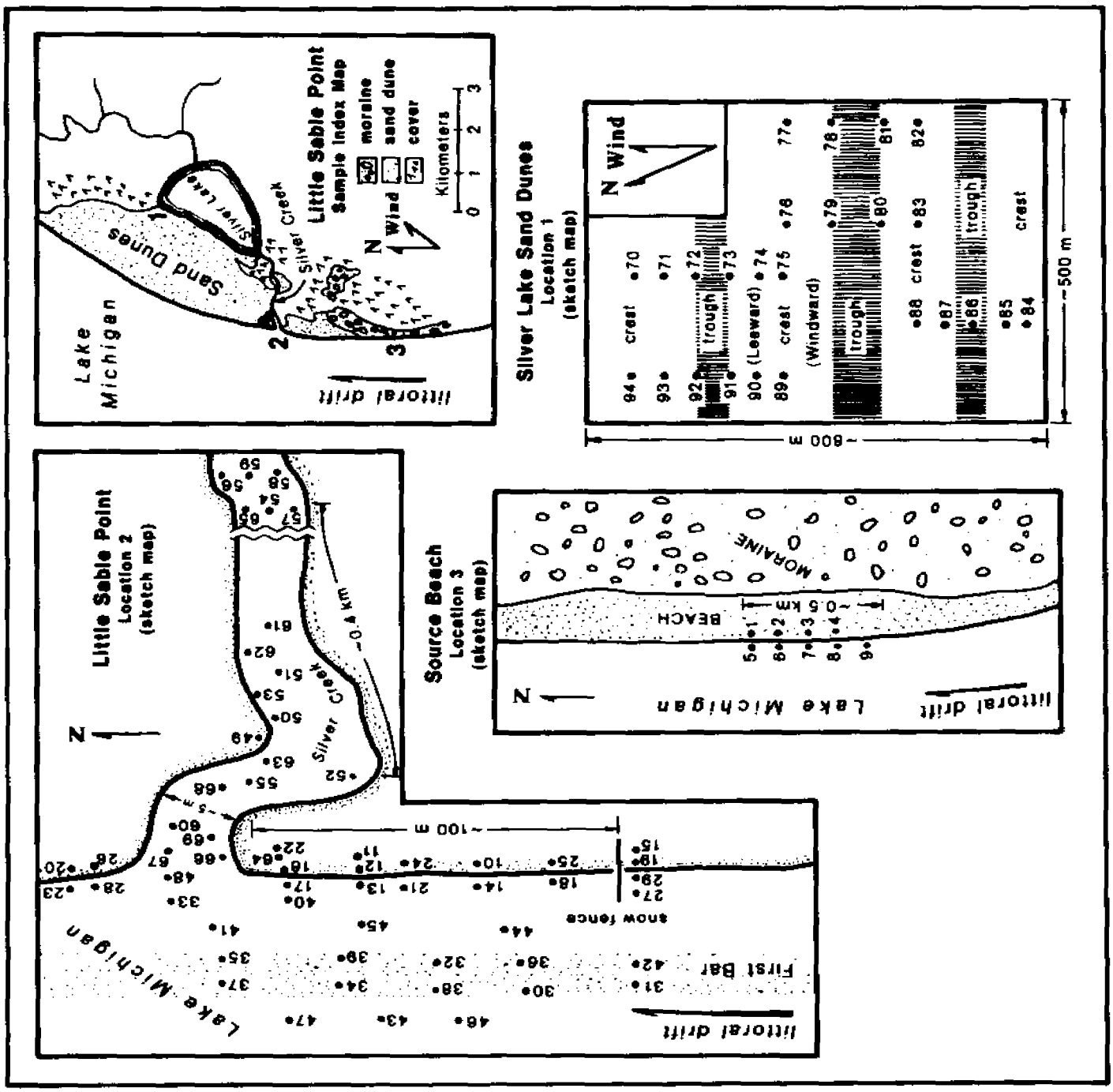
Little Sable Point
Sample Index Map
moraine
sand dune
cover
Kilometers
Wind
Silver Creek
Silver Lake
Sand Dunes
Lake Michigan
littoral drift
Silver Lake Sand Dunes
Location 1
(sketch map)
N Wind
crest
trough
(Leeward)
(Windward)
~800 m
~500 m
Source Beach
Location 3
(sketch map)
MORAINE
BEACH
~0.5 km
Lake Michigan
Little Sable Point
Location 2
(sketch map)
~0.4 km
~100 m
snow fence
First Bar

dunes, and Silver Creek. The Little Sable Point depositional system provides an excellent opportunity to study, under the constraints of a single source and a limited grain-size range, the grain-size distribution produced by different, adjacent hydrodynamic environments.

Two sample sets were collected: one set during early winter conditions in October 1972 (n = 52)*, the other during the spring conditions in late June 1973 (n = 42). Sampling was randomized by collecting sediment from the environments listed below during a random walk through an environment then noting their approximate position on a sketch map. The environments sampled include: 1) beach sediment at the morainic source area (n = 9); 2) beach sediment on Lake Michigan west of Silver Lake (n = 20); 3) offshore bars and troughs in the area of the beach just described (n = 18); 4) bed sediment from Silver Creek (n = 22); and 5) aeolian sediment between Silver Lake and Lake Michigan (n = 25). As suggested by Visher (1969), the samples were collected from the upper centimeter to reflect the physical conditions just prior to sampling. The data are listed in Appendix A.

Sleeping Bear Point/Manitou Passage area - This area (Figs. 1 and 4) is a region of both nearshore and open water environments, with different sedimentary processes operating in an area of mixed sediment provenances. The surficial sediments of Sleeping Bear Point

---

*N is the number of random samples collected.

and North and South Manitou Islands are morainic and glacial outwash, with large active sand dunes on Sleeping Bear Point (French, 1964).

Figure 3 shows the bathymetry for this area. The lake bottom physiography is complex and has been called the ridge-and-valley province of Lake Michigan (Hough, 1958). The major morphological zones in the study area are: 1) the shallow-water, Sleeping Bear Shoal, extending approximately 8 km northwest of Sleeping Bear Point, with water depths from 10-20 m; 2) deep, quiet water basins north and south of the shoal with water depths from 75-100 m; and 3) an intermediate depth area north to northeast of Sleeping Bear Point with depths from 20-75 m (French, 1964).

The most prominent feature of Sleeping Bear Point, the west face, has undergone extensive erosion in the past fifty years and has retreated more than 15 m during that time (Gillis and Bakeman, 1963). According to French (1964), the shoal areas with depths less than 20 m are floored with clean sands or with a pebble-cobble-boulder pavement overlaying clay till. The rocky-bottomed central portions of the shoal appear to be covered with lag concentrates eroded from the underlying till.

The northeast tip of Sleeping Bear Point has undergone at least two major episodes of mass wastage since the turn of the century. In 1906, approximately 8×10^5 square meters of unconsolidated glacial outwash and sand dune material slumped into the adjacent lake water (Upchurch, 1973). Eighty thousand square meters slumped into the lake again in March 1970 (U.S. Department of Commerce News, 1971) due to heavy rains and high water.

Figure 3: Bathymetric chart of the Sleeping Bear Point/Manitou Passage area, Lake Michigan

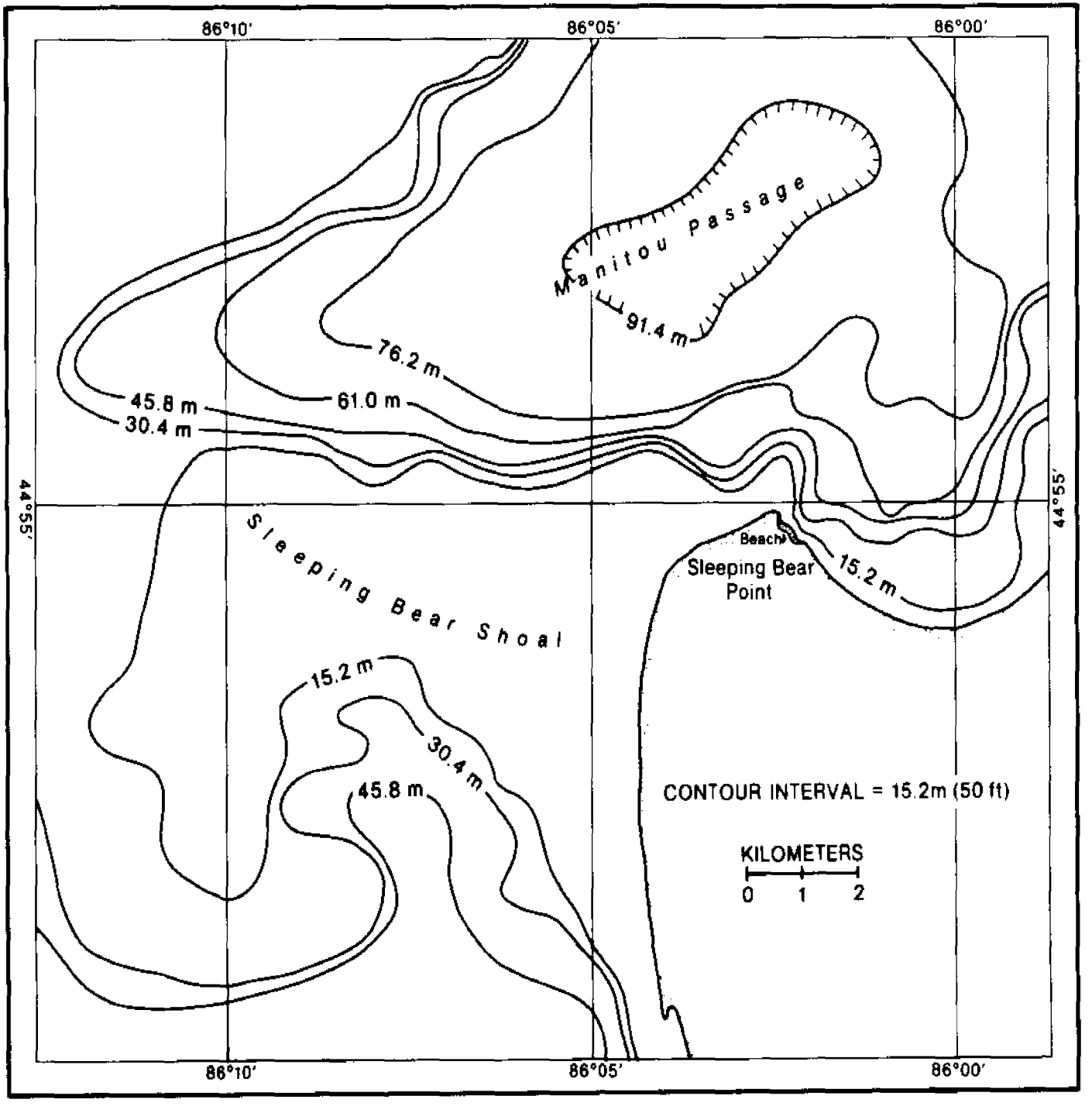
86°10'
86°05'
86°00'
44°55'
Manitou passage
91.4 m
76.2 m
61.0 m
45.8 m
30.4 m
Sleeping Bear Shoal
15.2 m
30.4 m
45.8 m
Beach
Sleeping Bear Point
15.2 m
CONTOUR INTERVAL = 15.2m (50 ft)
KILOMETERS
0 1 2

Forty-two surface samples and eighteen piston cores were collected from a 284 km^2 area encompassing the above environments (Fig. 4) during a one-week cruise in July 1973. All samples were collected from the Lake Survey research vessel SHENEHON. Bottom samples were collected at each station with a 400 cm^3 Shipek sediment sampler (Fig. 5a). The sampler recovers the upper 10 cm in an essentially undisturbed condition. Cores were collected with a 160 kg Alpine piston corer (Fig. 5b) that is capable of penetrating up to 3.5 m; with penetration dependent upon sediment type. Full penetration was possible in the silt-clay rich areas, while little penetration was possible in the coarse sand areas.

Sample Preparation and Size Analyses

Sample Preparation - Samples from the Sleeping Bear Point/Manitou Passage area were first treated with 10% HCl acid to remove shell material, and with 30% H_2O_2 to remove organic detritus. The samples were dried and weighed, then split at the 4.0Ø interval by wet-sieving methods. The coarse fraction was re-dried and weighed and the percent of total weight calculated. This portion was then ready for settling-tube analysis. The sediment finer than 4.0Ø was omitted from the multivariate tests to avoid the problems generated during multiple correlation analysis of closed number systems (page 29). The above procedures were not necessary for the Little Sable Point samples as they contained no shell fragments or organic detritus and were truncated at approximately 3Ø.

Figure 4: Sample locations at the Sleeping Bear Point/Manitou Passage area, Lake Michigan. Piston cores and surface samples were taken at locations indicated by a triangle. Only surface samples were collected at sites indicated by a dot

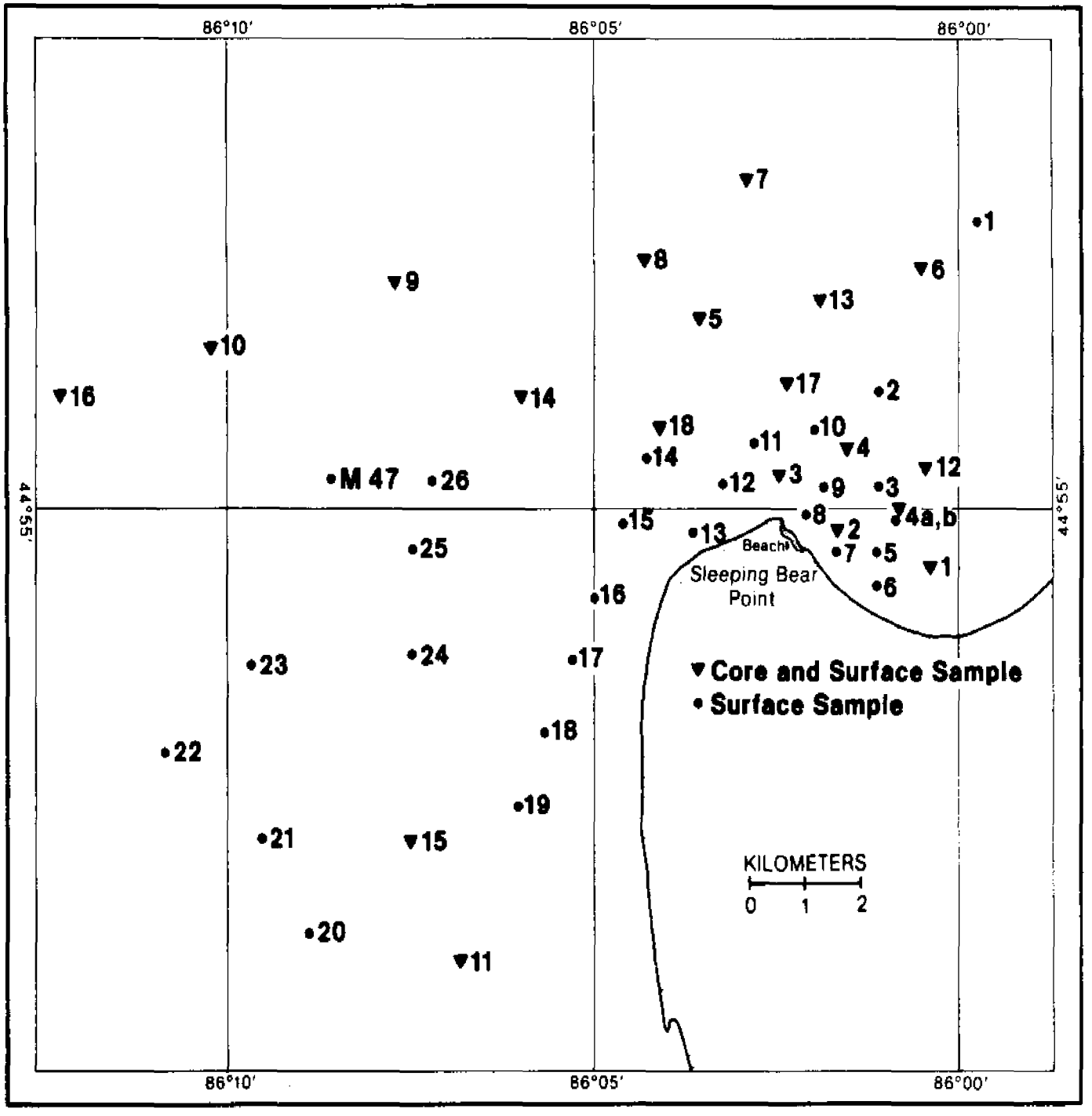
86°10'
86°05'
86°00'
44°55'
▼7
•1
▼8
▼6
▼9
▼13
▼5
▼10
▼16
▼14
▼17
•2
▼18
•10
•11
▼4
•14
•M 47
•26
•12
▼3
•9
•3
▼12
•15
•8
▼4a,b
•13
▼2
Beach
•7
•5
•25
▼1
Sleeping Bear
Point
•6
•16
•23
•24
•17
▼Core and Surface Sample
• Surface Sample
•18
•22
•19
•21
▼15
KILOMETERS
0 1 2
•20
▼11

Figure 5: Shipek surface sampler (a) and an Alpine piston corer (b) used for sample collection at the Sleeping Bear Point/ Manitou Passage area, Lake Michigan


a

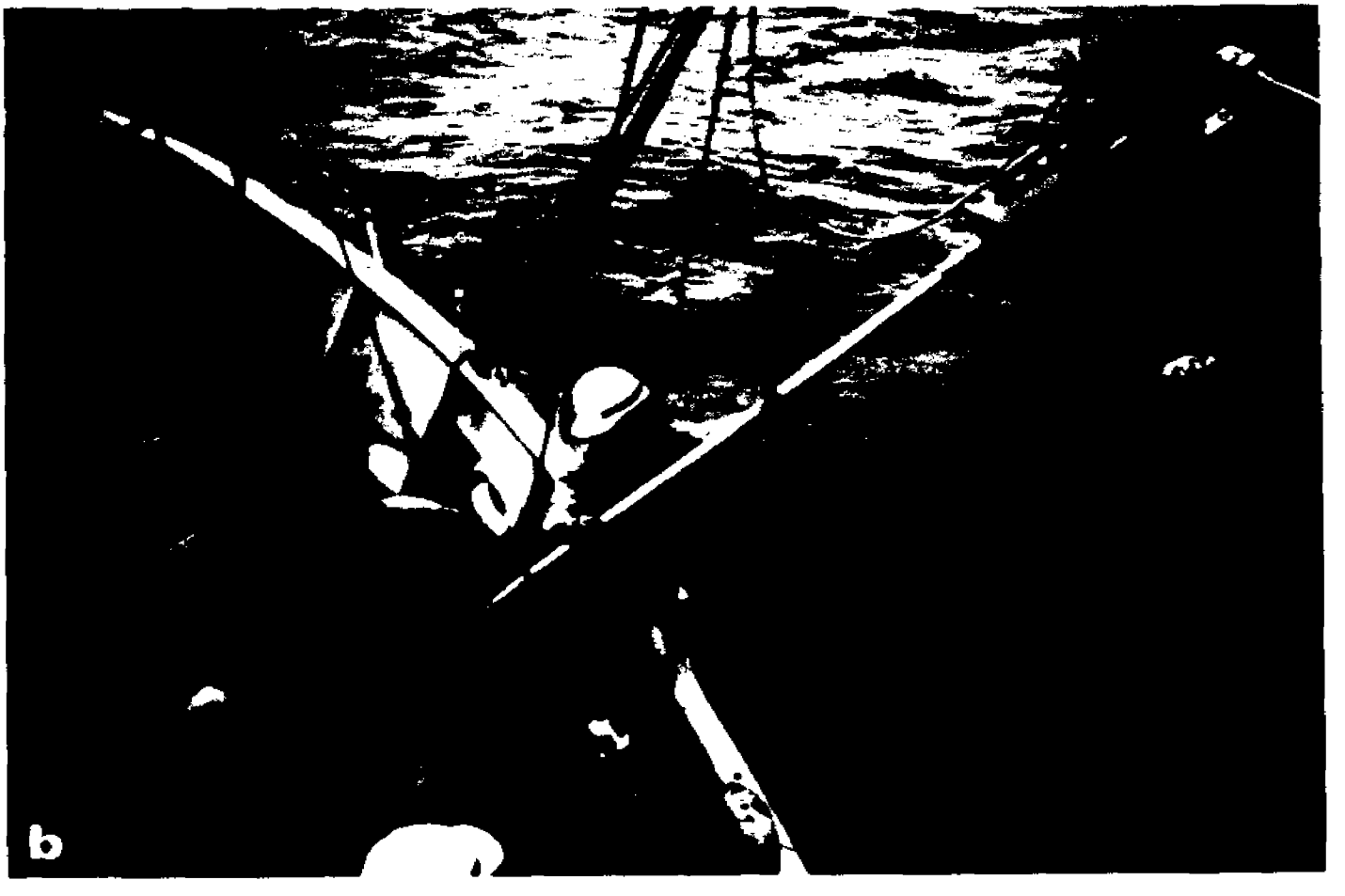
b

Size Analysis - A 12.5 cm inside-diameter settling tube utilizing a differential pressure transducer, carrier demodulator, and strip chart recorder were used to determine fall-velocity frequency distributions. The tube has a 140 cm effective fall length with a grain-size measuring range of -1Ø to 4Ø. Fall-velocity frequencies were converted to percent frequencies based on fall velocities of known quartz sand distributions.

The settling tube used in this study was built and calibrated by this author following the recommendations of Gibbs (1972). The calibration procedures were as follows: 1) pure, well sorted quartz sands ranging in size from -0.5Ø to 4.0Ø were carefully sieved at 1/4 Ø intervals; 2) ten repetitive 1 gram samples for each 1/4 Ø interval were introduced into the tube and allowed to settle; graphs of the fall times were recorded directly on a Perkin-Elmer recorder; 3) a template was prepared from the mean fall times; 4) a test sample was prepared by recombining weighed quantities of sediment from each of the 1/4 Ø size intervals; 5) ten repetitive 1 gram samples were introduced into the settling tube; 6) finally the grain-size distributions as determined by the settling tube were compared to the prepared test sample for precision.

The mean size of the sediment as determined by moments calculations for 10 settling tube frequency curves differed only by an average of $\pm$ 0.81% from the mean size of the prepared sample. The range of differences was found to be 0.43% to 1.07%. The reproducibility between the 10 runs was found to be better than $\pm$ 1%, ranging from 0.65% to 1.34%. As was found by Gibbs (1972)

a settling tube is a fast (up to 100 samples a day can be analyzed), accurate, and precise method for sizing sands.

For this study, a sample was split into two sub-samples and the average frequency distribution was used. It should be emphasized here that differences in mineralogical densities are taken into account because the settling tube measures hydraulic equivalences.

Variables - For this study, the variables are the relative frequencies of sediment from each sample which fall within specified size groups, which are at 0.5ø size intervals. These are the same variables used to compute the moment statistics, such as mean and standard deviation.

DATA ANALYSIS

Several multivariate methods were used in this study and include principal-components analysis, Q-mode factor analysis, and discriminant-function analysis, and are commonly cited in the geologic literature. These methods have been used in a wide variety of fields such as geochemistry, petrology, paleontology, and sedimentology. For excellent reviews of these methods see Imbrie (1963), Harbaugh and Merriam (1968), and Davis (1973). Suffice to mention the principal-components and Q-mode factor analyses are mathematical and statistical techniques that identify patterns of correlations in a data matrix. Using these techniques, the data are reduced to a small set of independent factors which account for a certain portion of the total variance in the original data matrix. Discriminant-function analysis mathematically determines the distance and percent overlap between multivariate normal populations as an indicator of separation of supposedly different populations.

By principal-components, which is an R-mode solution, it is possible to examine inter-relationships between the variables, in this case the grain-size fractions, and find the most efficient linear combination of the variables. Principal-components are the eigenvalues of the original data matrix. There are as many eigenvalues as there are variables, with each eigenvalue accounting for a certain proportion of the total variance. Normally the first

two or three components account for the greatest variance (Davis, 1973). Principal-components analysis was used in an effort to group grain-size classes into clusters that are correlated, which may aid in identifying major hydrodynamic processes operating within an environment.

Principal-components analysis follows three basic steps: 1) preparation of a product-moment correlation matrix; 2) extraction of initial factors; and 3) a varimax (orthogonal) rotation to a terminal solution (Nie, et al., 1970). The factors represent best fitted axes through clusters of data vectors in a hyperellipsoidal space. The first factor accounts for the most variability (the most prominent cluster), while factors 2, 3, ..., n represent the best fitted axes through the residual clusters. Although the axes are orthogonal, the variables they represent are not necessarily independent in nature making subsequent results sometimes difficult to interpret. In other words, a variable can be related to more than one factor axis. However, principal-components analysis is a useful technique in the absence of a hypothesis to account for the observed variations in the measured parameters.

Factor analysis is somewhat different from principal-components analysis. Although factor analysis can be carried out in the R-mode it is generally a Q-mode solution, which shows relationships between samples. Factor analysis is commonly regarded as a statistical technique rather than a mathematical principal-components analysis (Davis, 1973). Q-mode factor analysis was used

in this study to group the samples into similar textural suites that should represent different sedimentary environments. Q-mode factor analysis follows the same steps as principal-components except that in step one a cosine theta matrix is prepared, which measures the angles of the vectors projected into the data point clusters. This matrix shows better relations between samples as the variance is calculated across the variables (Davis, 1973). Unlike principal-components, Q-mode factor analysis requires some a priori knowledge about the structure of the data on the part of the investigator. This means that in the factor model, the significant number of factors p, must be known prior to the analysis. Other differences between principal-components and Q-mode factor analysis can be found in Davis (1973). Like principal-components analysis, the number of factors retained in Q-mode factor analysis is small, since only a few factors contain most of the variance. Some analysts only retain the factors which have eigenvalues ≥ 1, that is, only those factors which have variance greater than or equal to the variance of the original standardized variables are retained (Davis, 1973). The initial and rotated factor axes in Q-mode factor analysis are orthogonal to each other and a sample can be related to more than one factor. This is to be expected as sharp boundaries between adjacent environments are very rare indeed.

Discriminant-function analysis is a technique which finds the best linear combination of the variables which provides the maximum difference between the previously defined groups. To avoid cyclic arguments, the variables used in the analysis cannot include those

criteria used for the initial assumption of differences between the groups to be discriminated (Krumbein and Graybill, 1965; Morrison, 1967; and Davis, 1973). Discriminant-function analysis consists of finding a transform which gives the minimum ratio of differences between the multivariate means to the multivariate variance within the groups in question, which transforms the original data into a single discriminate score. This score represents the samples location along a line defined by the discriminant-function equation. This analysis follows six basic steps: 1) it finds row vector means of the groups; 2) it finds the differences in the row vector means; 3) it calculates the corrected sums of square for each group matrix; 4) the pooled variance-covariance matrix of the two groups is calculated, 5) the variance-covariance matrix is inverted; finally 6) step 2 is multiplied by step 5 to find the discriminant coefficients. The distance between the groups is the Mahalanobis D^2, which is expressed in terms of the pooled variance. This value can be tested for significance by substituting it for $[S]^{-1}$, the variance-covariance matrix, in the Hotelling T^2 statistic (Morrison, 1967; Davis, 1973); which has the following form:

$$T^2 = \frac{N_1 N_2}{N_1 + N_2} D^2$$

where N_1 is the number of samples in group 1 and N_2 is the number of samples in group 2. This converts a multivariate problem into univariate terms which can be tested using the F-statistic by

substituting T^2 into the following equation:

$$F = \frac{N_1 + N_2 - M - 1}{(N_1 + N_2 - 2)M} T^2$$

where the N's have the same meaning as above and M equals the number of variables. The value of F is tested for significance as an F with the following degrees of freedom:

$$F_{(1 - \alpha);\ M,\ N_1 + N_2 - 2 - 1}$$

Tests of significance for principal-components and factor analysis are available, however they are generally not used because of the difficulty in checking assumptions of multivariate normality and equality of the matrix structure (Morrison, 1967). Non-normality and inequality of the matrices does not seem to greatly affect the results of discriminant-function analysis as this procedure is robust to the above deviations, therefore the F-test can be used with certain confidence (Rothman, personal communication, 1975).

The computer programs used in this study were obtained from several sources. The principal-component program is from Nie, et al. (1970), the Q-mode factor program is from Davis (1973) and the discriminant-function program is from the UCLA, Biomedical Package, 1972.

INFORMATION CONTAINED IN GRAIN-SIZE FREQUENCY DISTRIBUTIONS

Introduction

The nature of the data used in the multivariate tests requires some explanation that will help place the results in perspective. The data are expressed as frequency percentages, and as percentages, the data form a closed array (the sum of the rows equal 100%) (Chayes, 1960, 1962; Krumbein and Graybill, 1965; Davis, 1973). This constant sum raises troublesome theoretical questions concerned with induced negative correlations in the principal-components analysis. The correlation matrix calculated from a closed data matrix is overdetermined; that is, it has more rows and columns than necessary, and some of these correlations are formed by the closed table and not true relationships in the data. For example, if A, B and C are known and if the total is fixed, then there is more information than is needed, because A and B determine the value of C. In correlation related analysis each variable can be represented by an eigenvalue and eigenvector with magnitude equivalent to the variability in the original data array. Therefore, if one of the variables is determined by constant summation, then one of the eigenvalues and corresponding eigenvector of the matrix will be zero and spurious correlations are formed (Davis 1973). Even though the variables constitute a closed array in principal-

components analysis, the array is not closed in Q-mode factor analysis. Real negative correlations can occur in an open or closed array and show real inverse relationships between the variables (Davis, 1973).

In order to avoid an overdetermined correlation matrix, closure can be prevented by excluding either A, B, or C from the original data matrix before the analysis is performed. For this study, one variable (the percentage of sediment within a size class interval) was eliminated to open the data array. For the Little Sable Point aeolian, bar and trough, and fluvial samples the 0 Ø variable was eliminated. This variable never accounted for more than 2% of the total sample and material in this size class was present in only 12 of 65 samples. The 3Ø variable was eliminated from the beach samples because more sediment was present in the 0 Ø size interval. Only 7 of the 29 beach samples had sediment in the 3Ø size class and represented less than 3% of the total sample. Even though many of the samples still sum to 100%, 19 samples do not and theoretically this should constitute an open data matrix (Huang and Rothman, personal communication, 1975). Also, if approximately 6 or more variables are used in a closed array, the effect of closure on induced negative correlation is reduced (Chayes, 1960, 1962; Krumbein and Graybill, 1965).

Nine test cases were prepared to evaluate the effect of closure on a closed data array using principal-components analysis (Fig. 6). These test cases represent a true, log-normal, sediment

Figure 6: Phi-probability graph of 4 of the 9 test cases used to determine the effect of closure on correlation coefficients

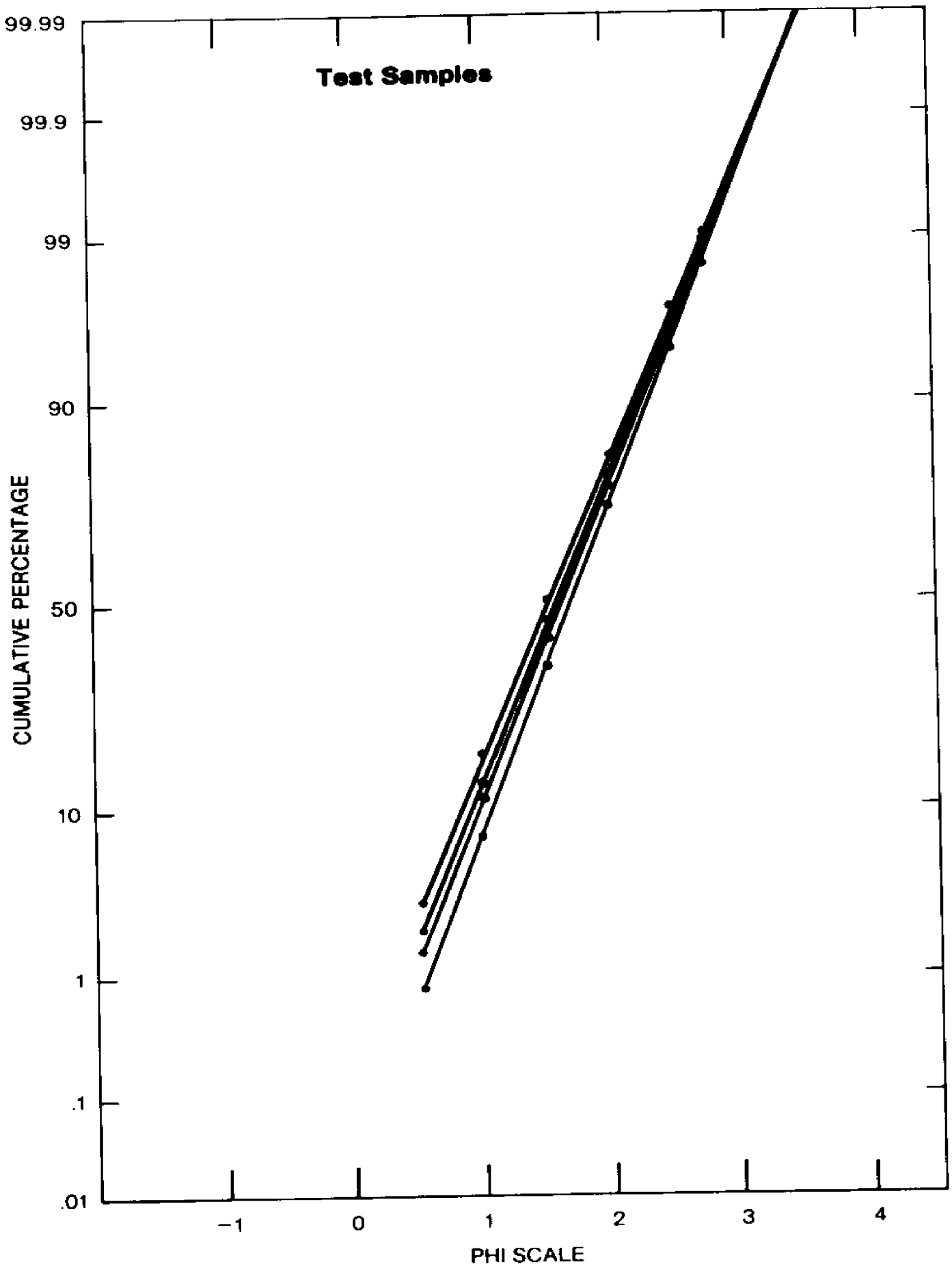
Test Samples
99.99
99.9
99
90
50
10
1
.1
.01
CUMULATIVE PERCENTAGE
−1
0
1
2
3
4
PHI SCALE

distribution similar to several aeolian samples collected at the Silver Lake State Park sand dunes. The variables used are percentages of the theoretical distributions in each 0.5Ø size interval from 0.5Ø to 2.5Ø. Examination of the correlation matrix (Table 1) shows that four significant negative correlations were formed; in a closed (3x3) matrix at least two negative correlations are induced (Chayes, 1960, 1962). Significance cannot be attached to these negative correlations because in a closed matrix the null hypothesis, $\rho = 0$, may be misleading (Chayes, 1960, 1962). The factor matrix (Table 1) shows that only one factor was extracted and accounts for 76.4% of the total variance. All the loading values (the degree to which a variable is associated with a factor) are very high, with variables 2.0Ø and 2.5Ø showing high-negative loading values.

An interesting comparison can be made between these test samples and factor III of Allen, et al. (1971). Their factor III represents the intermediate sand sizes from 0.6Ø to 3.0Ø, which is a similar size range of the test samples in this study. They divided this factor into two sub-groups on the basis of the signs of the factor loadings, hence one group is associated with size 3.0Ø to 2.0Ø (negative loading values), while the other group is represented by sizes 2.0Ø to 0.6Ø (positive loading values). These groups were interpreted to represent non-uniform suspension and saltation processes, respectively. Returning to Table 1, it is evident that these groups are present in the test samples and the loading value signs are also the same for each group. Allen, et al. (1971) did

TABLE 1

PRINCIPAL COMPONENTS RESULTS OF TEST CASES

Summary Statistics

Phi Size	0.5	1.0	1.5	2.0	2.5
Grand Means	0.01	2.2	43.5	50.4	3.6
Grand Standards Deviations	0.00	0.6	2.4	3.0	0.5

Product-Moment Correlation Matrix

Phi Size	0.5	1.0	1.5	2.0	2.5
0.5	1.00	.78*	.78*	-.63*	
1.0		1.00	.83**	0.84**	
1.5			1.00	-.93**	
2.0				1.00	-.68*
2.5					1.000

significant at $\alpha = 0.05$*, $\alpha = 0.01$**, n = 9, df = 7

Factor	Eigenvalue	Cumulative Percent of Eigenvalue
I	3.82	76.4

Rotated Factor Matrix

Phi Size	I
0.5	0.810
1.0	0.931
1.5	0.957
2.0	-0.932
2.5	-0.712

not take into account the effect of closure, therefore their interpretation may be erroneous. Bagnold (1966) noted that a change in sediment process occurs at approximately 2Ø. With the exception of the negative factor loadings it appears that, even when closure is present, the factors identified in principal-components analysis are insensitive to closure and are valid if caution is used in their interpretation. With the problem of closure and induced negative correlations identified the results of this study will be presented.

Little Sable Point Depositional Area

Statistical Analysis - The sediment collected for this study comes from an area with essentially one source or parent material (Upchurch, 1970b) and any differences in the size frequency distributions from offshore bars to beach, to aeolian, to fluvial environments should reflect changes in the processes operating in those environments. If the sediment from these environments are derived from one major source, the size distributions should be relatively constant through time and space due to the limitations imposed by the parent distribution. Student's-t and Chi-square (χ^2) tests were used to test for differences between the June and October sample sets.

Students-t test was used because the true population mean and variance are not known but are estimated from the collected samples. An amount of uncertainty is associated with these estimates, so decisions based upon them cannot be as precise as those based on

the Z test. When the number of samples are infinite, the t-distribution is equal to the Z or normal distribution (Davis, 1973). Three assumptions are necessary to perform this test (Davis, 1973). One is that the samples were collected randomly; which is so for this study. The second is that the samples are normally distributed. The Rankits method of testing for normality (Sokol and Rohlf, 1969) was used because the sample means have an apparent bimodal or slightly skewed distribution. This method allows somewhat for non-normality in the data. Figures 7 and 8 show a plot of Rankit values versus the ranked mean phi size of each sample for the October and June sampling periods. Although the observed distribution deviates from the normal Rankits distribution, the deviation is not a significant at $\alpha = 0.001$ as calculated by Chi-square. The third and most critical assumption is the equality of the grand variances of the June and October sample sets. The critical value of F between the two grand sample variances is 1.16 and is not significant at $\alpha = 0.05$. Therefore, there is no reason to suggest a difference in the grand sample variances. Having established the validity of the three basic assumptions, the Students-t test can be used to test for differences between the grand phi-size means of the June and October sample sets. The calculated value of t is 1.39, with 92 degrees of freedom. This value of t does not fall into the rejection region ($\alpha = 0.05$), and it must be concluded that there is no reason to suggest that the two sample sets came from populations with different grand means.

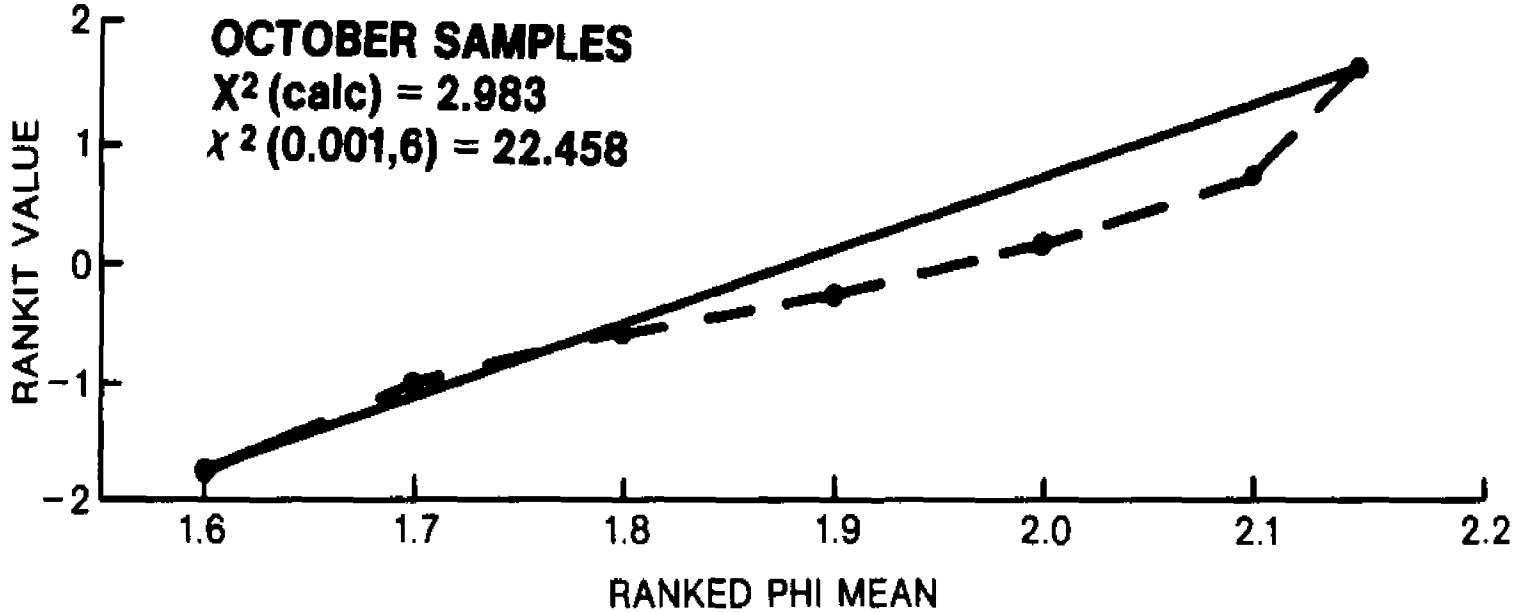

Figure 7: Rankit graph of the October 1972 sample set collected at Little Sable Point. Solid line is the Rankit normal curve, dashed line is the observed curve

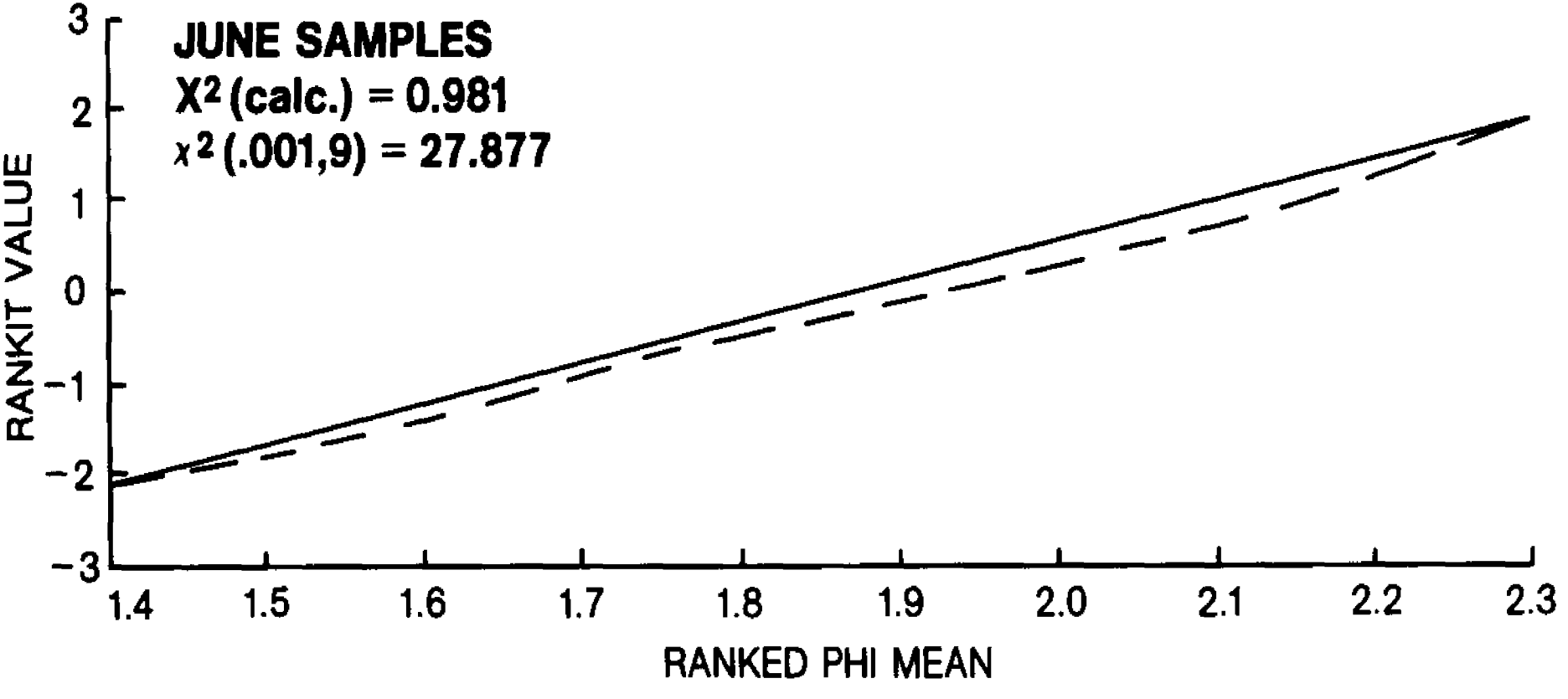

Figure 8: Rankit graph of the June 1973 sample set collected at Little Sable Point. Solid line represents the Rankit normal curve, dashed line is the observed curve

Chi-square was used to test for significant differences in the grand frequency distributions of the June and October sample sets. The calculated χ^2 value is 3.33, with six degrees of freedom is not significant at $\alpha = 0.05$. This suggests that there is no reason to assume that the two sample sets came from populations with different frequency distributions.

Results of these tests lend strong support to the previous assumption that one sediment source, or at least a very limited range in sizes, it available to the study area. Since these samples come from a limited parent population, it is possible to study textural responses to differing energy conditions in the various environments while discounting variability imposed by sediment introduced from multiple sources.

Principal-Components Analysis

Principal-components analysis was used to determine size limits and relationships between the sub-populations (e.g., those deposited by surface creep, saltation, and suspension) presumed to constitute the sediment (Visher, 1969). A uniform suspension population is not expected to be present in the Little Sable Point samples, because the sediment is truncated at approximately 3ø. The size limits represented by each factor will be compared to the same sub-populations plotted as cumulative probability curves after the method of Visher (1969). Although Visher (1969) studied sediment from a number of environments, the Little Point environments

do not appear to be directly analogous. This is largely due to the fact that Visher collected samples over a wide geographical area that represents many source types.

All Little Sable Point Samples - Table 2 lists the results of the principal-components analysis of all the Little Sable Point samples. The product-moment correlation matrix shows the intercorrelation among the variables that are significant at $\alpha = 0.05$ and 0.01. Two factors with eigenvalues >1 were extracted by principal-components analysis and account for 74.1% of the total variance. The values listed in the rotated factor matrix are loading values which show how each variable is associated with the extracted factors. The closer a factor loading approaches unity, the better the variable is explained. Communalities are the cumulative sums of squares of the factor loading in a row wise manner. The communalities indicate how well the factors with eigenvalues >1, describe the variables; as communalities approach unity the better the explanation.

Figure 9 is a cumulative probability plot of the grand means for each size class for all the Little Sable Point samples. Based on the segmentation of the line, three sub-populations are indicated on this graph: 1) sub-population A between 0.5Ø and 1.05Ø; 2) sub-population B between 1.05Ø and 2.5Ø; and 3) sub-population C finer than 2.5Ø. These sub-populations correspond with those identified by principal-components analysis.

TABLE 2

PRINCIPAL-COMPONENTS RESULTS OF ALL LITTLE SABLE POINT SAMPLES

	Summary Statistics					
Phi Size	0.5	1.0	1.5	2.0	2.5	3.0
Grand Means	0.6	3.6	23.3	52.8	17.2	2.2
Grand Standard Deviations	0.7	4.6	19.2	14.2	13.0	3.2

	Product-Moment Correlation Matrix					
Phi Size	0.5	1.0	1.5	2.0	2.5	3.0
0.5	1.00	.23*				
1.0		1.00	.56**	-.64**	0.44**	-.28**
1.5			1.00	-.67**	-.80**	-.55**
2.0				1.00		
2.5					1.00	.79**
3.0						1.00

significant at $\alpha = 0.05$*, $\alpha = 0.01$**, n = 94, df = 92

Factor	Eigenvalues	Cumulative Percentage of Eigenvalues
I	2.995	49.9
II	1.451	74.1

	Rotated Factor Matrix		Communalities
	I	II	
Phi Size			
0.5	-0.900	0.388	0.159
1.0	0.395	0.758	0.731
1.5	0.765	0.541	0.880
2.0	-0.086	-0.934	0.881
2.5	-0.956	-0.103	0.925
3.0	-0.918	0.158	0.869

Figure 9: Phi-probability graph of the grand frequency distribution of all Little Sable Point samples

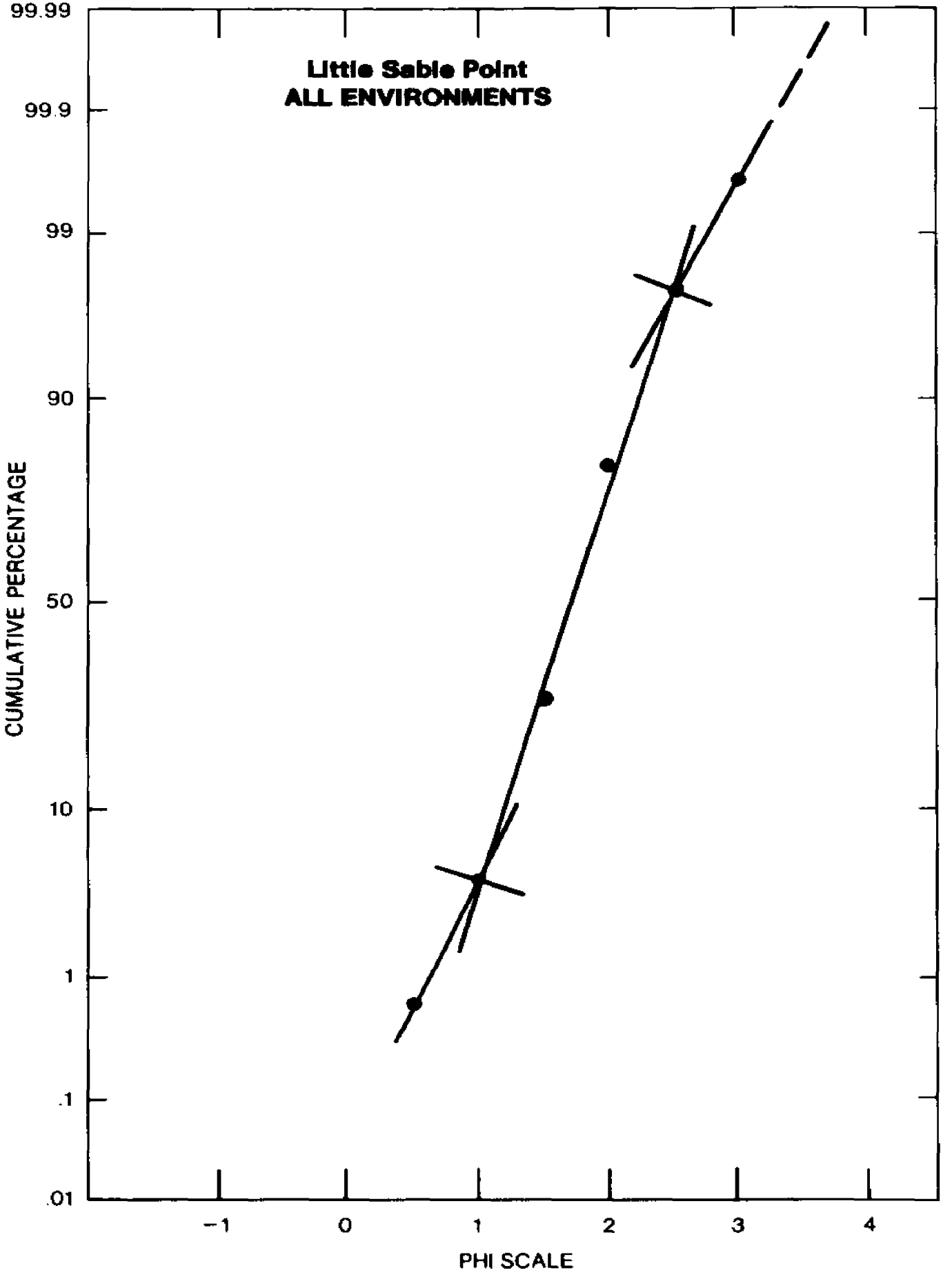
Little Sable Point
ALL ENVIRONMENTS
99.99
99.9
99
90
50
10
1
.1
.01
CUMULATIVE PERCENTAGE
−1
0
1
2
3
4
PHI SCALE

Factor I accounts for 49.9% of the total variance. This factor is associated with sizes finer than 2Ø, which have high negative loadings; and with the 1.5Ø size interval, which has a fairly high positive loading value. The other variables have negligible loadings values on factor I. Sub-population C on the probability graph accounts for 2.5% of the distribution and corresponds well with the 2.5Ø and 3.0Ø intervals of factor I.

Factor II accounts for 24.2% of the total variance. This factor is associated with sizes 2Ø and coarser. The 1.5Ø size class loads on both factors I and II, but only moderately high on factor II. The loading value of the 2.0Ø size class is highly negative. The 2.5Ø and 3.0Ø size class have negligible loading values on factor II. Except for the 0.5Ø size interval the communalities are high to very high and the two factors explain the data well. Sub-populations A and B of the probability graph account for 97.5% of the distribution and generally corresponds to factor II and the 1.5Ø interval of factor I.

It is important to note in principal-components analysis that a given grain-size interval can be affected by more than one factor, in this case the 1.5Ø interval, and a unique solution is not always possible. Although the factor axes are orthogonal the variables they represent are not entirely independent as is shown in the correlation matrix.

Sub-population A on Figure 9 would probably be interpreted by Visher (1969) as a surface creep transport mechanism, and sub-population B and C as a saltation transport mechanism. The high correlations

show that the transport mechanisms surface creep and saltation may not be entirely independent in a hydraulic sense. Therefore, size intervals loading on more than one factor can be expected. In principal-components analysis a break in the distribution is suggested as approximately 2Ø, at the change in sign of the loading values. This break is the size at which Bagnold (1966) noted a change between the bedload and non-uniform suspension-transport mechanisms. On this basis, the sediment approximately 2Ø and finer is interpreted as a non-uniform suspension, while the sediment coarser than 2Ø probably represents the surface creep and saltation transport mechanisms.

Beach Samples - The source beach samples and the beach samples collected on Lake Michigan west of Silver Lake State Park (Fig. 2) can be considered as a single, beach subsample for the following reason. The calculated χ^2 between the grand frequency distributions of the two samples (source beach and Lake Michigan beach) is 10.83 and is distributed approximately as χ^2_6 which is not significant at $\alpha = 0.05$. This suggests that the frequency distributions of the two samples are not different.

Table 3 lists the results of the principal-components analysis for the beach samples. Two factors with eigenvalues >1 were extracted and account for 75.4% of the total variance. The communalities are moderately high to very high. Variables with correlations significant at $\alpha = 0.01$ are also listed.

Figure 10 is a cumulative probability graph of the grand means of each size class for the beach subsamples. Two

TABLE 3

PRINCIPAL-COMPONENTS RESULTS OF LITTLE SABLE POINT BEACH SAMPLES

	Summary Statistics					
Phi Size	0.0	0.5	1.0	1.5	2.0	2.5
Grand Means	0.6	0.6	6.4	35.3	49.5	7.3
Grand Standard Deviations	1.0	0.8	7.2	16.4	17.7	6.6

	Product-Moment Correlation Matrix					
Phi Size	0.0	0.5	1.0	1.5	2.0	2.5
0.0	1.00					
0.5		1.00	.48**			
1.0			1.00	.68**	-.87**	-.48**
1.5				1.00	-.91**	-.77**
2.0					1.00	.54**
2.5						1.00

significant at $\alpha = 0.01$**, n = 29, df = 27

Factor	Eigenvalues	Cumulative Percentage of Eigenvalues
I	3.308	55.1
II	1.212	75.4

	Rotated Factor Matrix		Communalities
	I	II	
Phi Size			
0.0	-0.042	0.837	0.702
0.5	0.274	0.745	0.631
1.0	0.846	0.237	0.772
1.5	0.956	-0.042	0.917
2.0	-0.950	-0.059	0.907
2.5	-0.740	-0.201	0.589

Figure 10: Phi-probability graph of the grand frequency distribution of the Little Sable Point beach samples

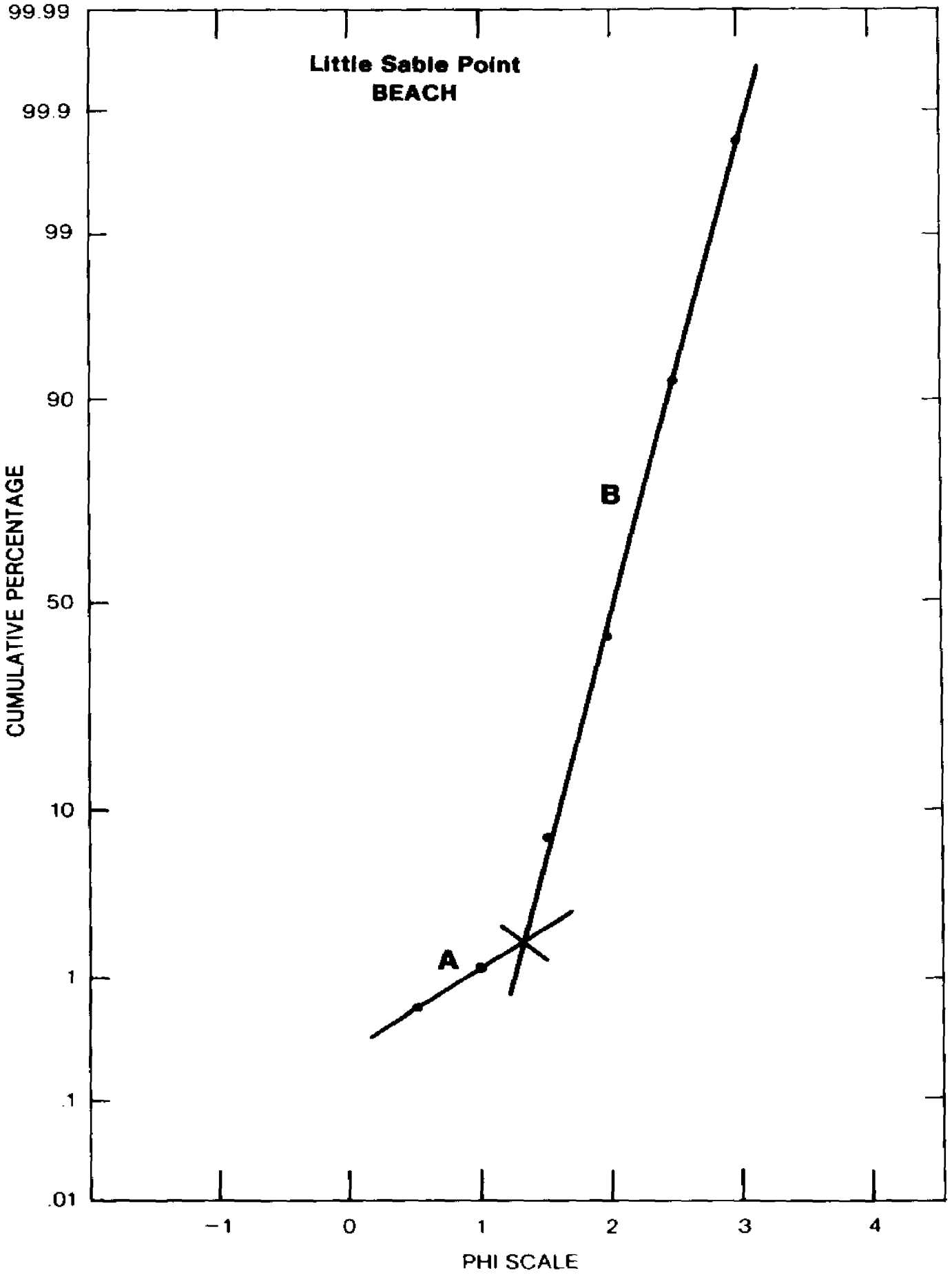
Little Sable Point
BEACH
99.99
99.9
99
90
50
10
1
.1
.01
CUMULATIVE PERCENTAGE
A
B
−1
0
1
2
3
4
PHI SCALE

sub-populations are indicated in this plot: 1) sub-population A coarser than 1.3Ø; and 2) sub-population B finer than 1.3Ø.

Factor I accounts for 55.1% of the total variance and is associated with sizes finer than 1.0Ø. Size 1.5Ø and 2.0Ø have high positive loading values, while the 2.5Ø and 3.0Ø have high negative loading values. Sub-population B which is indicated on the probability graph accounts for 98% of the distribution and corresponds very well with factor I.

Factor II has high positive loading values associated with 0.5Ø and 1.0Ø. This factor accounts for 19.3% of the total variance. The other size classes have very low loading values and are not associated with this factor. Factor II corresponds well with sub-population A on the probability graph which accounts for 2% of the distribution.

Offshore bar and trough samples - Table 4 lists the results of the principal-components analysis for the offshore bar and trough samples. Two factors with eigenvalues >1 were extracted and account for 71.9% of the total variance. Variables with correlations significant at $\alpha = 0.01$ are listed. The communalities are very high, except for the 0.5Ø and 1.0Ø size classes.

Figure 11 is a cumulative probability graph of the grand means of each size class for the bar and trough samples. The distribution is almost log-normal, however two sub-populations are indicated: 1) sub-population A coarser than 1.1Ø; and 2) sub-population B finer than 1.1Ø.

TABLE 4

PRINCIPAL-COMPONENTS RESULTS OF LITTLE SABLE POINT BAR AND TROUGH SAMPLES

	Summary Statistics					
Phi Size	0.5	1.0	1.5	2.0	2.5	3.0
Grand Means	0.4	3.3	25.8	34.4	15.2	1.2
Grand Standard Deviations	0.5	2.7	20.1	16.6	10.2	1.4

	Product-Moment Correlation Matrix					
Phi Size	0.5	1.0	1.5	2.0	2.5	3.0
0.5	1.00					
1.0		1.00				
1.5			1.00	-.82**	-.60**	
2.0				1.00		
2.5					1.00	.88**
3.0						1.00

significant at $\alpha = 0.01$**, n = 18, df = 16

Factor	Eigenvalues	Cumulative Percentage of Eigenvalues
I	2.706	45.1
II	1.608	71.9

	Rotated Factor Matrix		Communalities
	I	II	
Phi Size			
0.5	-0.489	-0.007	0.240
1.0	0.367	0.500	0.386
1.5	0.308	0.907	0.918
2.0	0.252	-0.958	0.981
2.5	-0.920	-0.312	0.944
3.0	-0.918	0.033	0.844

Figure 11: Phi-probability graph of the grand frequency distribution of the Little Sable Point bar and trough samples

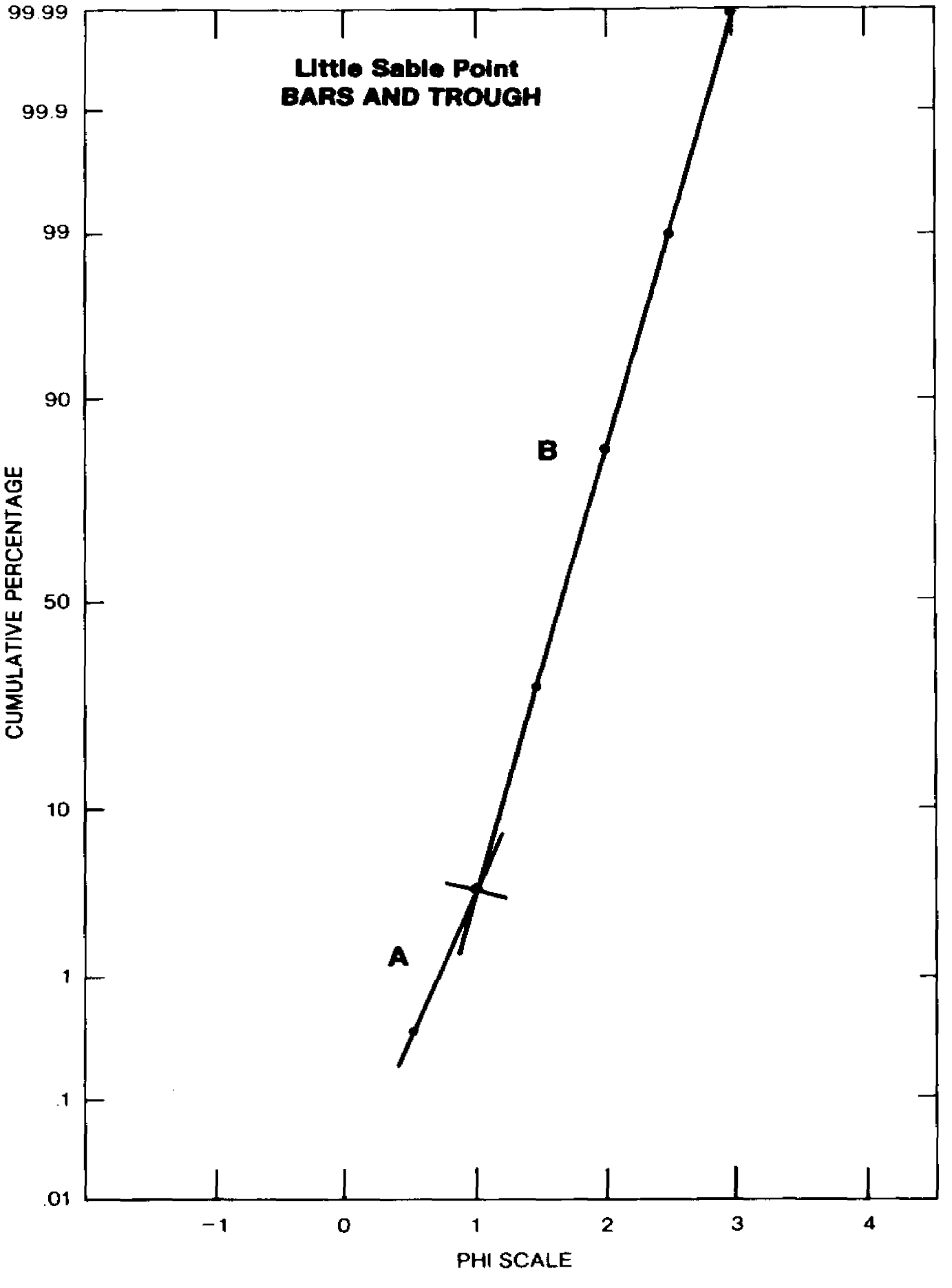
Little Sable Point
BARS AND TROUGH
99.99
99.9
99
90
50
10
1
.1
.01
CUMULATIVE PERCENTAGE
A
B
−1
0
1
2
3
4
PHI SCALE

Factor I is associated with sizes finer than 2.0Ø (high negative loading values) and is moderately associated with 0.5Ø. This factor accounts for 45.1% of the sample variance. The other size intervals have small loading values on this factor.

Factor II, which accounts for 26.8% of the total variance, is associated with sizes finer than 0.5Ø and coarser than 2.5Ø. The 1.0Ø and 1.5Ø size class have moderate to very high positive loading values, while the 2.0Ø size class has a high negative value. The other size classes have small loading values on this factor. The factor axes do not correlate very well with the sub-populations on the probability graph. Sub-population A accounts for 4% of the distribution, while sub-population B accounts for 96% of the distribution.

Silver Creek bed samples - Table 5 lists the results of the principal-components analysis of the Silver Creek samples. Variables with correlations significant at $\alpha = 0.01$ are listed in this table. Two factors with eigenvalues >1 were extracted and account for 81.5% of the total variance. Communalities are high to very high.

Three sub-populations are indicated on the cumulative probability graph (Fig. 12): 1) sub-population A with sizes finer than 1.25Ø; 2) sub-population B with sizes between 1.25Ø and 2.5Ø; and 3) sub-population C with sizes finer than 2.5Ø.

Factor I accounts for 59.8% of the total variance and is related to sizes finer than 0.5Ø. The sizes 1.0Ø and 1.5Ø have high positive loading values, while those finer than 1.5Ø have high

TABLE 5

PRINCIPAL-COMPONENTS RESULTS OF LITTLE SABLE POINT SILVER CREEK BED SAMPLES

	Summary Statistics					
Phi Size	0.5	1.0	1.5	2.0	2.5	3.0
Grand Means	0.7	2.5	19.1	57.3	18.6	1.4
Grand Standard Deviations	0.7	1.3	17.9	9.7	12.2	1.4

	Product-Moment Correlation Matrix					
Phi Size	0.5	1.0	1.5	2.0	2.5	3.0
0.5	1.00					
1.0		1.00	.75**	-.68**	-.61**	-.53**
1.5			1.00	-.75**	-.88**	-.74**
2.0				1.00		
2.5					1.00	.77**
3.0						1.00

significant at $\alpha = 0.01$**, n + 22, df = 20

Factor	Eigenvalues	Cumulative Percentage OF Eigenvalues
I	3.589	59.9
**	1.300	81.5

	Rotated Factor Matrix		Communalities
	I	II	
Phi Size			
0.5	-0.089	0.875	0.775
1.0	0.835	0.201	0.737
1.5	0.975	0.069	0.956
2.0	-0.705	-0.548	0.798
2.5	-0.875	0.236	0.822
3.0	-0.816	0.362	0.799

Figure 12: Phi-probability graph of the grand frequency distribution of the Little Sable Point Silver Creek bed samples

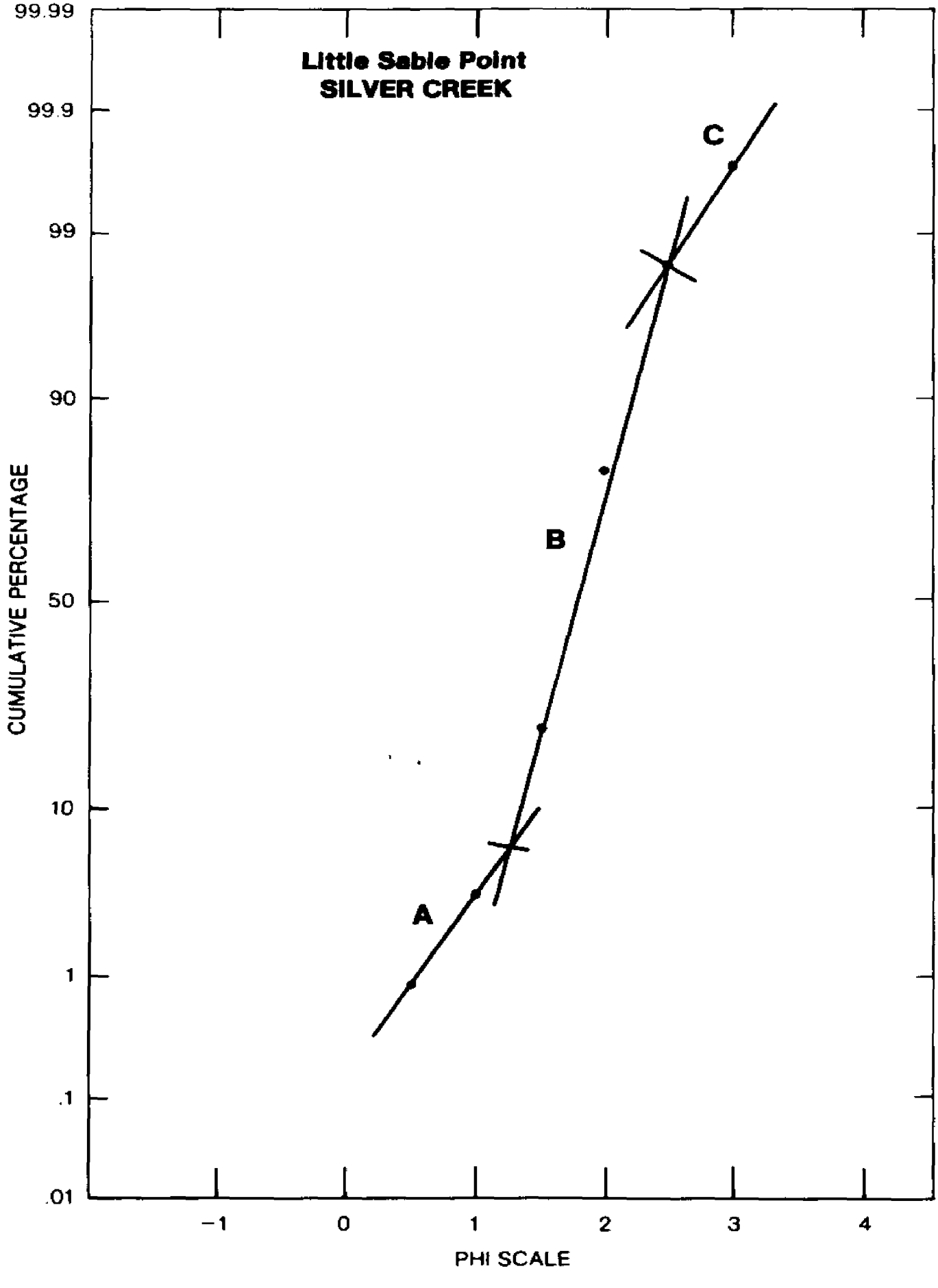
Little Sable Point
SILVER CREEK
99.99
99.9
99
90
50
10
1
.1
.01
CUMULATIVE PERCENTAGE
A
B
C
−1
0
1
2
3
4
PHI SCALE

negative values. This factor correlates well with the sub-populations B and C defined on the probability graph, with sub-population B corresponding to the sizes with positive loading values, and C corresponding to the size classes with negative loading values. Sub-populations B and C on the probability graph account for 95% of the total distribution.

Factor II is related to the 0.5Ø size class and accounts for 20.7% of the total variance. The 2.0Ø size class is moderately related to this factor. This factor correlates to sub-population A on the probability graph, which accounts for only 5% of the total distribution.

Aeolian samples - Table 6 lists the principal-components results for the aeolian samples. Variables significantly correlated at α = 0.05 and 0.01 are listed. Three factors with eigenvalues >1 were extracted and account for 83.1% of the total variance. Communalities are moderately high to very high.

Figure 13 is a cumulative probability graph of the grand frequency distribution of the aeolian samples. The graph shows the presence of two sub-populations: 1) sub-population A with sizes coarser than 1.25Ø; and 2) sub-population B with sizes finer than 1.25Ø.

Factor I accounts for 42% of the total variance and is related to the 1.5, 2.5, and 3.0Ø size classes. The sizes 2.5Ø and finer have high negative loading values, while 1.5Ø has a high positive loading value.

TABLE 6

PRINCIPAL-COMPONENTS RESULTS OF LITTLE SABLE POINT AEOLIAN SAMPLES

	Summary Statistics					
Phi Size	0.5	1.0	1.5	2.0	2.5	3.0
Grand Means	0.6	1.5	11.4	51.4	28.8	5.7
Grand Standard Deviations	0.8	1.2	14.3	10.1	11.6	4.0

	Product-Moment Correlation Matrix					
Phi Size	0.5	1.0	1.5	2.0	2.5	3.0
0.5	1.00					
1.0		1.00				
1.5			1.00		-.73**	-.55**
2.0				1.00		-.48**
2.5					1.00	.80**
3.0						1.00

significant at $\alpha = 0.05$*, $\alpha = 0.01$**, n = 26, df = 24

Factor	Eigenvalues	Cumulative Percentage of Eigenvalues
I	2.519	42.0
II	1.450	66.2
III	1.013	83.1

	Rotated Factor Matrix			Communalities
	I	II	III	
Phi Size				
0.5	0.106	0.298	0.736	0.642
1.0	-0.013	-0.462	0.688	0.687
1.5	0.885	-0.423	-0.056	0.967
2.0	0.127	0.937	0.053	0.897
2.5	-0.937	-0.211	-0.071	0.927
3.0	-0.843	-0.360	-0.143	0.861

Figure 13: Phi-probability graph of the grand frequency distribution of the Little Sable Point aeolian samples

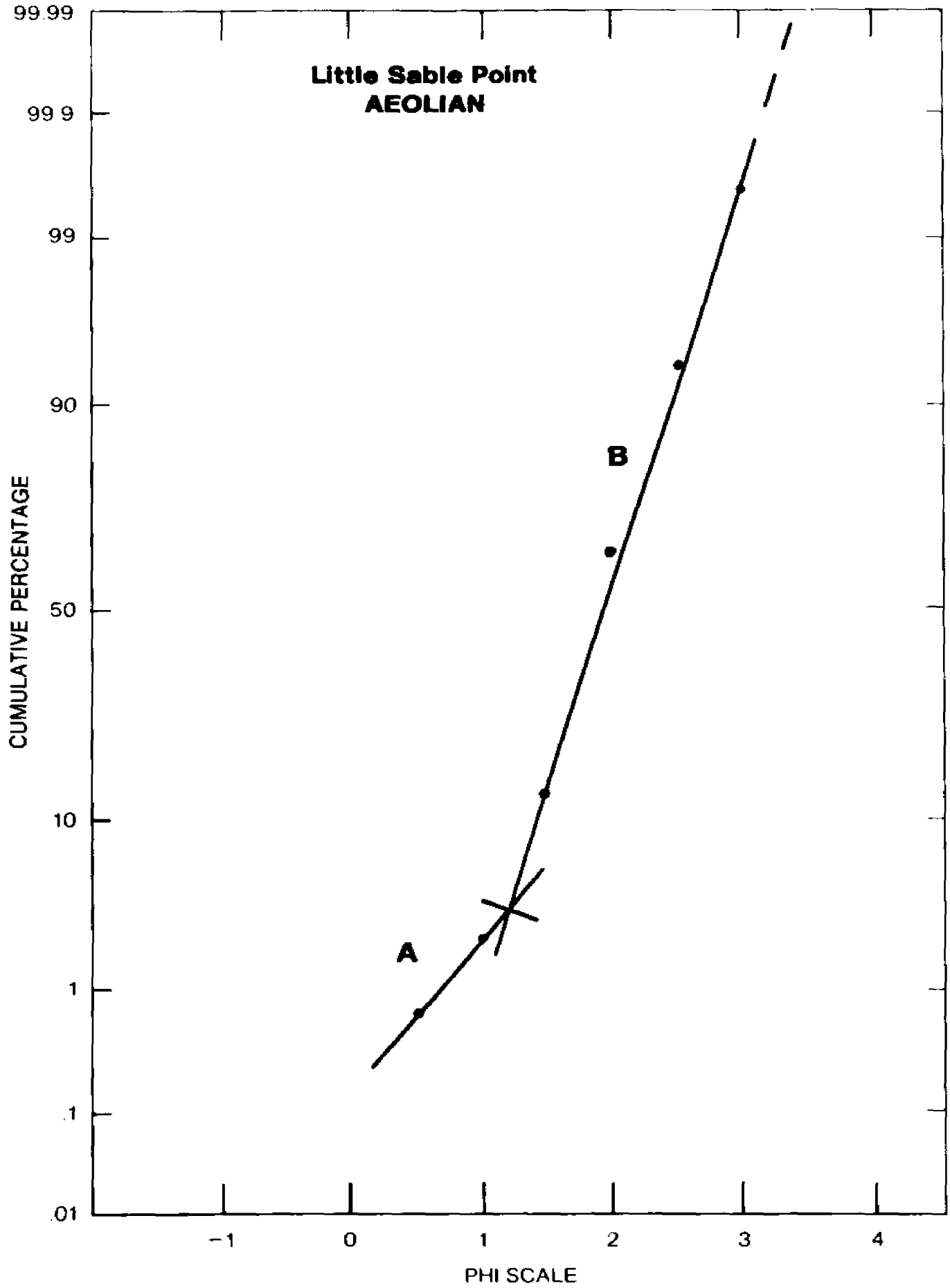
Little Sable Point
AEOLIAN
99.99
99.9
99
90
50
10
1
.1
.01
CUMULATIVE PERCENTAGE
A
B
−1
0
1
2
3
4
PHI SCALE

Factor II is related to the 2.0Ø size class and accounts for 24.4% of the total variance, with a high positive loading value. Sub-population B of the probability graph accounts for 96% of the total distribution and correlates very well with factors I and II.

Factor III accounts for 16.9% of the total variance and is associated with sizes coarser than 1.5Ø. This factor correlates well with sub-population A on the probability graph, which accounts for only 5% of the total distribution.

Discussion of the Principal-Components Analysis and Probability Graphs of the Little Sable Point Samples

Assignment of the sediment sub-populations identified in this study, on the basis of principal-components analysis and cumulative probability graphs, to distinct hydrodynamic sedimentary processes follows the results of earlier workers (e.g., Bagnold, 1966; Visher, 1969; and Allen et al. 1971).

An important feature to notice on the probability graph is that the size frequency distribution can be divided into two or more log-linear sub-populations (Visher, 1969) and that each sub-population can be correlated in most cases (bar and trough samples are an exception) to one or two principal axes. These axes are orthogonal, hence statistically independent, therefore each sub-population may reflect a different transportational/depositional history (Allen et al.,1971).

Figure 14 illustrates factor loading profiles for each environment. These graphs show the relationship of each size class

Figure 14: Loading profiles of each Little Sable Point environment

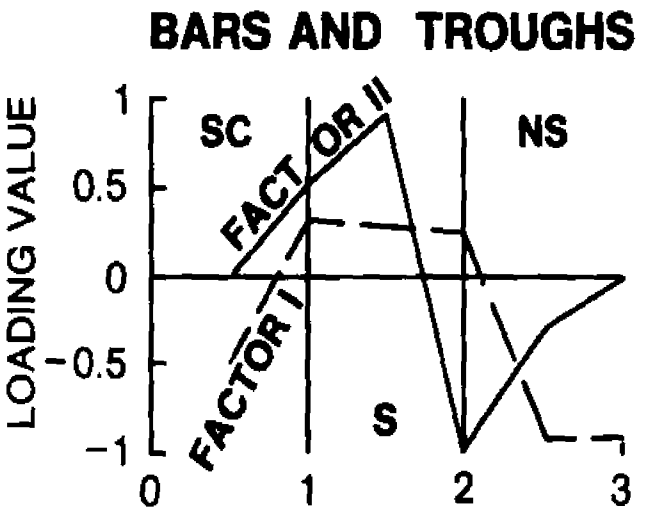

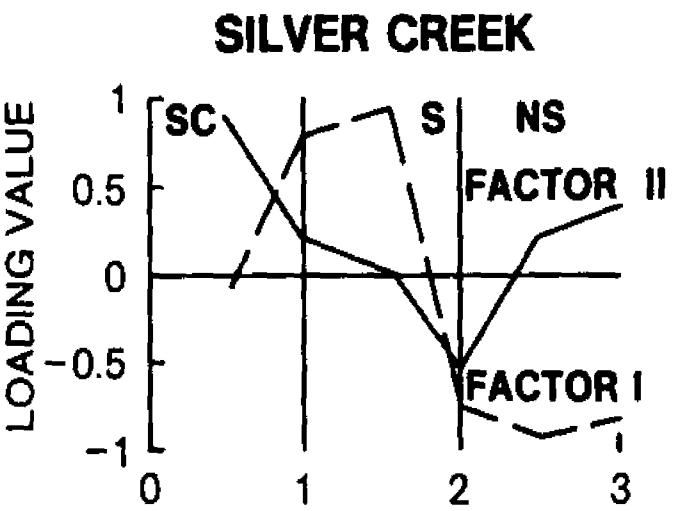

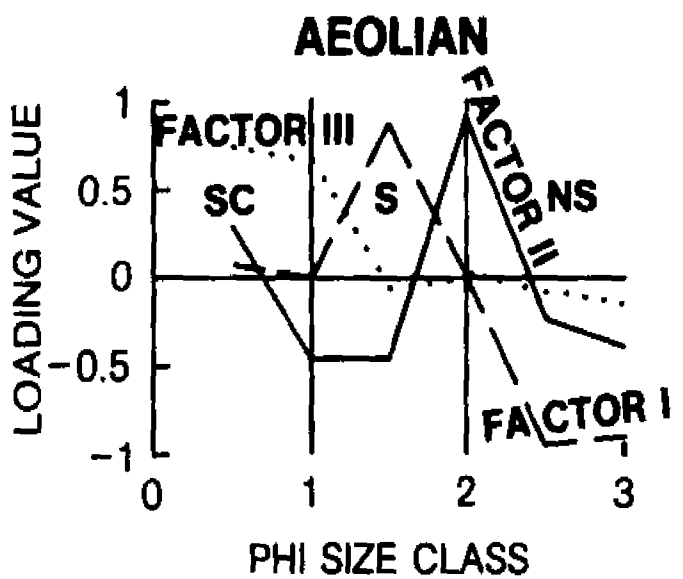

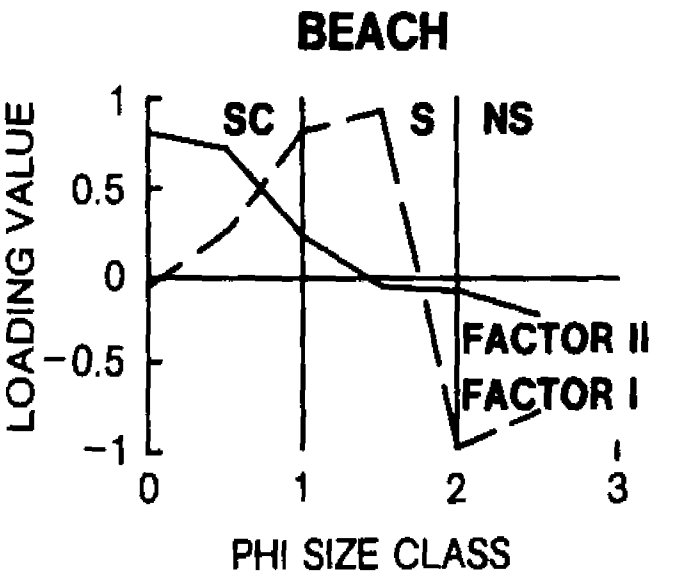

SC=Surface Creep S=Saltation NS=Non-Uniform Suspension

to the extracted factors by plotting the loading values on each factor by each size class interval. The relationship of each size class interval cannot be interpreted rigidly, but these plots do show that breaks occur in the loading profiles when all factors are plotted together.

On the basis of this study and Allen, et al. (1973), the sediment ranging from approximately 1Ø to 3Ø can be assigned to the saltation process of Visher (1969). However, Allen, et al. (1971) suggested that this sand-size group might represent a transition between two end-member transport processes (surface creep and suspension). It was found in this study and in Allen, et al. (1971) that a definite break occurs at 2Ø corresponding to a change in sign of the factor loading values, also noted by Bagnold (1966). Bagnold (1966) suggested that sediment coarser than 2Ø would be transported as bedload and those sizes finer than 2Ø would be transported as a non-uniform suspension (cf. Fig. 14).

The sediment 1Ø and coarser is interpreted to represent the surface creep mode and corresponds well to the interpretation of Visher (1969) and Allen, et al. (1971).

Within the limitations of the size range of the sediment collected in this study, the percent of sediment in each sub-population and the number of sub-populations and the truncation points on the probability graphs are comparable to the same environments studied by Visher (1969). It has also been shown in this study that the sub-populations delineated on probability graphs correlate well with a principal-components analysis of the same

samples. There are some major differences in the information extracted by these methods however. The major difference is in the amount of variance explained by the two methods. Visher (1969) states that if it is assumed that each sediment transport process is reflected in a separate log-normal population, the proportion of each population should be related to the relative importance of the corresponding process in the information contained in the whole distribution. Visher assumes that the total variance of the sample is accounted for by the sum of the proportions of the sub-populations, but does not take into account variance produced by sampling error, measurement error and local fluctuations in the prevailing energy conditions. If these variances are taken into account, then the proportions will account for something less than 100% of the total variance. Another type of error is inherent in the plotting of data on log-probability paper (Hoel, 1962). In this type of graph the confidence limits placed about the mean distribution are very wide in both tails of the graph (i.e., in the 95 to 99.99% region and in the 0.001 to 5% region on the graph paper), thus the frequency percentages in these regions are overwhelmed by their own variances.

Results of the principal-components analysis show that the total variance is not explained in each environment, assuming of course that only those factor axes with eigenvalues >1 are considered as significant, whereas the truncation points and number of populations are basically identical to those defined on probability paper.

Another difference between principal-components analysis and probability graphs is more subtle than the variance problem and is concerned with the number of populations delineated in the size range of 1Ø to 3Ø. In most cases only one population (one log-linear segment) is defined on the probability paper. It has been suggested by Allen et al.(1971) and this writer, on the basis of principal-components analysis, that two sub-groups are present in this size range in every environment as denoted by a change in sign of the factor loadings. However, it is possible in this study that the matrix was acting as a closed array and negative correlations were induced resulting in high negative factor loading. This is certainly the case for Allen, et al.(1971) as they made no apparent attempt to open their matrix. Visher (1969) states that in the samples he analyzed only the beach samples contained two sub-groups in this size range and that the break occurs at 2Ø, which he attributed to swash-backwash beach processes.

On the basis of principal-components and probability graphs the size frequency distributions were divided into three energy/process related sub-populations which are described below in the terms of Moss (1962, 1963), Bagnold (1966), Visher (1969), and Allen, et al. (1971):

Sub-population I - this population is generally described by sediments coarser than 1Ø and related to a surface creep process.

Sub-population II - this population is generally described by two sub-groups in the size range of 1Ø to 3Ø;

Group A - grain-sizes from 1Ø to 2Ø, transported by saltation.

Group B - grain-sizes from 2Ø to 3Ø, transported as non-uniform suspension.

Principal-component factors account for 74-84% of the total grain-size variance in the Little Sable Point environments, the remainder of the variance not explained can be assigned to random fluctuations in the transport processes, sampling and measurement errors (Imbrie, 1963; and Allen, et al., 1971).

In sedimentological terms the populations listed above are the best textural delineators of the hydrodynamic processes operating in the Little Sable Point environments. Principal-components analysis seems to refine and quantify the graphical conclusions of Visher (1969) and support the theoretical results about juncture points between processes as described by Bagnold (1966).

Discriminant-Function Analysis

Discriminant-function analysis was used on the Little Sable Point samples to test for significant differences between the sampled environments. The a priori criteria used to test for differences in the Little Sable Point samples is based on the mode of sample collection; that is, each sub-set of samples was collected from a different environment.

The Mahalanobis D^2 for the beach, aeolian, bar and trough, and fluvial multivariate means (not the true means, but the D or Z score means between the four populations) is 109.03. This value is distributed approximately as χ^2_{18} and at α >0.001 is highly significant and suggests that at least one environment is significantly different from the others. Table 7 lists the discriminant classification of the functional groups tested.

TABLE 7

Discriminant-function Classification of the Functional Groups Tested at Little Sable Point

Functional Group Tested	Aeolian	Silver Creek	Beach	Bars and Troughs	Total
Aeolian	17	5	0	3	25
Silver Creek	1	11	10	0	22
Beach	0	5	23	1	29
Bars and Troughs	2	6	9	1	18

Comparing Table 7 to Figure 15, a graphical representation of the first canonical variable versus the second, suggests that the aeolian samples constitute one textural group (environment) while the beach, offshore bars and trough, and Silver Creek samples constitute another textural group. The beach samples discriminant better (less samples were mis-classified) than the other groups, however as can be seen in Table 7 and Figure 15, there is much more textural overlap

Figure 15: Discriminant-function analysis classification of the Little Sable Point environments

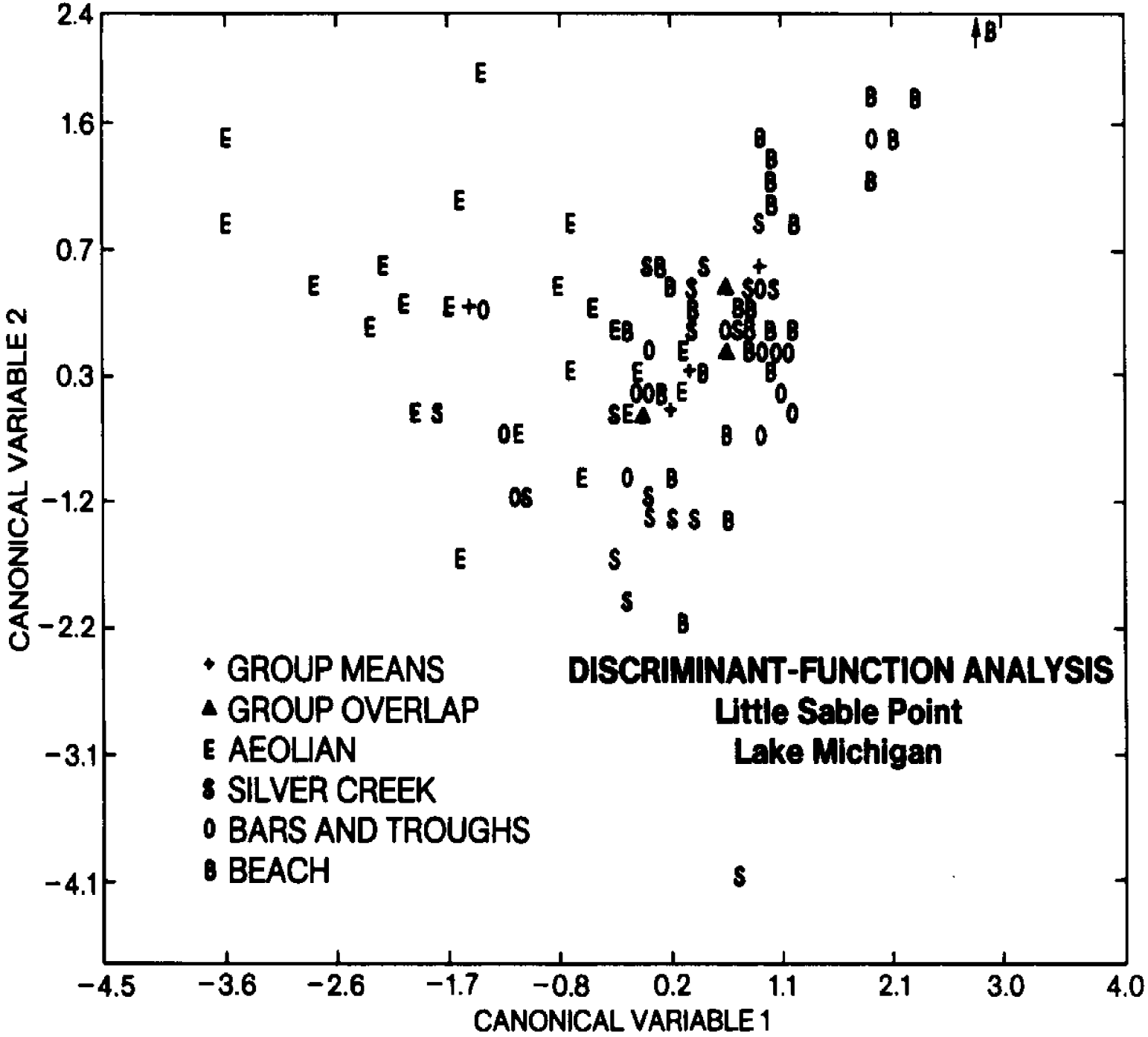
2.4
1.6
0.7
−0.3
−1.2
−2.2
−3.1
−4.1
CANONICAL VARIABLE 2
−4.5
−3.6
−2.6
−1.7
−0.8
0.2
1.1
2.1
3.0
4.0
CANONICAL VARIABLE 1
GROUP MEANS
GROUP OVERLAP
E AEOLIAN
S SILVER CREEK
0 BARS AND TROUGHS
B BEACH
DISCRIMINANT-FUNCTION ANALYSIS
Little Sable Point
Lake Michigan

between the beach, Silver Creek and offshore bars and trough samples than there is between the aeolian samples and the other groups. The bar and trough samples show the greatest textural overlap of any group, being classified mainly as beach and fluvial sediment. This may reflect an inter-play between the beach-fluvial and littoral drift component in the area showing a feedback between these environments. Saylor and Hands (1970) tried to distinguish textural differences in the bar and trough sediment but with little success. Very little is known about this environment (Blatt, et al., 1972).

Almost half of the Silver Creek samples were classified as beach sediment. As will be more clearly seen in the next section (Q-mode factor analysis), the beach processes seem to override the fluvial processes at the mouth of Silver Creek.

It is apparent from the discriminant analysis that there is a great deal of textural overlap between adjacent environments at Little Sable Point, much more than would normally be expected on the basis of transport competency of the processes in these environments. The single sediment source in this area seems to be a dominant factor for environmental discrimination. Unless all sizes are available to the system, the differences in energy levels of the different environments will not be reflected in the sediment.

Q-Mode Factor Analysis

Q-Mode factor analysis was used to classify the sediments into similar groups by calculating the variance across the sample variables. Four factors were retained for varimax rotation, one factor for each environment. Under ideal conditions each environment would be

associated with one and only one factor. However, this should not be expected for two reasons: 1) on the basis of discriminant-function analysis it has already been shown that there is a great amount of textural overlap in samples from these environments; and 2) one would not expect perfect separation in nature because of transitional zones between adjacent environments.

The results of the Q-Mode factor analysis for all Little Sable Point samples are listed in Appendix C. Only three independent factors with eigenvalues >1 were extracted and these explain 99.5% of the total sample variance. Communalities for the three factors are all very high, exceeding 0.992. Although the eigenvalue for factor III is >1, it only accounts for 2.7% of the total variance and has insignificant factor loadings.

Figure 16 is a ternary diagram of normalized factor loadings. Each factor loading was normalized by dividing the square of the loading value by its corresponding communality (Klovan, 1966). This procedure provides results similar to the oblique-projection method of Imbrie and Van Andel (1964) in that more emphasis is placed on the larger factor loadings; however, the axes are still orthogonal.

The samples loading highest on factor I are the aeolian samples and those collected from the main part of Silver Creek, which flows across the dune field. Beach, source beach and the fluvial samples from the mouth of Silver Creek load on factor II. Offshore bar samples are distributed between both factors I and II. It is evident in Figure 16 that there is great textural overlap in the samples.

Figure 16: Ternary diagram of normalized Q-mode factor loadings of the Little Sable Point samples

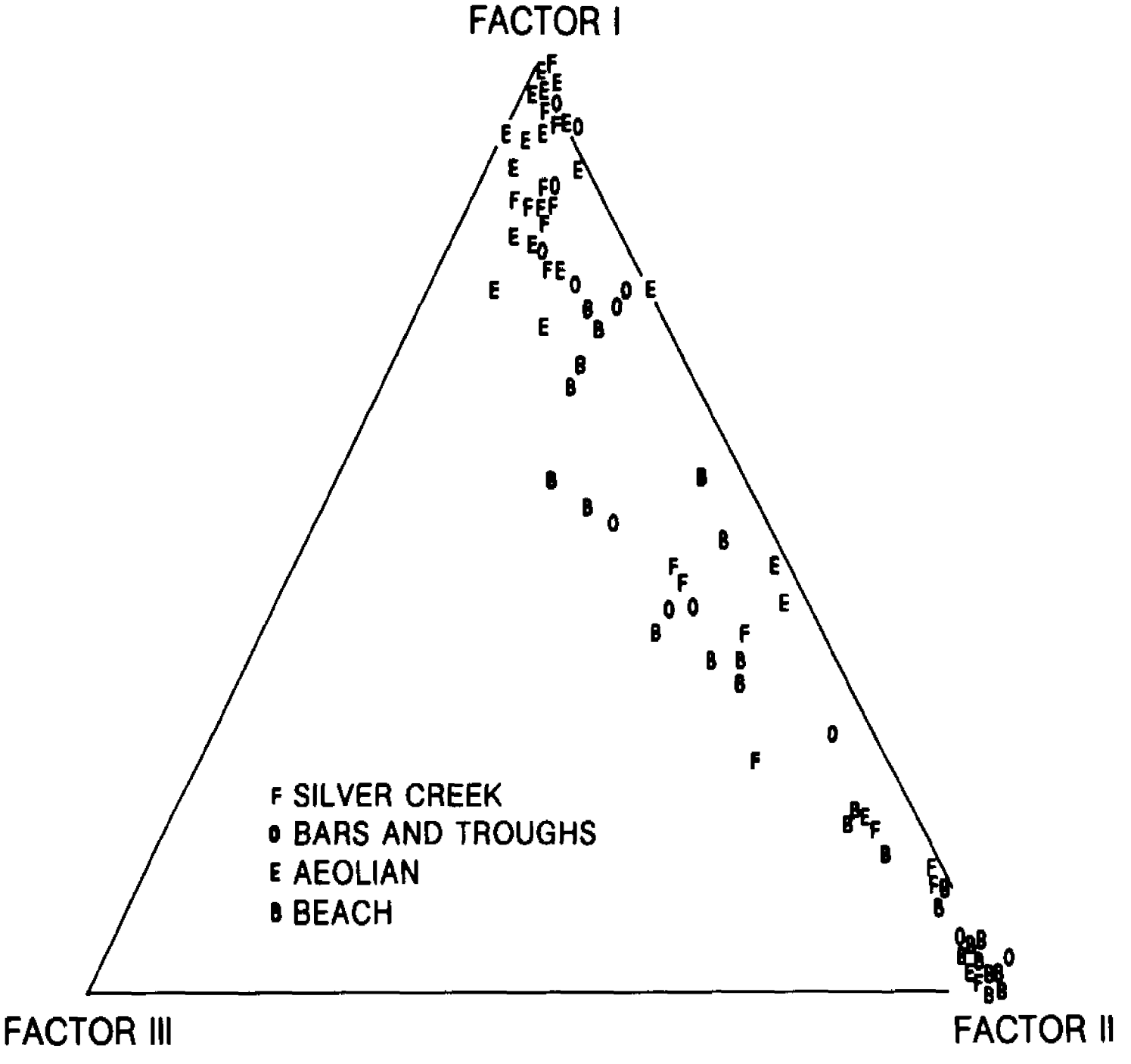
FACTOR I
F SILVER CREEK
O BARS AND TROUGHS
E AEOLIAN
B BEACH
FACTOR III
FACTOR II

As shown in Figure 17 for the most part, the beach and nearshore trough samples load on factor II. Five beach samples load factor I, four of these are south of a snow fence which may slightly impede littoral drift to the north and cause a change in texture. Notice that the samples collected in and near the mouth of Silver Creek load on factor II, while the other fluvial samples load on factor I. Those fluvial samples loading on factor I are from the stream within the dune train, which serves as a sediment source for Silver Creek, while those loading on factor II are dominated by introduction of material by littoral drift and beach processes. Beall (1970) noted the dominance of beach processes over fluvial processes in a beach-deltaic system. The bar and trough samples load on factor I or II, or load moderately on both I and II. The aeolian dune samples load almost entirely on factor I, while the source beach samples load on factor II.

Q-Mode factor analysis emphasizes a lack of environmental differentiation as shown in the previous section with discriminant-function analysis. The beach processes, due to wave surge, seem to override the fluvial processes affecting Silver Creek as much as 6-10 meters upstream of the mouth. The offshore bar and trough samples show great textural variance, which probably reflects feedback between the beach and Silver Creek sediment. Samples from the second trough load on factor I and may represent material deposited by backwash action from the first bar. Although this study deals with major environmental groupings (i.e., fluvial, strandline, and aeolian) there appears, as should be expected, to be different sub-environments within each major group.

Figure 17: Areal distribution of two Q-mode factors for the Little Sable Point Samples

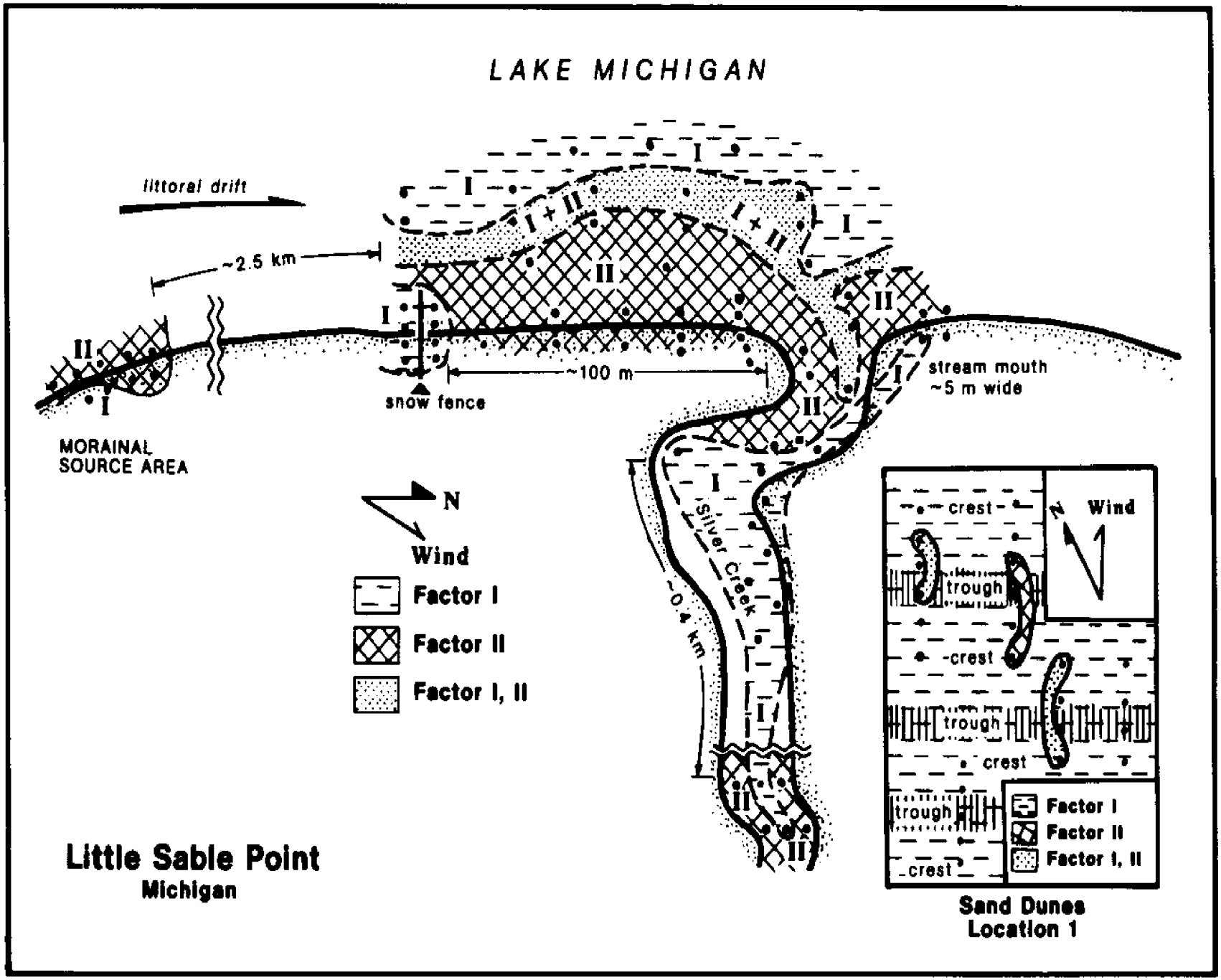
LAKE MICHIGAN
littoral drift
~2.5 km
~100 m
snow fence
MORAINAL
SOURCE AREA
stream mouth
~5 m wide
Silver Creek
~0.4 km
N
Wind
Factor I
Factor II
Factor I, II
Little Sable Point
Michigan
crest
trough
Wind
Factor I
Factor II
Factor I, II
Sand Dunes
Location 1

Figure 17 illustrates the spatial distribution of the Q-Mode factors for the Little Sable Point samples. Discriminant-function analysis has shown that environmental differentiation of these sediments is somewhat tenuous when dealing with sands from one source with a truncated or winnowed distribution. It is important to note however in Figure 17 that there is some spatial distribution of sediment patterns. Although samples were collected from supposedly different energy environments, the energy related processes in this study area are generally not sufficiently distinct enough to cause significant changes in the size distributions in the sands with the above characteristics.

Sleeping Bear Point/Manitou Passage Depositional Area

The sediment in the Sleeping Bear Point/Manitou Passage area have multiple source areas with a range in grain-sizes from lag gravel deposits and coarse sand on Sleeping Bear Shoal to fine silt and clay in the profundal basin north of the shoal (Fig. 18). The fact that the sediments are not truncated at the fine end of the distribution may provide for a better means of environmental discrimination. Many authors have shown that the finer sediments are deposited under lower hydrodynamic conditions which can be depth dependent (e.g., Passega, 1957, 1972; Visher, 1969). The fines winnowed from the higher energy shoal environment should be deposited in the lower energy profundal environment.

Before any of the Sleeping Bear Point/Manitou Passage samples were analyzed the study area was divided into four areas

that appear to be different depositional/erosional environments. The a priori criterion used for this classification is based on the morphological open water zones noted by French (1964), which are based on the bathymetry of the area. The first environment is the shoal and nearshore zone where twenty-one samples were collected. Five of the samples were not analyzed because of their coarse clast size. These samples appear to be part of the lag deposits described by French (1964). The second environment includes the beach area on the northeastern tip of Sleeping Bear Point where twenty-nine samples were collected. The west side of the point was not sampled because the base of the west face consists of lag beach gravels of morainic sediments (French, 1964). The nine samples from the profundal area north of Sleeping Bear Point constitute the third environment, with the fourth environment making up the transitional area between the profundal basin and the shoal and nearshore. Fifteen samples were collected in the transitional area. The data are listed in Appendix B.

Discriminant-Function Analysis

Figure 18 is an index map of the Sleeping Bear Point/Manitou Passage area and locates the environments defined on the basis of bathymetry. The Mahalanobis D^2 of the four multivariate means is 1634.35. This value is distributed approximately as χ^2_{27} and at $\alpha>0.001$, is highly significant and suggests that at least one environment is significantly different from the others. Table 8 lists the discriminant classification of the functional

Figure 18: Index map of the environments at the Sleeping Bear Point/Manitou Passage area used in the discriminant-function analysis. The environments were defined after French (1964)

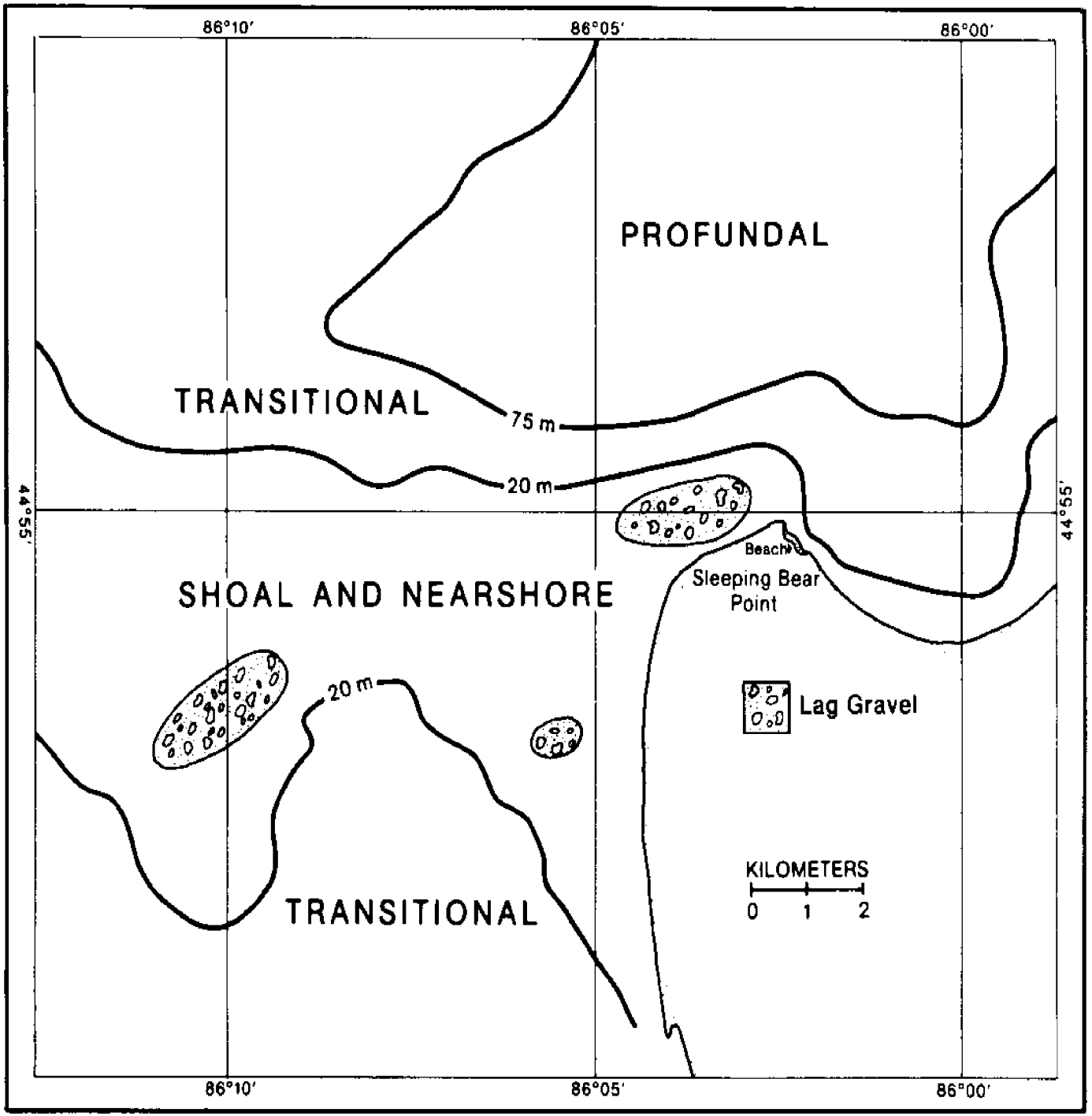
86°10′
86°05′
86°00′
PROFUNDAL
TRANSITIONAL
75 m
20 m
44°55′
Beach
Sleeping Bear Point
SHOAL AND NEARSHORE
20 m
Lag Gravel
KILOMETERS
0 1 2
TRANSITIONAL

groups tested. Comparing Table 8 to Figure 19, a graphical plot of the first canonical variable against the second, shows that all the environments are significantly different. Three beach samples were classified with the shoal and nearshore samples, while three shoal samples were classified in the transitional group. Some textural overlap between the beach and shoal and nearshore environments should be expected as they are both areas of high energy wind induced wave processes.

TABLE 8

Discriminant-Function Classification of the Functional Groups Tested at the Sleeping Bear Point/ Manitou Passage Area

	Profundal	Nearshore and Shoal	Transitional	Beach	Total
Profundal	9	0	0	0	9
Nearshore & Shoal	0	13	3	0	16
Transitional	0	0	15	0	15
Beach	0	3	0	26	29

The discriminant classification provides a basis for evaluating, by means of principal-components analysis, different transport processes in these environments. Discriminant-function analysis shows statistically that the size distributions represent distince environments on the basis of their multivariate means.

Figure 19: Discriminant-function classification of the Sleeping Bear Point/Manitou Passage environments

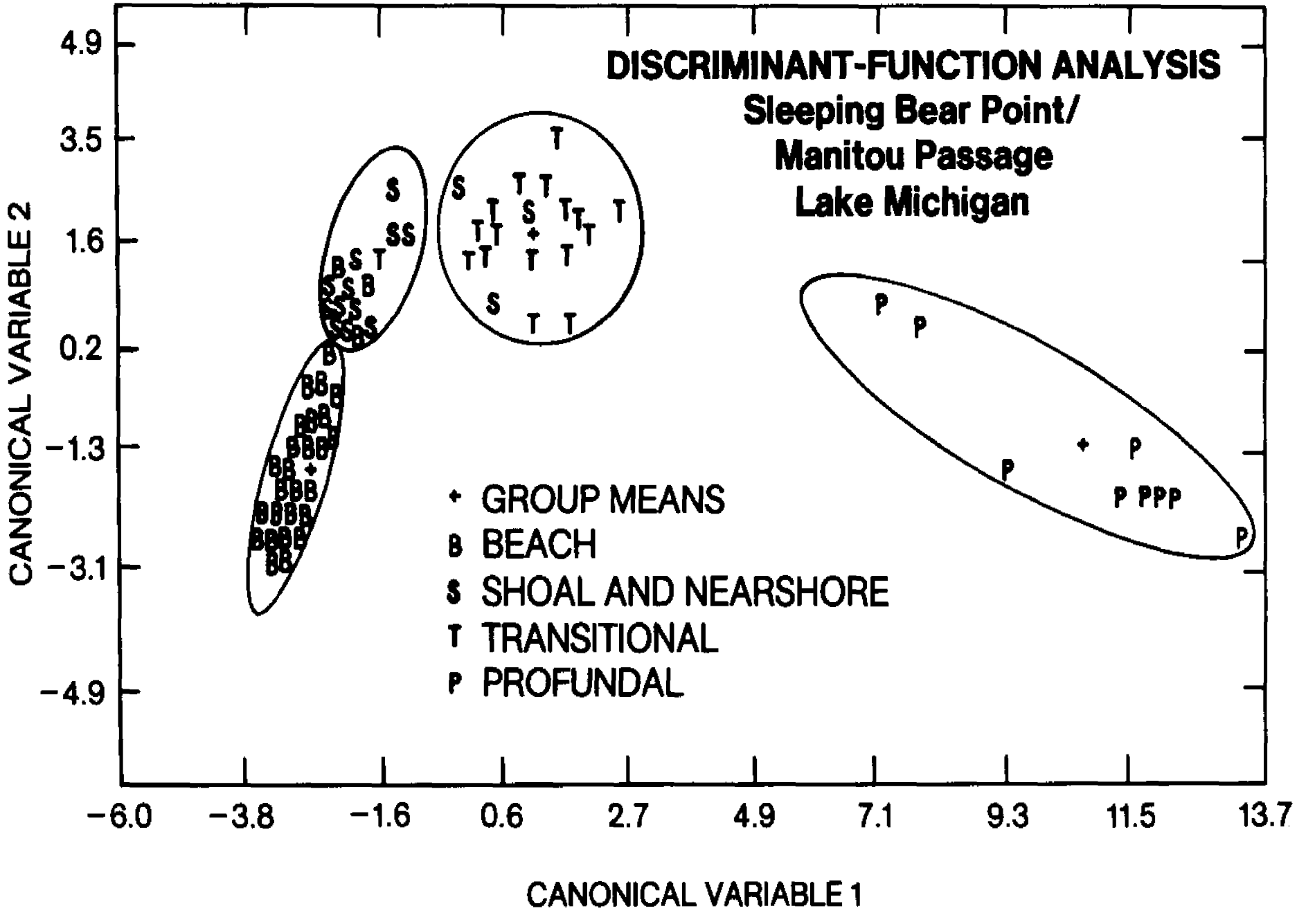
DISCRIMINANT-FUNCTION ANALYSIS
Sleeping Bear Point/
Manitou Passage
Lake Michigan
GROUP MEANS
B BEACH
S SHOAL AND NEARSHORE
T TRANSITIONAL
P PROFUNDAL
CANONICAL VARIABLE 2
CANONICAL VARIABLE 1
4.9
3.5
1.6
0.2
−1.3
−3.1
−4.9
−6.0
−3.8
−1.6
0.6
2.7
4.9
7.1
9.3
11.5
13.7

Principal-Components Analysis

The shoal and nearshore, profundal, transitional, and beach samples were subjected to principal-components analysis to determine the relationships between the sub-populations of their size frequency distributions in an effort to delineate transport processes operating in the four environments. The sediment finer than 4Ø was not included in this analysis for two reasons; 1) excluding this fraction will open the data array and avoid the closure problem discussed earlier; and 2) it has been assumed by several workers that this size group represents the suspension transport mechanism and should therefore load on an independent factor (e.g., Bagnold, 1956; Passega, 1957, 1972; Visher, 1969; Davis, 1970; Allen, et al., 1971).

Shoal and nearshore area - Table 9 lists the principal-components results for the shoal and nearshore samples. Variables correlated at α = .05 and .01 are listed in this table. Two factors with eigenvalues >1 were extracted and account for 80.4% of the total variance. The communalities are high to very high.

Figure 20 is a cumulative-probability graph of the grand frequency distribution of the shoal and nearshore samples. Four sub-populations are indicated in this distribution with truncation points at: 1) 2.0Ø between A and B; 2) 3.3Ø between B and C; and 3) 4.0Ø between C and D.

Factor I is closely related to the size classes 0.5Ø to 1.5Ø (high positive loading values) and the size class 2.5Ø

TABLE 9

PRINCIPAL-COMPONENTS RESULTS OF SLEEPING BEAR POINT/ MANITOU PASSAGE SHOAL AND NEARSHORE SAMPLES

	Summary Statistics							
Phi Size	0.5	1.0	1.5	2.0	2.5	3.0	3.5	4.0
Grand Means	4.7	12.1	25.6	30.6	13.8	6.3	3.4	0.8
Grand Standard Deviations	3.9	8.8	11.7	13.4	8.7	8.3	6.6	1.2

	Product-Moment Correlation Matrix							
Phi Size	0.5	1.0	1.5	2.0	2.5	3.0	3.5	4.0
0.5	1.00	.85**	.58*		-.53*	-.55*	-.51*	-.55*
1.0		1.00	.64**		-.72**	-.50**		
1.5			1.00		-.65**	-.71**	-.57*	-.60*
2.0				1.00			.65**	
2.5					1.00			
3.0						1.00	.88**	.72**
3.5							1.00	.63**
4.0								1.00

significant at $\alpha = 0.05$*, $\alpha = 0.01$**, n = 16, df = 14

Factor	Eigenvalues	Cumulative Percentage of Eigenvalues
I	4.501	56.3
II	1.930	80.4

	Rotated Factor Matrix		Communalities
Phi Size			
0.5	0.838	0.226	0.753
1.0	0.960	-0.001	0.922
1.5	0.781	0.365	0.743
2.0	-0.459	0.835	0.892
2.5	-0.764	-0.205	0.626
3.0	-0.524	-0.809	0.929
3.5	-0.531	-0.854	0.853
4.0	-0.345	-0.767	0.708

Figure 20: Phi-probability graph of the grand frequency distribution of the Sleeping Bear Point/Manitou Passage shoal and nearshore samples

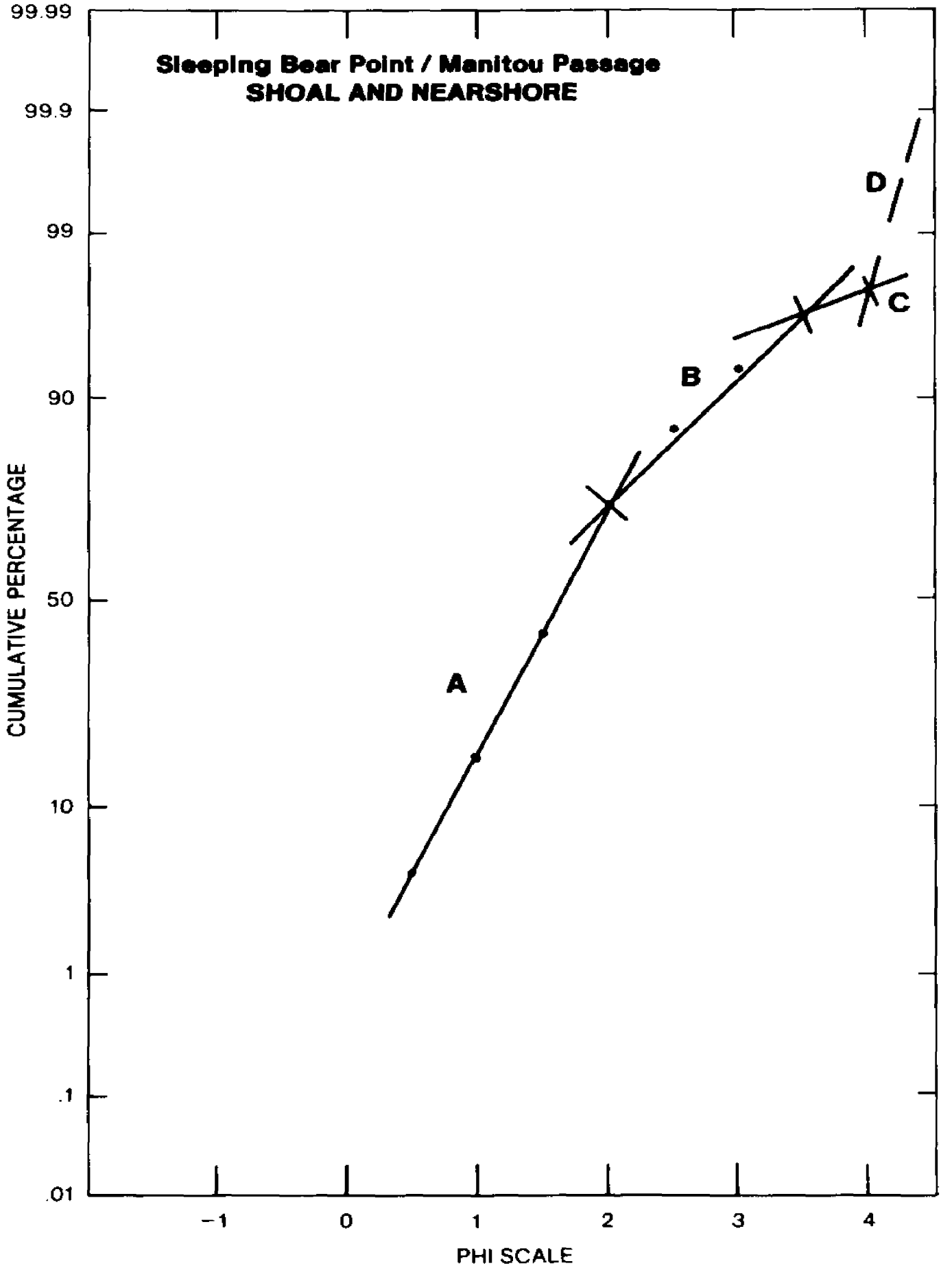
Sleeping Bear Point / Manitou Passage
SHOAL AND NEARSHORE
99.99
99.9
99
90
50
10
1
.1
.01
CUMULATIVE PERCENTAGE
−1
0
1
2
3
4
PHI SCALE
A
B
C
D

(moderately high negative loading value). This factor accounts for 56.3% of the total variance. Sub-population A on the probability graph accounts for 70% of the total distribution and correlates well with this factor.

Factor II accounts for 24.1% of the total variance and is related to the size classes 3.0Ø and finer (high negative loadings) and with the 2.0Ø size class (high positive loading). Sub-population C on the probability graph accounts for 4% of the total distribution and seems to correlate with this factor.

Sub-population B on the probability graph accounts for 25% of the total distribution and correlates with both factor I (high negative loading values) and factor II (high positive loading values).

Beach samples - Table 10 lists the principal components results for the beach samples. Two factors with eigenvalues >1 were extracted and account for 85.2% of the total variance. The communalities are high to very high. Variables significantly correlated at α = .05 and .01 are also listed.

Figure 21 is a cumulative-probability graph of the grand frequency distribution for these samples. Three sub-populations are shown on this graph with truncation points at: 1) 0.5Ø between A and B; and 2) at 1.7Ø between B and C.

Factor I is related to the 1.0Ø size class (high positive loading) and those 2.0Ø and finer (very high negative loadings). This factor accounts for 30.3% of the total variance. This factor

TABLE 10

PRINCIPAL-COMPONENTS RESULTS OF SLEEPING BEAR POINT/ MANITOU PASSAGE BEACH SAMPLES

	Summary Statistics					
Phi Size	0.0	0.5	1.0	1.5	2.0	2.5
Grand Means	1.7	4.6	44.6	32.1	12.0	3.1
Grand Standard Deviations	2.5	3.9	18.3	11.6	11.5	6.3

	Product-Moment Correlation Matrix					
Phi Size	0.0	0.5	1.0	1.5	2.0	2.5
0.0	1.00	.75**	-.53**			
0.5		1.00	.42**	-.67**	-.54**	-.37*
1.0			1.00		-.87**	-.74**
1.5				1.00		
2.0					1.00	.88*
2.5						1.00

significant at $\alpha = 0.05$*, $\alpha = 0.01$**, n = 29, df = 27

Factor	Eigenvalues	Cumulative Percentage of Eigenvalues
I	3.291	54.9
II	1.821	85.2

	Rotated Factor Matrix		Communalities
Phi Size	I	II	
0.0	0.165	-0.836	0.727
0.5	0.382	-0.863	0.892
1.0	0.873	-0.193	0.800
1.5	0.114	0.890	0.805
2.0	-0.960	0.207	0.965
2.5	-0.958	-0.041	0.920

Figure 21: Phi-probability graph of the grand frequency distribution of the Sleeping Bear Point/Manitou Passage beach samples

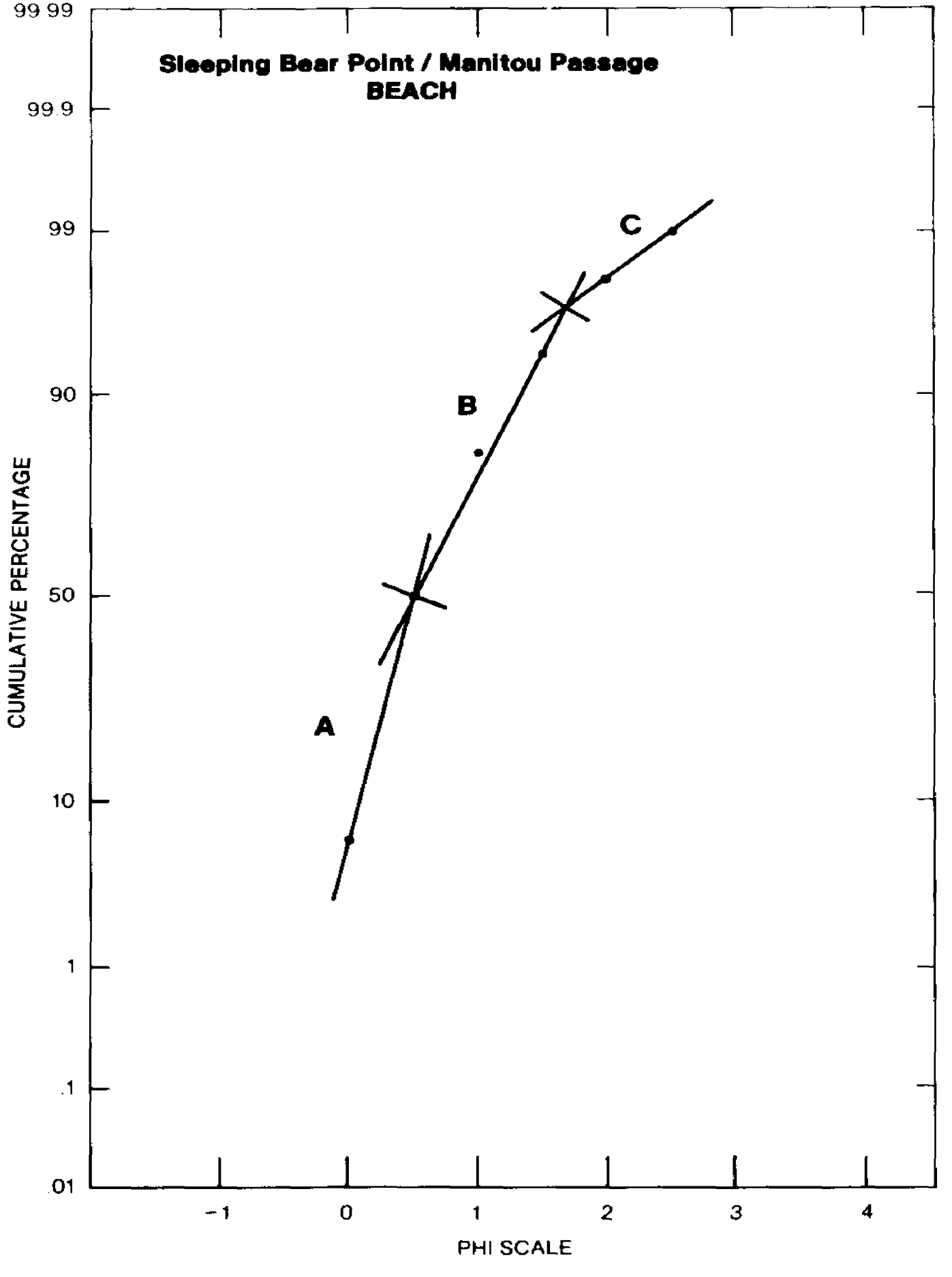
Sleeping Bear Point / Manitou Passage
BEACH
99.99
99.9
99
90
50
10
1
.1
.01
CUMULATIVE PERCENTAGE
A
B
C
-1
0
1
2
3
4
PHI SCALE

relates well with sub-population A on the probability graph which accounts for 50% of the total population.

Factor II accounts for 54.9% of the total variance. The size classes related to this factor are the 0.0Ø to 0.5Ø (high negative loadings) and the 1.5Ø interval (high positive loading). This factor corresponds well with sub-populations B and C on the probability graph which account for 50% of the total distribution.

Profundal sediments - Table 11 lists the principal-components results for the profundal sediments. Two factors with eigenvalues >1 were extracted and account for 89.9% of the total variance. Correlations significant at α = .05 and .01 are listed. The communalities are high to very high.

Figure 22 shows the grand frequency distribution of the profundal sediments. Three sub-populations are present with truncation points at: 1) 2.0Ø between A and B; and 2) at 4.0Ø between B and C.

Factor I is related to the size classes 2.0Ø and coarser (high to very high loading values). This factor accounts for 67.7% of the total variance and correlates well with sub-population A on the probability plot which accounts for 10% of the total size distribution.

Factor II accounts for 22.2% of the variance and is related to sizes finer than 2.0Ø (high positive loadings). This factor correlates well with sub-population B on the probability graph which

TABLE 11

PRINCIPAL-COMPONENTS RESULTS OF SLEEPING BEAR POINT/ MANITOU PASSAGE PROFUNDAL SAMPLES

Summary Statistics

Phi Size	0.5	1.0	1.5	2.0	2.5	3.0	3.5	4.0
Grand Means	0.6	1.7	2.7	5.0	1.9	4.0	3.5	1.5
Grand Standard Deviastions	0.4	1.4	2.2	2.9	1.0	5.5	3.2	1.8

Product-Moment Correlation Matrix

Phi Size	0.5	1.0	1.5	2.0	2.5	3.0	3.5	4.0
0.5	1.00	.95**	.92**	.74*				
1.0		1.00	.99**	.85*				
1.5			1.00	.88**				
2.0				1.00				
2.5					1.00	.72*	.86**	.78**
3.0						1.00	.91**	.70**
4.0								1.00

significant at $\alpha = 0.05$*, $\alpha = 0.01$**, n = 9, df - 7

Factor	Eigenvalues	Cumulative Percentage of Eigenvalues
I	5.415	67.7
II	1.778	89.9

	Rotated Factor Matrix		Communalities
	I	II	
Phi Size			
0.5	0.940	0.138	0.903
1.0	0.969	0.215	0.987
1.5	0.952	0.288	0.991
2.0	0.844	0.273	0.788
2.5	0.295	0.863	0.832
3.0	0.186	0.908	0.860
3.5	0.110	0.981	0.975
4.0	0.565	0.731	0.855

Figure 22: Phi-probability graph of the grand frequency distribution of the Sleeping Bear Point/Manitou Passage profundal samples

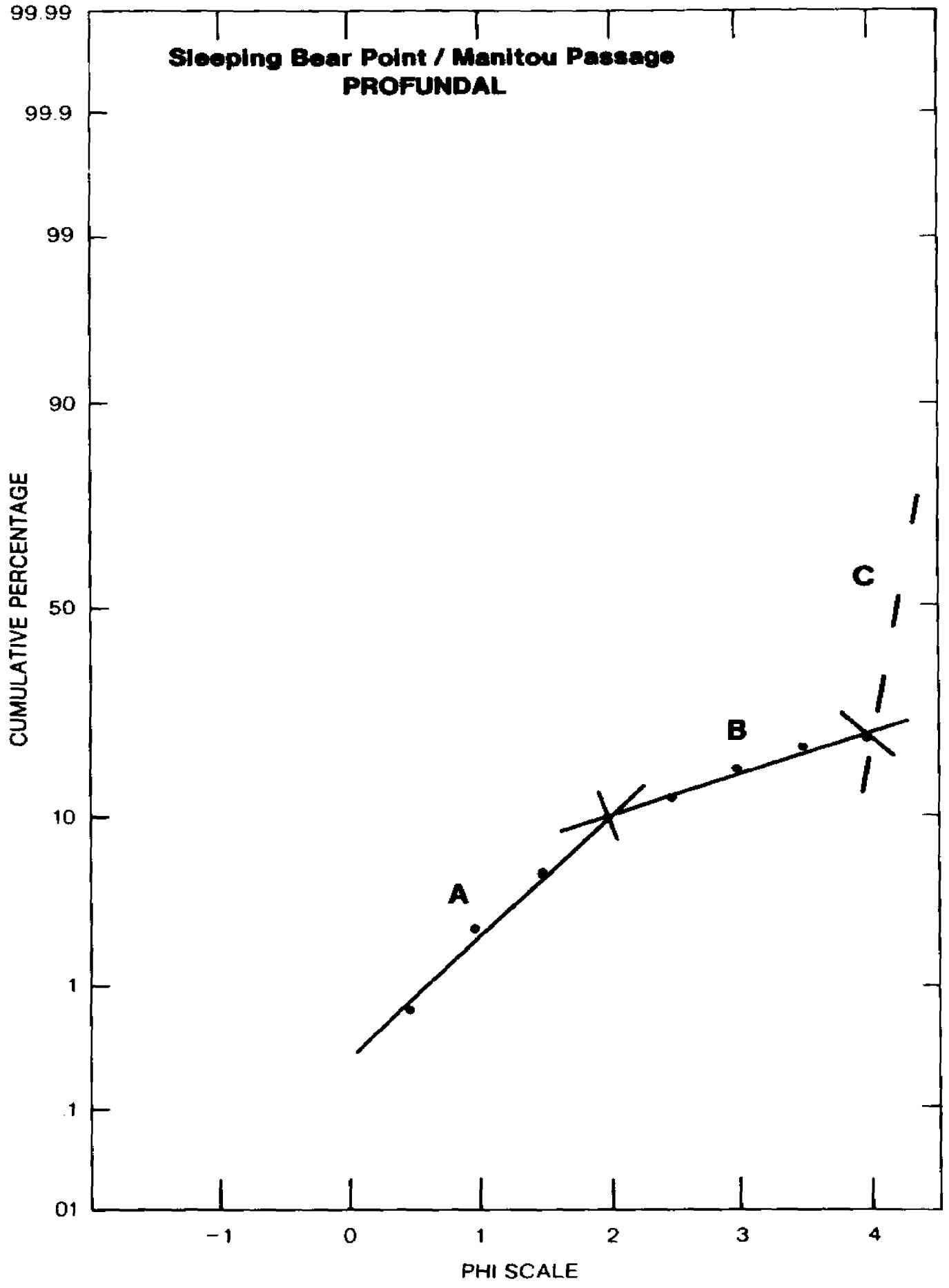
Sleeping Bear Point / Manitou Passage
PROFUNDAL
99.99
99.9
99
90
50
10
1
.1
01
CUMULATIVE PERCENTAGE
A
B
C
−1
0
1
2
3
4
PHI SCALE

accounts for 10% of the distribution. Sub-population C on the porbability graph is related to sizes 4.0Ø and finer and accounts for 80% of the total distribution.

Transitional sediments - Table 12 lists the principal-components results for the transitional sediments. Two factors were extracted with eigenvalues >1 and account for 79.4% of the total variance. The communalities are moderately high to high in value. Figure 23 shows the grand frequency distribution of the transitional samples. Three sub-populations are present with truncation points at: 1) 3.25Ø between A and B; and 2) at 4.0Ø between B and C.

Factor I is related to sizes 1.5Ø and coarser (high positive) loadings) and sizes 2.0Ø and 2.5Ø (moderately high negative loadings). This factor accounts for 47.3% of the total variance.

Factor II accounts for 32.1% of the total variance. The sizes related to this factor are the intervals 3.0Ø (high negative loading) and 3.5Ø to 4.0Ø (high positive loadings).

Sub-populations A and B on the probability graph are related to factors I and II; these sub-populations account for 86% of the total population. Population C relates to sizes finer than 4Ø and accounts for 13% of the population.

TABLE 12

PRINCIPAL-COMPONENTS RESULTS OF THE SLEEPING BEAR POINT/ MANITOU PASSAGE TRANSITIONAL SAMPLES

Summary Statistics

Phi Size	0.5	1.0	1.5	2.0	2.5	3.0	3.5	4.0
Grand Means	1.6	5.2	8.1	15.4	17.0	25.6	10.5	3.8
Grand Standard Deviations	1.6	4.5	6.6	8.8	12.9	12.3	7.4	2.7

Product-Moment Correlation Matrix

Phi Size	0.5	1.0	1.5	2.0	2.5	3.0	3.5	4.0
0.5	1.00	-.64**	-.72**			-.61*		
1.0		1.00	.86**		-.67**	-.64**		
1.5			1.00			-.74**		
2.0				1.00		-.77**	-.61*	
2.5					1.00			-.69**
3.0						1.00		
3.5							1.00	
4.0								1.00

significant at $\alpha = 0.05$*, $\alpha = 0.01$**, n = 15, df = 13

Factor	Eigenvalues	Cumulative Percentage of Eigenvalues
I	3.780	47.3
II	2.575	79.4

	Rotated Factor Matrix		Communalities
	I	II	
Phi Size			
0.5	0.812	-0.149	0.681
1.0	0.909	0.135	0.846
1.5	0.957	-0.098	0.927
2.0	0.423	-0.761	0.758
2.5	-0.662	-0.708	0.940
3.0	-0.769	0.520	0.863
3.5	-0.152	0.775	0.624
4.0	0.107	0.837	0.713

Figure 23: Phi-probability graph of the grand frequency distribution of the Sleeping Bear Point/Manitou Passage transitional samples

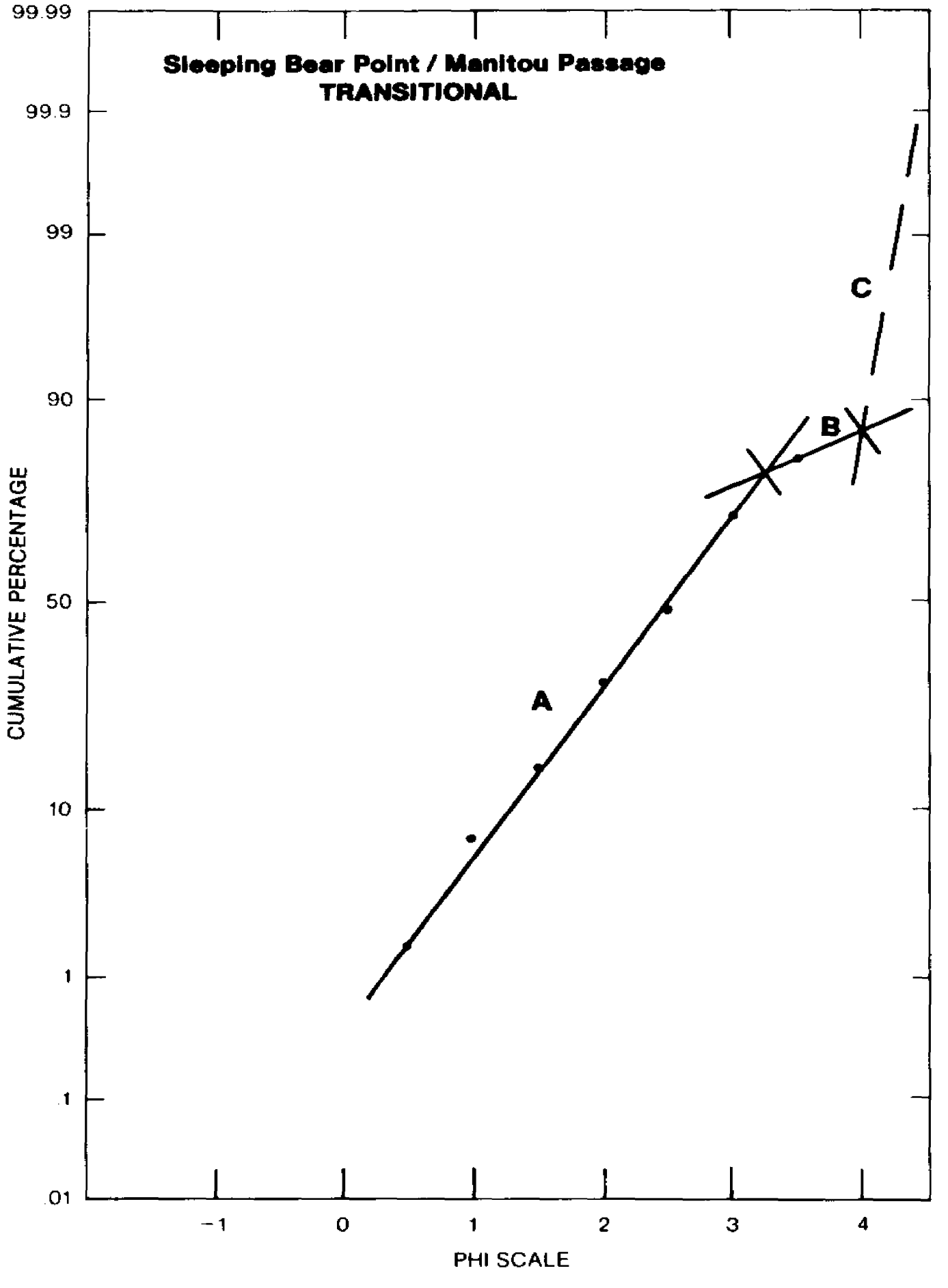
Sleeping Bear Point / Manitou Passage
TRANSITIONAL
99.99
99.9
99
90
50
10
1
.1
.01
CUMULATIVE PERCENTAGE
−1
0
1
2
3
4
PHI SCALE
A
B
C

Discussion of the Principal-Components and Probability Graph Results for the Sleeping Bear Point/Manitou Passage Environments

Figure 24 is a plot of the loading values versus phi size for each of the four environments. The reader is reminded here that the pure suspension mode (>4Ø sizes) is not represented in the principal-components analysis, omission of this size fraction should not affect the loading values of the other sizes on the factors. The sediment finer than 4Ø in the profundal sediments accounts for 50-95% of the total sample by weight, 15-35% in the transitional sediments, less than 5% in the shoal and nearshore samples, and none in the beach sediment. As this material accounts for a great proportion of the total weight in the profundal sediment, the amount of variance accounted for by the two factors is grossly over estimated. The variance accounted for by the two factors in the transitional and shoal and nearshore sediments should be only moderately over estimated. Therefore, only trends in the loading profiles can be used significantly for the profundal sediments.

The cumulative-probability graphs (cf., Figs. 20, 21, 22, and 23) of the Sleeping Bear Point/Manitou Passage sediments correlate well with the factors extracted by the principal-components analyses (Fig. 24). The probability graphs suggest the presence of 3 to 4 sub-populations, while the principal-components results suggest that the size distributions can be divided into 3 subgroups, which probably correspond to the following transport mechanisms:

Figure 24: Loading profiles of each Sleeping Bear Point/Manitou Passage environment

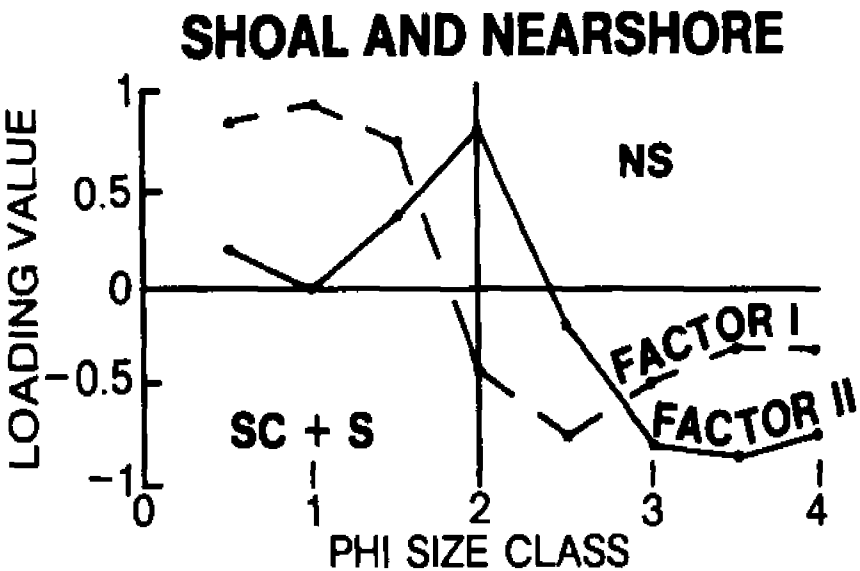

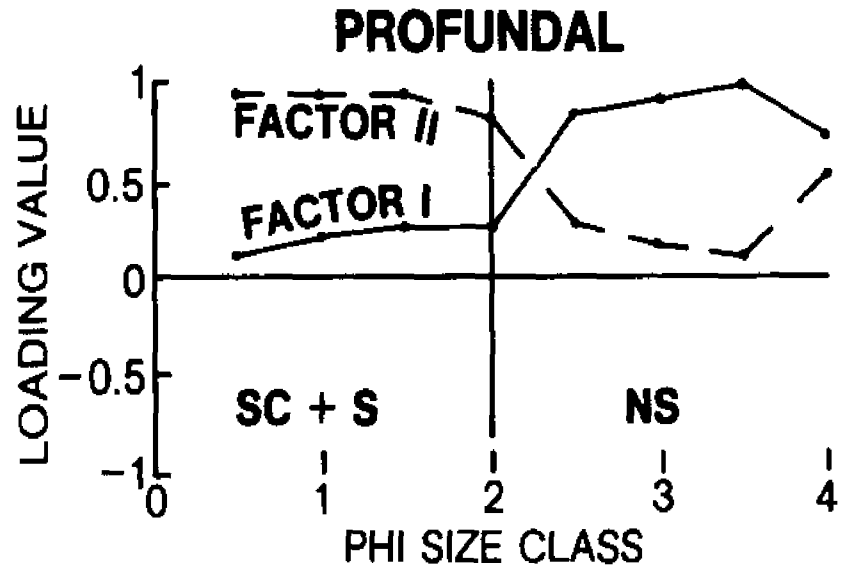

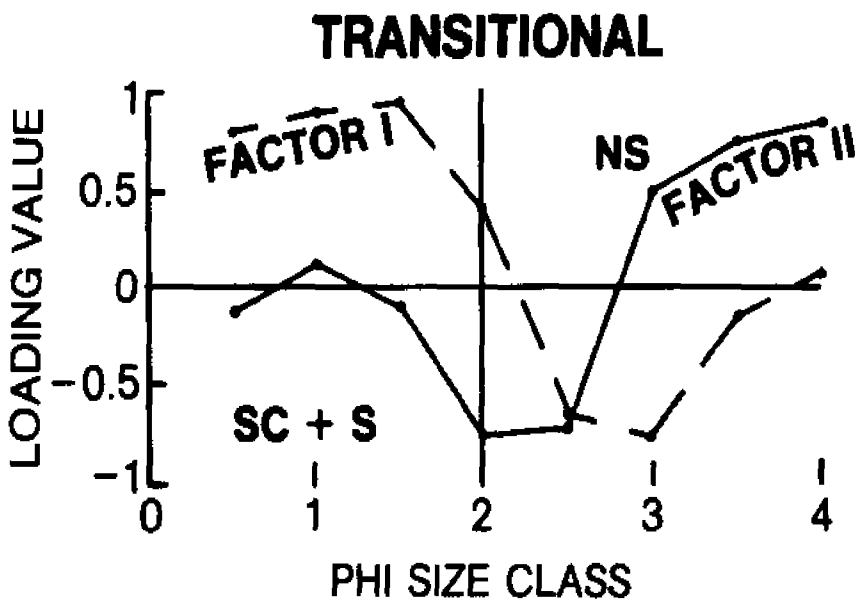

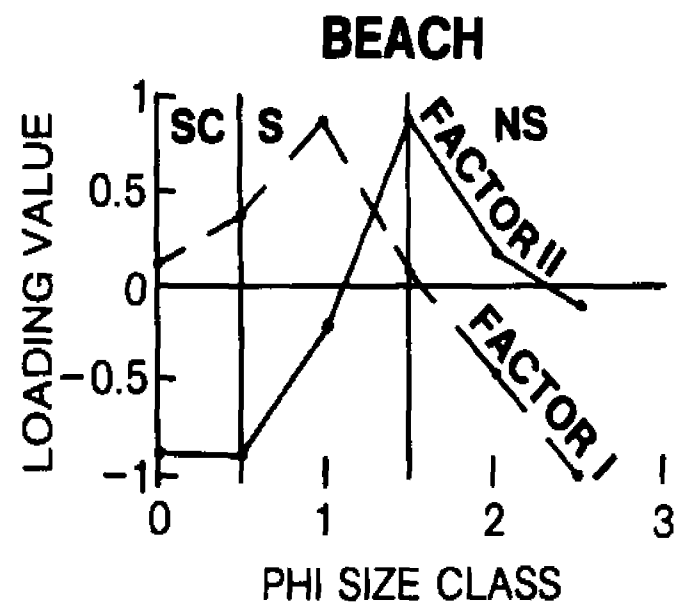

SC=Surface Creep S=Saltation NS=Non-Uniform Suspension

Sub-population I - coarse sand (1.0Ø and coarser) affected by surface creep.

Sub-population II - intermediate sand sizes (1.0Ø to 4.0Ø) affected by two mechanisms:

1) saltation (1.0Ø to 2.0Ø)
2) non-uniform suspension (2.0Ø to 4.0Ø)

Sub-population III - silt and clay (4Ø and finer) affected by a pure suspension mechanism.

These sub-populations described here are very similar to the sub-populations described for the Little Sable Point samples.

COMPARISON OF THE LITTLE SABLE POINT AND THE SLEEPING BEAR POINT/MANITOU PASSAGE ENVIRONMENTS

Even a cursory examination of the multivariate results of the environments studied indicate differences in the effectiveness of environmental discrimination on the basis of grain-sizes alone (cf. Figs. 15 and 19). Discrimination of environments using textural data was most effective at the Sleeping Bear Point/Manitou Passage area, while little discrimination was possible for the Little Sable Point environments.

The grain-size distributions of the two study areas differ significantly in terms of the range of sizes available to the systems. The samples at Little Sable Point have a very restricted size range, which is limited to the sand-size range (0Ø to 3Ø), while the samples from the Sleeping Bear Point/Manitou Passage area range from lag gravels to very fine deep water silt and clay.

Both study areas have a wide range in energy conditions from the lower energy profundal environment at the Sleeping Bear Point/Manitou Passage area and the aeolian environment at Little Sable Point to the higher energy beach environments in both areas. If it is assumed that textural modifications are energy-dependent, passage into or through any environment should result in modification of the original grain-size distribution, provided that the new environment has sufficient energy to modify the distribution,

or that the sediment remains in any environment long enough to acquire the textural characteristics of that environment.

The loading profiles (cf. Figs. 14 and 24) of the environments from each study area shows that truncation points of grain-size frequency distributions occur at relatively the same phi size intervals. This suggests that regardless of sediment type, the same basic transport mechanisms are reflected in samples from different environments. The proportions of the sub-populations may vary between environments which is evident in the Sleeping Bear Point/Manitou Passage environments.

The problem of induced negative correlations formed by closed matrices, particularly concerning the change in sign of factor loading values at 2Ø, can now be further evaluated by comparing the factor loading profiles (cf. Figs. 14 and 24) from the two study areas. It was stated that the break at 2Ø for the test cases was due to closure, but this same break occurs in the samples from Little Sable Point, which theoretically form an open matrix. The principal-components results of the transitional and profundal environments form an open matrix when the sediment finer than 4Ø is excluded from the analysis. The transitional sediments have a percentage range of sediment finer than 4Ø from 15 to 35%, while those from the profundal environment range from 50-95% finer than 4Ø. The 2Ø break in the loading profile for the transitional sediments (Fig. 24) occurs with a change in sign of the loading value (high negative value) as before, however, for the profundal

samples, the 2Ø break occurs where factor I changes from high to low positive values, and factor II changes from low to high positive values (Fig. 24). These results tend to support Bagnold's (1966) assumption that a change in hydrodynamic process occurs at approximately 2Ø.

It is not possible to compare the amount of explained variance between the two study areas because the amount of total variance contributed by the silt and clay by the Sleeping Bear Point/Manitou Passage samples is not known.

Environmental Interpretation of Sedimentary Environments

The profundal sediments in the Sleeping Bear Point/Manitou Passage area are characterized by a predominance of silt and clay (50-95%) which is carried as a suspended load and deposited by gravitational settling. Coarser grained material may be introduced by saltation and/or surface creep during storms, or by slumping from the adjacent Sleeping Bear Point. Airborne material may also be derived from the adjacent Sleeping Bear sand dunes.

Decreasing water depths with a consequent increase in wind generated wave energy into the shoal and nearshore area results in the winnowing of the silt/clay fraction. This area is characterized by lag gravels and coarse to medium sand sizes. The sand is predominantly carried as saltation, non-uniform suspension and/or surface creep. The maximum depth of erosion in this area is approximately 20m (French 1964). French (1964) noted that much of the material forming the extensive sediment plume on the northeast

tip of Sleeping Bear Point is fine sand derived from erosion on the shoal, the silt/clay fraction is carried lakeward by strong currents in this area.

Most of the fine sand and silt in the transitional sediments, Sleeping Bear Point/Manitou Passage, is derived from the shoal and nearshore and is probably transported as a saltation and/or non-uniform suspension load.

Finally, in the beach environment of both areas two types of saltation modes were distinctly recognized, and probably result from the swash and backwash in the foreshore zone as described by Visher (1969). The swash, being the strongest process, probably transports material as primarily non-uniform suspension and/or suspension, while the backwash processes probably transport sand mainly as saltation and/or non-uniform suspension.

The bar and trough samples in the Little Sable Point area show much textural overlap with the beach samples, presumably the same processes and in relatively the same proportions are affecting these samples.

The significance of saltation in wind transport of sediments in the aeolian environment has been emphasized by Williams (1963), Hoyt (1965), and Visher (1969). In addition to the dominant saltation mode, these authors have also shown that small amounts of suspended material may be present (not present in the Little Sable Point aeolian samples), but very little surface creep material (less than 1-2%. Visher, 1969). Despite the differences in beach

and dune transport mechanisms, these two environments at Little Sable Point cannot be perfectly separated without some overlap on the basis of texture alone. Others have also noted that in many cases beach and dune sands cannot be distinguished texturally (Shepard and Young, 1961, Schlee, et al., 1964, Davies and Ethridge, 1975).

CONCLUSIONS

Several multivariate methods, principal-components, Q-mode factor, and discriminant function, analyses were applied to an entire range of grain-sizes to test the effectiveness of sediment size distributions as environmental discriminators for several different environments. In the case of the Little Sable Point samples, the results showed little separation of the environments studied, however, the environments in the Sleeping Bear Point/ Manitou Passage area discriminated very well. These results can be explained in terms of a very simple causal relationship: the grain-size distribution of the parent material (i.e., those grains available to the system) seems to control the efficiency of environmental discrimination. If it is assumed that textural modifications are energy-dependent then systems with a limited grain-size range, such as the Little Sable Point system, may not reflect the entire energy spectrum of the system, whereas systems with unlimited grain-size ranges, such as the Sleeping Bear Point/Manitou Passage system, can reflect different energy levels in their sediment distributions (Fig. 25).

The results of this study tend to confirm, on the basis of principal-components analysis, that grain-size distributions are composed of two or more sub-populations, which may be related to

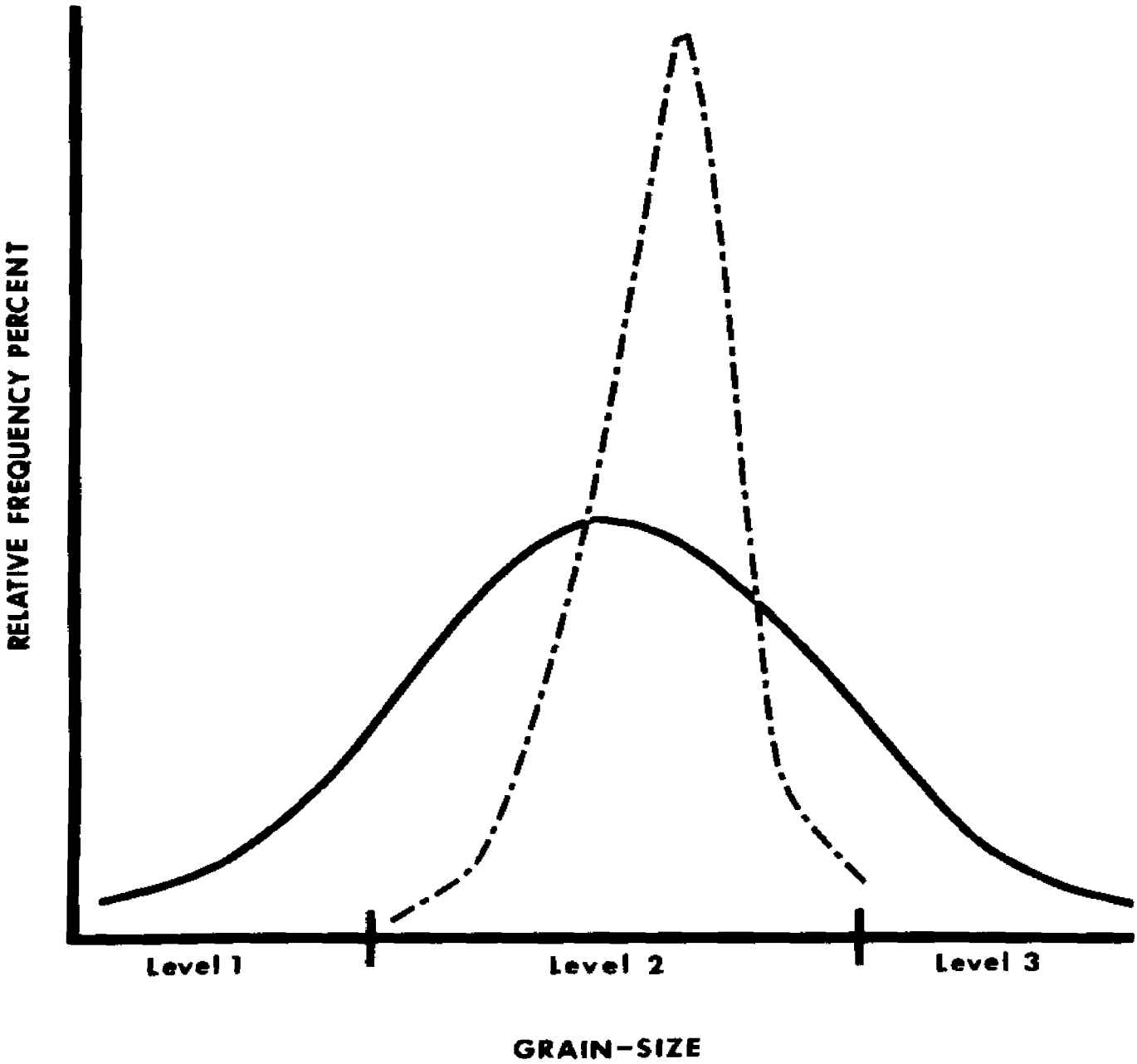

Figure 25: Diagrammatic grain-size frequency distributions. Dashed line represents a narrow grain-size distribution which reflects only one energy level, while the solid line represents a wider grain-size distribution reflecting three energy levels

different transport mechanisms. Although this technique does not determine which mechanisms control grain-size distributions it does show that two, and in one case three, factor axes are needed to explain a major portion of the variance in a set of grain-size data. It has also been shown that certain grain-size entities cluster around the same factors and are comparable in most cases to straight-line segments on log-probability grain-size graphs.

Although Q-mode factor analysis was used on a limited basis in this study, because the broad categories of depositional environments were known before hand, it is felt that this technique has much potential in the field of sedimentology. Samples can be classified into groups which show both geographical and geological meaningful trends without any a priori knowledge of the spatial position of the samples (Klovan, 1966). This is a very important point. For years, many investigators have used arbitrary indices in an effort to characterize sediment from different environments. Arbitrary in the sense that these indices were defined by the author in a special way. For example, Mason and Folk (1958) suggested that a graph of skewness versus kurtosis was appropriate for discriminating between different environments. However, even with different symbols, it was difficult to see any trends in the samples. Klovan (1966) states "...It is precisely from such unquantified data that we try to reconstruct environments of deposition..." If we can not distinguish differences between recent depositional environments our task is confounded immensely when we turn to the ancient deposits.

Passega (1957, 1972), Bagnold (1966), Klovan (1966), Koldijk (1968), and others suggest that the presence of the fine tail (silt/clay fraction) is a sensitive environmental indicator. This fraction was shown, indirectly, to be a significant factor for environmental discrimination of the Sleeping Bear Point/Manitou Passage samples. Indirectly, in the sense that the matrix was normalized prior to analysis which took into account the absence of this fraction from the analysis. The presence of the fine tail in the Sleeping Bear Point/Manitou Passage area samples allowed for a more effective reflection of the energy spectrum in this depositional system.

The present study shows only the results of applying several multivariate techniques to two areas of recent sedimentation. The causal process of sediment transport postualted here are not all inclusive. Many other processes or mechanisms not studied here are subject to review (i.e., turbidity currents) as well as other aspects such as rate of sediment supply, rate of subsidence, storm frequencies and intensity changes in source areas, which would complicate the patterns found.

As shown in this study, it is difficult to state with certainty whether depositional environments can be uniquely identified in recent deposits using only grain-size analysis. The problem of environmental discrimination is further complicated in ancient deposits particularly with respect to lithification and diagenesis of the sediment.

There is a great need at this time for more experimental flume and wave tank studies with much more sophisticated *in situ* measurements and collection techniques in order to establish the hydrodynamic aspects of sediment transport mechanisms which up to now have been mainly studied by some type of grain-size analysis. Once these techniques have been established and a reasonable data base established, the multivariate techniques used in this study could be used to establish a more objective classification of sediment types and processes. Even if environments can not be distinctly identified, in the fossil deposits, knowledge of energy-transport relationships of recent or experimental deposits will help to better interpret paleo-flow regimes.

APPENDICES

APPENDIX A

APPENDIX A

List of Phi Size Classes and Frequency Percentages of Each Little Sable Point Environment

Sample Number	0.0Ø	0.5Ø	1.0Ø	1.5Ø	2.0Ø	2.5Ø	3.0Ø
				Source Beach			
1	0.00	0.00	16.0	54.0	28.0	1.9	0.0
2	0.00	1.00	2.5	31.7	58.3	6.4	0.0
3	0.00	0.00	2.0	27.5	67.5	2.9	0.0
4	2.00	3.00	30.5	49.4	13.6	1.4	0.0
5	1.00	0.50	16.5	56.5	24.0	1.7	0.0
6	1.80	0.30	2.4	30.5	61.0	4.9	0.0
7	3.00	0.00	2.0	48.0	42.3	4.6	0.0
8	0.00	0.00	1.8	42.2	52.5	3.4	0.0
9	0.00	0.00	2.0	42.0	53.0	2.9	0.0
				Beach Samples West of Silver Lake			
10	0.0	0.0	2.0	23.5	66.7	7.8	0.0
11	0.0	0.0	2.5	32.5	60.5	4.5	0.0
12	2.3	1.7	1.0	19.0	68.5	7.5	0.0
13	3.0	0.5	0.30	15.9	71.1	8.2	1.0
14	0.0	0.0	13.0	47.5	36.0	3.5	0.0
15	0.0	1.0	0.80	14.2	70.5	13.5	0.0
16	1.5	1.0	7.80	39.0	45.9	2.8	0.0
17	0.0	0.8	10.4	52.3	30.0	6.0	0.5
18	0.5	2.5	10.0	46.5	37.0	3.5	0.0
19	0.0	1.5	1.0	10.5	72.7	13.3	1.0
20	0.0	1.0	4.5	50.5	39.2	4.8	0.0
21	0.0	1.0	19.0	50.5	27.0	2.5	0.0
22	0.0	0.0	2.0	8.0	60.0	30.0	0.0
23	0.0	0.0	9.5	58.7	29.1	2.7	0.0
24	0.5	0.5	2.0	14.5	72.5	9.5	0.5
25	1.0	1.0	12.0	54.0	26.5	4.8	0.7
26	0.0	0.0	1.5	15.0	63.0	18.5	2.0
27	0.0	0.0	2.0	13.5	65.0	19.5	0.0
28	0.4	1.1	8.3	50.2	37.2	2.8	0.0
29	0.0	0.0	1.5	25.0	55.5	15.5	2.5

Offshore Bars and Trough

Sample Number	0Ø	.5Ø	1Ø	1.5Ø	2Ø	2.5Ø	3Ø
30	0.0	0.0	2.5	17.5	70.0	10.0	0.0
31	0.0	0.0	2.0	10.8	76.2	11.0	0.0
32	0.6	0.6	1.3	77.5	3.5	14.5	2.0
33	0.0	0.0	6.5	40.5	44.8	7.40	0.6
34	0.0	0.5	3.5	16.5	64.5	15.0	0.0
35	0.0	0.0	2.0	12.0	63.0	20.5	2.5
36	0.0	0.0	3.0	28.0	61.5	7.5	0.0
37	0.0	0.0	2.0	27.0	65.8	5.2	0.0
38	1.5	1.0	1.7	22.0	65.3	8.5	0.0
39	1.5	0.1	2.9	56.5	44.7	4.3	0.0
40	0.0	0.9	3.4	36.7	49.8	9.2	0.0
41	0.0	1.5	3.0	16.5	55.0	22.5	1.5
42	1.0	0.5	2.0	7.5	61.0	26.5	1.5
43	0.0	0.0	3.0	16.5	57.5	20.8	2.2
44	0.0	0.0	13.0	54.5	32.3	0.2	0.0
45	0.0	1.0	3.0	9.0	64.5	20.0	2.5
46	0.0	0.0	2.2	8.8	50.5	34.0	4.5
47	0.0	1.0	3.0	6.0	50.0	36.5	3.5

Silver Creek Bed

	0Ø	.5Ø	1Ø	1.5Ø	2Ø	2.5Ø	3Ø
48	0.0	1.5	2.0	26.5	61.5	8.5	0.0
49	0.0	0.0	1.0	5.5	65.5	26.4	1.6
50	0.0	0.0	2.0	5.0	59.0	32.0	2.0
51	0.0	0.0	2.0	7.0	66.0	24.0	1.0
52	0.0	0.0	3.0	9.0	67.5	15.2	3.3
53	0.0	1.5	3.0	7.0	63.0	23.4	2.1
54	0.0	0.9	1.1	3.8	69.0	24.2	1.0
55	1.0	1.0	3.0	35.5	59.5	0.0	0.0
56	0.0	1.5	1.5	5.0	51.5	37.5	3.0
57	0.0	0.0	3.0	4.0	56.8	34.7	1.5
58	0.0	1.5	2.0	3.0	66.5	24.5	2.5
59	1.5	0.5	3.5	25.5	60.0	9.0	0.0
60	0.0	0.0	3.8	42.7	50.7	2.8	0.0
61	0.0	0.0	1.0	6.5	66.0	24.7	1.8
62	0.0	1.0	1.0	9.0	67.0	20.1	1.9
63	0.0	1.5	1.5	4.5	55.0	34.5	3.0
64	0.0	1.0	6.0	43.0	42.7	7.3	0.0
65	0.0	2.0	1.3	2.7	53.0	36.0	5.0
66	0.0	1.5	5.5	56.5	31.0	5.5	0.0
67	0.0	0.0	2.5	30.7	56.3	8.7	1.8
68	1.0	0.5	2.8	41.2	50.5	4.0	0.0
69	1.0	0.5	2.7	46.8	41.8	7.2	0.0

Aeolian

Sample Number	0Ø	.5Ø	1Ø	1.5Ø	2Ø	2.5Ø	3Ø
70	0.0	1.0	1.0	2.5	65.5	14.5	5.5
71	0.0	0.0	1.8	0.2	67.0	26.5	4.5
72	0.0	0.0	1.0	56.5	37.0	5.5	0.0
73	1.8	1.2	2.0	7.0	63.5	21.0	3.5
74	0.0	0.0	1.0	3.0	47.8	39.8	9.0
75	0.0	2.0	1.0	2.0	52.0	34.5	8.5
76	2.0	1.0	3.6	28.6	46.0	16.0	3.0
77	0.0	0.5	0.5	4.4	46.1	37.5	11.0
78	0.0	0.0	0.0	2.5	40.0	44.0	13.5
79	0.0	0.0	0.0	6.5	55.0	31.5	9.0
80	0.0	0.0	0.5	10.5	66.0	20.5	2.5
81	0.0	2.2	2.0	2.2	39.7	44.1	9.8
82	0.0	1.5	0.7	4.0	59.3	30.7	3.8
83	0.0	2.5	1.5	31.0	49.2	14.0	1.8
84	0.0	0.0	1.0	4.0	50.0	37.5	7.5
85	0.0	1.0	3.4	19.1	46.3	24.7	6.5
86	0.0	0.0	5.0	3.2	47.7	37.1	7.0
87	0.0	1.5	1.5	1.5	63.5	29.5	2.5
88	0.7	0.8	1.0	2.0	72.5	22.0	1.0
89	0.0	0.0	1.5	14.0	44.5	32.5	7.5
90	0.0	0.9	0.9	39.2	48.5	10.5	0.0
91	0.0	0.0	0.5	5.0	48.8	41.7	4.0
92	0.0	0.0	1.5	26.5	53.0	17.0	2.0
93	0.0	0.0	1.8	4.0	36.2	44.3	15.7
94	0.0	0.0	4.0	6.5	41.0	42.3	6.2

APPENDIX B

APPENDIX B

List of Phi Size Classes and Frequency Percentages of Each Sleeping Bear Point/Manitou Passage Environment

Shoal and Nearshore

Sample Number	0.5	1.0Ø	1.5Ø	2Ø	2.5Ø	3Ø	3.5Ø	4Ø	>4Ø
S6	3.7	14.8	23.0	17.8	14.7	14.6	8.0	3.0	0.4
S11	0.0	1.96	8.80	10.8	21.5	27.5	25.4	2.0	2.0
S14	6.5	15.0	32.4	37.5	6.5	1.9	0.1	0.0	0.1
S16	1.0	10.0	30.0	45.9	11.0	1.9	0.0	0.0	0.1
S17	2.0	3.50	21.0	52.4	17.5	3.4	0.0	0.0	0.1
S19	4.0	15.9	48.7	8.40	15.4	5.1	1.8	0.1	0.6
S20	8.0	18.5	28.4	36.5	7.5	1.0	0.0	0.0	0.1
S21	4.5	6.70	19.4	43.2	20.9	4.9	0.1	0.0	0.2
S24	6.5	11.3	20.2	41.8	16.5	3.4	0.2	0.0	0.1
S25	9.0	17.7	38.6	28.8	5.6	0.2	0.0	0.0	0.1
S26	7.0	10.3	37.6	37.5	6.9	0.6	0.0	0.0	0.1
M47	5.0	6.00	21.0	31.8	30.2	5.7	0.2	0.0	0.0
C12	0.5	1.45	2.1	26.0	30.5	24.0	8.7	2.9	3.3
C15	1.7	13.3	22.5	27.9	7.0	4.7	5.5	2.6	14.8
C16	15.0	38.4	36.5	9.00	0.9	0.2	0.0	0.0	0.1

Profundal

Sample Number	0.5	1.0Ø	1.5Ø	2Ø	2.5Ø	3Ø	3.5Ø	4Ø	>4Ø
S1	0.1	0.2	0.2	0.5	0.2	0.2	0.3	0.1	98.2
S2	1.6	5.1	7.7	9.7	2.6	6.7	4.9	4.8	56.8
C5	0.9	1.5	2.0	3.9	1.6	2.0	3.4	0.4	84.3
C6	0.5	1.3	2.5	4.3	2.0	0.6	2.9	1.9	84.0
C7	0.5	1.3	2.4	6.0	1.9	0.3	0.8	0.4	86.4
C8	0.4	1.0	1.4	2.7	2.2	0.9	2.6	0.7	88.1
C9	0.3	0.8	1.1	3.5	1.4	0.9	2.4	0.7	88.9
C13	0.6	2.2	3.6	8.9	1.5	7.8	2.8	0.6	72.0
C14	0.5	1.6	3.0	5.6	3.7	16.7	11.1	4.2	53.6

Beach

Sample Number	0.0Ø	0.5Ø	1.0Ø	1.5Ø	2.0Ø	2.5Ø	3.0Ø
101	2.6	6.6	55.3	32.0	3.5	0.0	0.0
102	1.8	5.7	52.0	33.3	7.2	0.0	0.0
103	0.0	0.6	23.2	56.5	15.7	2.0	2.0
104	0.0	1.3	24.0	50.2	23.0	1.5	0.0
105	0.0	3.3	35.9	47.6	12.2	2.0	0.0
106	0.0	0.0	4.5	10.8	51.2	26.0	7.0
108	1.3	3.2	6.5	23.6	35.4	20.0	9.2
111	0.0	1.8	15.8	42.7	29.0	6.6	4.1
112	1.2	4.8	59.0	28.5	3.9	0.6	0.0
113	0.5	1.0	14.0	36.0	32.2	11.0	4.7
114	2.5	1.0	47.0	40.9	7.8	7.8	0.0
115	2.2	4.6	54.2	30.8	6.5	1.7	0.0
116	1.0	2.5	46.5	38.0	10.5	1.5	0.0
117	0.0	4.0	39.8	41.2	7.0	4.0	0.0
118	1.8	4.2	54.0	33.7	6.3	0.0	0.0
119	1.5	6.8	68.0	19.2	3.0	1.5	0.0
120	0.8	4.7	57.8	28.7	6.5	1.5	0.0
121	11.2	17.8	28.7	11.0	2.8	0.0	0.0
122	3.2	2.5	51.4	32.8	10.0	0.0	0.0
123	8.0	10.5	60.5	16.2	4.0	0.8	0.0
124	0.5	11.8	67.2	16.0	4.5	0.0	0.0
125	0.0	2.0	40.5	45.0	12.5	0.0	0.0
126	0.0	5.2	51.5	33.0	8.0	0.0	0.0
127	1.2	3.3	53.2	32.3	10.0	0.0	0.0
128	0.0	2.7	46.8	39.5	10.3	0.7	0.0
129	0.0	4.0	54.5	32.5	9.0	0.0	0.0
130	0.0	4.0	62.0	28.0	6.0	0.0	0.0
131	3.0	3.0	48.5	37.3	8.2	0.0	0.0
132	4.2	10.6	69.9	13.3	2.0	0.0	0.0

Transitional

Sample Number	.5Ø	1Ø	1.5Ø	2Ø	2.5Ø	3Ø	3.5Ø	4Ø	>4Ø
S3	3.4	10.5	8.2	10.1	4.9	25.3	17.3	4.6	15.7
S4	2.9	14.1	23.4	21.8	6.2	4.2	2.0	2.3	22.7
S5	0.6	1.9	3.3	5.30	19.7	36.5	12.6	3.9	16.1
S7	0.0	0.9	1.0	4.20	35.3	34.8	12.5	3.3	7.1
S8	1.2	1.6	3.2	32.1	35.1	16.9	1.9	0.9	7.1
S9	4.0	12.2	17.6	17.8	6.6	13.0	5.3	4.4	19.1
S10	2.4	6.3	5.9	8.90	13.7	24.1	23.1	2.6	13.0
C1	0.8	6.5	12.2	25.6	10.9	13.5	13.7	5.7	11.0
C2	0.0	0.0	1.9	19.0	45.3	24.6	2.2	1.1	5.9
C3	0.0	0.0	0.9	2.20	4.4	56.6	15.7	8.9	11.3
C4A	0.0	6.3	8.8	13.3	6.9	18.9	24.0	5.2	16.7
C4B	1.8	2.3	5.5	21.5	26.6	26.6	7.1	0.9	7.6
C10	4.8	4.3	15.5	25.0	12.7	10.7	1.5	4.8	20.7
C17	1.6	8.1	10.0	14.2	9.1	22.7	10.1	4.8	19.4
C18	0.0	3.1	3.7	9.70	18.0	40.0	7.8	3.4	14.3
C11	0.8	8.4	19.3	34.9	8.0	2.3	4.8	1.6	19.7

APPENDIX C

APPENDIX C

List of Q-Mode Factor Results for Little Sable Point Samples

Factor	Eigenvalue	Cumulative Percentage of Eigenvalues
1	78.65	83.67
2	12.29	96.75
3	2.62	99.53
4	0.34	99.90
5	0.07	99.97
6	0.02	100.00
7	0.00	100.00
.	.	.
.	.	.
.	.	.
94	0.00	100.00

Rotated Factor Matrix

Sample Number	Factor I	Factor II	Factor III	Communality
1	0.18	0.97	0.08	0.998
2	0.60	0.68	0.41	0.999
3	0.61	0.60	0.50	0.999
4	0.03	0.92	-0.08	0.998
5	0.13	0.98	0.03	0.999
6	0.60	0.66	0.44	0.999
7	0.38	0.88	0.24	0.998
8	0.47	0.80	0.35	0.999
9	0.47	0.79	0.36	0.999

Rotated Factor Matrix

Sample Number	Factor I	Factor II	Factor III	Communality
10	0.67	0.56	0.47	0.999
11	0.58	0.68	0.43	0.999
12	0.70	0.50	0.50	0.997
13	0.72	0.45	0.51	0.998
14	0.32	0.92	0.17	0.999
15	0.77	0.43	0.46	0.999
16	0.45	0.82	0.32	0.999
17	0.26	0.96	0.07	0.999
18	0.33	0.91	0.20	0.999
19	0.78	0.38	0.48	0.999
20	0.34	0.91	0.19	0.999
21	0.19	0.96	0.07	0.995
22	0.18	0.97	0.08	0.999
23	0.90	0.33	0.24	0.999
24	0.74	0.44	0.50	0.999
25	0.20	0.97	0.04	0.998
26	0.81	0.45	0.37	0.999
27	0.81	0.42	0.37	0.999
28	0.30	0.93	0.19	0.999
29	0.72	0.60	0.32	0.999
30	0.72	0.48	0.48	0.999
31	0.76	0.38	0.51	0.999
32	-0.01	0.94	-0.28	0.999
33	0.48	0.83	0.25	0.999
34	0.77	0.47	0.41	0.999
35	0.83	0.41	0.35	0.999
36	0.64	0.63	0.43	0.999
37	0.63	0.60	0.48	0.999
38	0.69	0.54	0.46	0.999

Rotated Factor Matrix

Sample Number	Factor I	Factor II	Factor III	Communality
39	0.34	0.91	0.21	0.999
40	0.55	0.77	0.30	0.999
41	0.83	0.48	0.26	0.999
42	0.89	0.33	0.29	0.998
43	0.82	0.48	0.30	0.999
-44	0.20	0.96	0.14	0.999
-45	0.84	0.37	0.37	0.999
46	0.93	0.33	0.10	0.999
47	0.95	0.29	0.08	0.997
48	0.66	0.61	0.43	0.999
49	0.89	0.30	0.32	0.998
50	0.93	0.29	0.21	0.997
51	0.87	0.33	0.34	0.998
52	0.81	0.37	0.44	0.998
53	0.87	0.33	0.33	0.999
54	0.88	0.28	0.37	0.999
55	0.51	0.71	0.46	0.998
56	0.65	0.74	-0.02	0.997
57	0.94	0.27	0.17	0.995
58	0.89	0.28	0.35	0.999
59	0.66	0.61	0.42	0.999
60	0.45	0.81	0.34	0.999
61	0.88	0.32	0.34	0.999
62	0.84	0.36	0.39	0.999
63	0.94	0.27	0.15	0.997
64	0.45	0.86	0.23	0.999
65	0.96	0.24	0.12	0.998
66	0.24	0.96	0.08	0.999
67	0.62	0.68	0.37	0.998

Rotated Factor Matrix

Sample Number	Factor I	II	III	Communality
68	0.47	0.80	0.34	0.999
69	0.41	0.88	0.21	0.999
70	0.83	0.28	0.46	0.995
71	0.91	0.23	0.33	0.999
72	0.29	0.93	0.14	0.998
73	0.86	0.34	0.36	0.998
74	0.97	0.22	0.01	0.998
75	0.33	0.92	0.11	0.998
76	0.68	0.69	0.22	0.995
77	0.96	0.25	0.01	0.993
78	0.96	0.18	-0.12	0.999
79	0.84	0.38	0.37	0.999
80	0.93	0.30	0.17	0.998
81	0.97	0.19	-0.12	0.998
82	0.93	0.27	0.23	0.999
83	0.65	0.70	0.27	0.998
84	0.96	0.25	0.06	0.999
85	0.83	0.53	0.14	0.997
86	0.96	0.24	0.04	0.999
87	0.92	0.24	0.28	0.998
88	0.86	0.26	0.41	0.999
89	0.90	0.42	0.03	0.998
90	0.54	0.78	0.27	0.999
91	0.96	0.25	0.01	0.996
92	0.72	0.62	0.28	0.999
93	0.95	0.20	-0.18	0.986
94	0.95	0.27	-0.09	0.998

LIST OF REFERENCES

LIST OF REFERENCES

Allen, G. P., P. Castaing, and A. Klingebiel, 1971, Distinction of elementary sand populations in the Gironde estuary (France) by R-mode factor analysis of grain-size data: Sedimentology, V. 19, pp. 21-35.

Ayers, J. C., D. C. Chandler, G. H. Lauff, C. F. Power and E. B. Henson, 1958, Currents and Water Masses of Lake Michigan: Pub. 3, Great Lakes Res. Div., Univ. of Michigan, p. 169.

Bagnold, R. A., 1956, Flow of cohensionless grains in fluids: Royal Soc. Philos. Trans. (London), V. 249, pp. 235-297.

_____, 1966, An approach to the sediment transport problem from general physics: U.S. Geol. Surv. Prof. Pap., 422 (I), pp. 11-137.

_____, 1967, Deposition in the process of hydraulic transport: Sedimentology, V. 10, pp. 45-56.

Beall, A. O., 1970, Textural analysis within the fine sand grade: Journ. Geol., V. 78, pp. 77-93.

Blatt, H., G. Middleton, and R. Murray, 1972, Origin of Sedimentary Rocks: Prentice-Hall, Inc., N.J.

Buller, A. T. and J. McManus, 1972, Simple metric sedimentary statistics used to recognize different environments: Sedimentology, V. 18, pp. 1-21.

Chayes, F., 1960, On correlation between variables of constant sums: Journ. Geophys. Res., V. 65, No. 12, pp. 4185-4193.

_____, 1962, Numerical correlation and petrographic variation: Journ. Geol., V. 70, pp. 440-452.

Davis, J.C., 1970, Information contained in sediment-size analysis: Journ. of Math. Geol., V. 2, No. 2, pp. 105-112.

_____, 1973, Statistics and Data Analysis in Geology: John Wiley and Sons, Inc., N. Y.

Davis, D. K. and F. G. Ethridge, 1975, Sandstone composition and depositional environment: Am. Assoc. Petroleum Geol. V. 59, No. 2, pp. 239-264.

Doeglas, D. J., 1946, Interpretation of the results of mechanical analysis: Journ. Sed. Petrol., V. 16, pp. 19-40.

French, W. E., 1964, A correlation of currents and sedimentary activity in the Manitou Passage area of Lake Michigan: Pub. no. 11, Great Lakes Research Div., The University of Michigan, Ann Arbor.

Friedman, G. M., 1967, Dynamic processes and statistical parameters compared for size frequency distribution of beach and river sands: Journ. Sed. Petrol. V. 37, No. 2, pp. 327-354.

Fuller, A. O., 1961, Size characteristics of shallow marine sands from Cape of Good Hope, South Africa: Journ. Sed. Petrol. V. 31, pp. 256-261.

Folk, R. F. and W. C. Ward, 1957, Brazos River bar, a study in the significance of grain-size parameters: Jour. Sed. Petrol., V. 27, pp. 3-26.

Gibbs, G., 1972, Accuracy of sediment analysis by use of settling tubes: Journ. Sed. Petrol., March.

Gillis, W. T. and K. I. Bakeman, 1963, The disappearing Sleeping Bear Sand Dune: Mich. Botanist, V. 2, pp. 45-54.

Harbaugh, J. W. and F. Demirmen, 1968, Computer Applications in Stratigraphic Analysis: John Wiley and Sons, N. Y.

Hough, J. L., 1958, Geology of the Great Lakes: Univ. of Illinois Press, Urbana.

Hoel, P. G., 1962, Introduction to Mathematical Statistics: John Wiley and Sons, N. Y., 3rd ed.

Hoyt, J. H., 1966, Air and sand movements to the lee of dunes: Sedimentology, V. 7, pp. 137-143.

Imbrie, J., 1963, Factor and vector analysis programs for analyzing geologic data: Northwestern Univ., Evanston, Ill., Tech. Rept. 6, O.N.R. Task No. 389-135, Contr. No. 1228 (26).

_____ and T. H. Van Andel, 1964, Vector analysis of heavy mineral data: Bull of Geol. Soc. of America, V. 75, pp. 1131-1156.

Inman, D. L., 1949, Sorting of sediment in light of fluvial mechanics: Journ. Sed. Petrol, V. 19, pp. 51-70.

Klovan, J. E., 1966, The use of factor analysis in determining depositional environments from grain-size distributions: Journ. Sed. Petrol., V. 36, pp. 115-125.

Koldijk, W. S., 1968, On environment-sensitive grain-size parameters: Sedimentology, V. 10, pp. 57-69.

Krumbein, W. C., 1937, Sediments and exponential curves: Journ. Geol., V. 45, pp. 577-601.

_____, 1938, Size frequency distributions and the normal phi curve: Journ. Sed. Petrol, V. 8, pp. 84-90.

_____, and F. A. Graybill, 1965, An Introduction to Statistical Models in Geology: McGraw-Hill Co., N. Y.

Mason, C. C. and R. L. Folk, 1958, Differentiation of beach, dune, and aeolian flat environments by size analysis, Mustang Island: Journ. Sed. Petrol., V. 28, pp. 211-226.

Mather, P. M., 1972, Study of factors influencing variation in size characteristics of fluvioglacial sediments: Journ. Math. Geol., V. 4, No. 3, pp. 219-234.

Morrison, D. F., 1967, Multivariate Statistical Methods: McGraw Hill, Inc., N. Y.

Moss, A. J., 1962, The physical nature of common sandy and pebbly deposits, II: Am. Journ. Sci., V. 261, pp. 297-343.

_____, 1963, The physical nature of common sandy and pebbly deposits II: Am. Journ. Sci., V. 261, pp. 297-343.

Nie, N. H., D. H. Bent and C. H. Hull, 1970, Statistical Package for Social Sciences: McGraw Hill, Inc., p. 343.

Otto, G. M., 1939, A modified logarithmic probability graph for the interpretation of mechanical analyses of sediments: Journ. Sed. Petrol., V. 9, pp. 62-75.

Passega, R., 1957, Texture as characteristic of clastic deposition: Am. Assoc. Petroleum Geol. Bull., V. 41, pp. 1304-1319.

_____, 1972, Sediment sorting related to basin mobility and environment: Am. Assoc. Petroleum Geol. Bull. V. 56, pp. 2440-2450.

Sahu, B. K., 1964, Depositional mechanisms from size analysis of clastic sediments: Journ. Sed. Petrol. V. 34, pp. 73-83.

Saylor, J. H. and E. B. Hands, 1970, Properties of longshore bars in the Great Lakes: Proc. of 12th Coastal Engineering Conf. Washington, D. C., pp. 839-853.

Schlee, J. S., E. Uchupi and J. V. A. Trumball, 1964, Statistical parameters of Cape Cod beach and aeolian sands: U.S.G.S. Prof. Pap. 501-D, pp. D-118-D122.

Shephard, F. P. and R. Young, 1961, Distinguishing between beach and dune sands: Jour. Sed. Petrol., V. 31, pp. 196-214.

Sokal, R. R. and F. J. Rohlf, 1969, Biometry: W. H. Freeman and Co., San Francisco.

_____, 1969, Statistical Tables: W. H. Freeman and Co., San Francisco.

Solhub, J. T. and J. E. Klovan, 1970, Evaluation of grain-size parameters in lacustrine environments. Jour. Sed. Petrol., V. 40, pp. 81-101.

Spencer, D. W., 1963, The interpretation of grain-size distribution curves of clastic sediments: Journ. Sed. Petrol., V. 33, pp. 180-190.

Upchurch, S. B., 1970a, Sedimentation on the Bermuda platform: U.S. Lake Survey Research Report 2-2, Department of the Army, U.S. Lake Survey District, Corps of Engineers, 172 pp.

_____, 1970b, Mixed-population sediment in nearshore environments: Proc. 13th Conf. Great Lakes Res., pp. 768-778.

_____, 1972, Discriminant analysis of Bermuda carbonate strand-line sediment: Bull. of the Geol. Soc. of America, V. 83, pp. 87-94.

_____, 1973, Lake Michigan coastal processes: Leland to Manistee, Michigan, in Geology and the Environment, R. L. Chambers and W. T. Straw, eds., published by Michigan Basin Geological Society, pp. 54-66.

United States Department of Commerce News, 1971, No hazards found at Sleeping Bear dunes slide site. Circular N/R 71-40 (Oct. 1971) OB-0-5-7-75-9-55B-5NB-75B-55-5N-7N., published by the Lake Survey Center, NOAA, Detroit, Michigan.

Visher, G. S., 1965, Fluvial processes as interpreted from ancient and recent fluvial sediments; in Primary sedimentary structures and their hydrodynamic interpretations: G. V. Middleton, ed., Soc. Econ. Paleon. and Mineral. Sp. Pap. 12, pp. 116-133.

_____, 1969, Grain size distributions and depositional processes: Journ. Sed. Petrol., V. 39, No. 3, pp. 1074-1106.

Williams, G., 1964, Some aspects of the eolian saltation load: Sedimentology, V. 3, pp. 257-287.